

CDP NR 5

Conceptual Design Project (CH3843)

MSc Chemical Engineering
ChemE - Faculty of Applied Sciences
Delft University of Technology

Safe Spent Research Reactor Fuel Disposal

Authors	Study nr.
Kevin Koets	4752988
Deniz Erkan	5599938
Agneta Meiksane	5619610
Alexandros Mantzanas	5621909
Jakob Bregman	4982711

Keywords: Nuclear waste management, cementitious materials, spent research reactor fuel, geological disposal

Assignment issued: 25-04-2022
Report issued: 27-06-2022
Appraisal: 28-06-2022

Summary

The Central Organisation for Radioactive Waste (COVRA) currently stores high-level waste (HLW), intermediate-level waste (ILW) and low-level waste (LLW) for at least the coming 100 years, while further disposal options are being researched. One approach is based on a natural concept, where the radionuclides are immobilised in the host rock. Based on this case, the underground repository is being designed for long term safe disposal and possible retrieval of the waste before the final closure of the repository [1].

Multiple barriers are used to improve the containment of the waste, consisting of a concrete housing with a steel canister (ECN canister) inside. These barriers are usually referred to in total as the engineered barrier system. The scope of this project was to find a suitable cementitious fluid that could cover the aluminium cladding around the UAl_x fuel in spent research reactor fuel rods, which are placed inside the ECN canister. This is needed to inhibit the formation of hydrogen gas by corrosion of the cladding around the fuel meat, since this would most likely jeopardize the integrity of the barriers due to pressure build up. Since safety is the number one concern in the storage and handling of nuclear waste, this additional fail-safe barrier is researched here in case the engineered barrier system is compromised.

The main way to ensure the containment of the waste, is by preventing the corrosion of the outer aluminium cladding of the waste elements. Cement-based solutions were preferred due to the expertise COVRA has in working with them. Corrosion prevention can occur, either by forming an insoluble layer on the aluminium cement interface or by providing a controlled environment that inhibits corrosion by pH induced passivation [2]. Magnesium potassium phosphate cement (MKPC) was identified to be most suited barrier. It was selected for its eventually low pore water pH (between 7 and 9) and comparatively workable setting time. With a cement selected, then came the consideration for the ratios of magnesium to phosphate (M/P) and water to cement (W/C), both having an effect on the setting time and the pH of the pore water. From a literature review it was gathered that a M/P ratio of 1.50 gave a pH of 7 to 8. With increasing W/C the porosity and setting time rose, which had to be balanced with each other. Keeping the W/C in line with M/P, the W/C has to be around 0.20. Further additives were also researched to design for even more preferable characteristics. Therefore, we suggest adding 15 w% of boric acid to provide a tripling of the setting time.

In terms of economics, the MKPC cement was found to be more compelling than the previously reported benchmark solution of a Portland cement blend with $LiNO_3$. Furthermore, the annual expenses of implementing such cement were calculated. However, there is still the option of significantly reducing the cost by using COVRA's existing equipment or purchasing pre-mixed components from other companies. Further experiments are needed to validate the properties of the final cement mixture and to determine whether the findings from the literature are applicable in the long term safe storage of the fuel assemblies.

Contents

List of Figures	1
List of Tables	2
Abbreviations	4
List of Symbols	5
1 Introduction and Project Charter	6
1.1 Scope of the Project	9
2 Waste Disposal System and Physical Processes	10
2.1 Physical and chemical components of the disposal cell	10
2.2 Physical processes	12
2.2.1 Water diffusion	13
2.2.2 H ₂ generation by the corrosion of aluminium	14
2.2.3 Dissolution of H ₂ into pore waters	17
2.2.4 Criticality	18
3 Product concepts and selection	21
3.1 Preexisting Solution: Lithium Nitrate	21
3.2 Product concepts	21
3.2.1 Low pH Cements	22
3.2.2 Conversion coatings	23
3.3 Product selection	24
4 Concept stage	26
4.1 Market Analysis	26
4.1.1 Quantity of product required	26
4.1.2 Competitor activities	26
4.1.3 Collaborations	26
4.2 Product Design	27
4.2.1 MKPC Cement	27
4.2.2 House of Quality	29
4.2.3 Cement Mixture Parameters	30
4.3 Final formulation	35
5 Manufacturing of the product	36
5.1 Production of magnesium oxide	36
5.2 Production of monopotassium phosphate	38
6 Process control	39
6.1 MgO-production	39
6.1.1 Calcination temperature	39
6.1.2 Air for combustion of natural gas	39
6.1.3 Hot spots monitoring	39
6.2 MKP production	39
7 Balances and Utility requirements	41
7.1 Plant capacity	41
7.2 Assumptions	41
7.3 Mass balances	42
7.4 Energy balances	43
7.4.1 MgO production	43

7.4.2	KH ₂ PO ₄ production	43
7.5	Utility requirements	44
7.5.1	Hot utilities	44
7.5.2	Cold utilities	44
7.6	Heat integration	44
8	Equipment List and Unit Design	48
8.1	MgO-production	48
8.2	KH ₂ PO ₄ -production	48
8.3	Mixing of solids	49
9	Safety, Health, Environment and Sustainability	50
9.1	Safety analysis	50
9.1.1	Bow-Tie for the Disposal System	50
9.1.2	MPC Manufacturing safety analysis	51
9.2	Criticality	53
10	Economics	55
11	Creativity and Group Process Tools	58
11.1	Creativity Tools	58
11.2	Group Process Tools	58
	Conclusion and further recommendations	60
11.3	Conclusion	60
11.4	Recommendations	60
11.4.1	Experimental work	60
11.4.2	Addition of additives	60
11.4.3	External production	61
	Reference list	62
	Appendices	
A	Appendix A	1
A.1	Chromate Hydroxide Coating	1
A.2	Cerium salts	2
A.3	Phosphate conversion coating	2
A.4	Molybdate Coating	2
B	Appendix B	4
B.1	Thermodynamic data	4
B.1.1	Heat capacities	4
B.1.2	Standard Enthalpies of formation	4
B.2	General energy balance	5
B.3	Mass fractions of streams	6
C	Appendix E	7
C.1	Serpent code used for the criticality calculations	7

List of Figures

1.1	Artist's rendition of the planned Dutch Geological Disposal Facility [1]	7
1.2	Multibarrier approach of the GDF [1]	7
2.1	Scaled side view cross-section of the EBS	11
2.2	Schematic top view of the fuel plates for spent research reactor fuel [1]	11
2.3	Summary of physical processes.	12
2.4	Diffusion path of water	13
2.5	Al ₂ O ₃ protective layer formation	15
2.6	Al corrosion in cements [3]	16
2.7	Corrosion types that occur at different pH levels [4]	16
2.8	Neutrons scattering from direction Ω and energy E to direction Ω' and energy E' [5].	20
3.1	Setting time with respect to temperature[6].	23
4.1	OCP measurements on aluminium electrode as a function of time [7].	29
4.2	Effect of the M/P ratio, on the pore water pH (left)[8] & on the setting time and and strength of the cement mixture (right)[9].	32
4.3	setting time and cement strength with respect to borax content [9].	33
4.4	Compressive strength and setting time with respect to W/C ratio [10].	34
4.5	Theoretical W/C mass ratio with respect to the M/P ratio [11]	34
4.6	Compressive strength and setting time with respect to W/C ratio [12].	35
5.1	Simple schematic of a countercurrent flow rotary kiln [13]	37
5.2	Schematic of MgO production	37
5.3	Schematic of KH ₂ PO ₄ manufacturing	38
7.1	Flow diagram of the whole process	47
9.1	Bow-tie analysis: Foreign material entering fuel assembly	51
9.2	ECN canister Geometry and materials	53
9.3	The multiplication factor k with respect to the spacing for different number of fuel rods (left) and with respect to salt content of water % w/w(right).	54
9.4	The multiplication factor k with respect to water content(from ingress by the surrounding rock) of MKPC cement % w/w.	54
A.1	Layer formation mechanism [14](left) and application process(right)	1
A.2	Schematic illustration of the inhibition mechanism for aluminium corrosion in 10mM MoO ₄ ²⁻ concentration in concrete pore solutions	3

List of Tables

2.1	Modelled pore water composition for the seawater scenario [15]	14
2.2	Diffusion coefficients in water cement mixtures	18
3.1	H ₂ gas generation comparison between cements with pore water pH inside the passivation range compared to Portland cement.	22
3.2	Different types of conversion coatings and their characteristics	24
3.3	Pugh Matrix	25
4.1	Hydration products of MKPCs [16]	28
4.2	House of quality	30
4.3	Summary of MKPC pore water pH studies	31
4.4	Peak Heat Flow (W/g)[17]	35
4.5	Mass fractions of raw materials in final product	35
5.1	Classification of type of magnesia according to their calcination temperature [6, 18]	37
7.1	Assumptions made concerning the production capacity	41
7.2	Stream summary	42
7.3	Errors in overall mass balances of both production processes	42
7.4	Heating requirements for the MgO production	43
7.5	Cooling requirements for the MgO production	43
7.6	Heating requirements for the KH ₂ PO ₄ production	43
7.7	Cooling requirements for the KH ₂ PO ₄ production	43
7.8	Errors in overall energy balances of both production processes	43
7.9	Hot utility requirements for the production of MgO	44
7.10	Hot utility requirements for the production of MKP	44
7.11	Cold utility requirements for the production of MgO	44
7.12	Cold utility requirements for the production of MKP	44
7.13	Hot and cold streams in the MgO-process suitable for heat integration	45
7.14	Reduction in duties by heat integration in MgO-process	45
7.15	Natural gas utility review	45
7.16	Cooling water utility review	45
7.17	Chilled water utility review	45
7.18	Chilled air cooling utility review	46
9.1	Hazard(s) identification information of materials involved in MPC manufacturing [19]	51
9.2	Hazard & Operability Analysis (HAZOP) for the Spray Dryer	52
9.3	Hazard & Operability Analysis (HAZOP) for the Rotary Kiln	52
10.1	Material requirements for the production of 1 kg of final product	56
10.2	Manual labor cost	56
10.3	Maintenance cost	57
11.1	Team Member Responsibilities	59
A.1	K_{sp} and equilibrium pH in pure water of hydroxide compounds	2
B.1	Heat capacities constants that were used for the energy balances. All of this data is retrieved from the 'NIST-JANAF Thermochemical Tables' [20]	4
B.2	Standard enthalpies of formation of the used chemicals	4

B.3	Energy flows in the MgO-process	5
B.4	Energy flows in the KH_2PO_4 -process	5
B.5	Fraction table	6

Abbreviations

COVRA Central Organization for Radioactive Waste.

DBM Dead-Burned Magnesia.

DOE Department of Energy.

EBS Engineered Barrier System.

ECN Energy Research Center of Netherlands.

ERDO European Repository Development Organisation.

FA Fly ash.

GDF Geological Disposal Facility.

HABOG The High-Level Radioactive Waste Treatment and Storage Building.

HAZOP Hazard and Operability Study.

HEU High Enriched Uranium.

HHV Higher Heating Value.

HLW High-Level Waste.

ILW Intermediate-Level Waste.

LCA Life Cycle Assessment.

LEU Low Enriched Uranium.

LHV Lower Heating Value.

LLW Low-Level Waste.

MKPC Magnesium potassium phosphate cement.

MPC Magnesium Phosphate Cement.

SF Silica Fume.

List of Symbols

Symbol	Description	Symbol	Description
D	diffusion coefficient	V	Volume
E	energy	x	position
g	acceleration of gravity		
J	neutron net flow	<i>Greek</i>	
k	permeability	μ	viscosity
K	hydraulic conductivity	ν	emitted neutrons after fission
k_{eff}	criticality multiplication factor	ρ	density
n	number of neutrons	σ	neutron cross sectional area
N	neutron density	Σ	neutron cross section
P	probability	χ	energy distribution of fission neutrons
r	neutron rate of change	ψ	neutron angular flux
t	time	Ω	angle
v	speed(magnitude)	ω	direction
		<i>Vectors</i>	
F	vector field	r	position vector
n	unit vector perpendicular to S	<i>Greek</i>	
		Ω	direction vector
		<i>Other</i>	
S	surface		

1

Introduction and Project Charter

Radioactive waste is generated from a variety of human activities including nuclear power generation, mining, nuclear weapons processing, as well as from the use of radioactive materials in industries like medicine, agriculture and research. Depending on its level of radioactivity, the length of time it remains hazardous, and the heat generation, radioactive wastes can be separated into three categories: low-level waste (LLW), intermediate-level waste (ILW) and high-level waste (HLW) [21].

Regardless of type, it is essential to have a safe, secure and sustainable management plan for radioactive wastes as they are potentially hazardous to the environment and subsequently, public health. Although the wastes are primarily managed in accordance with the national government's policies, which usually have been prepared in compliance with relevant international legislation and standards, these approaches are recognized to be a result of a complex network of multinational measures. In the Netherlands, the current policy on the nuclear waste management is divided into two parts [22]:

1. Storage of all types of radioactive waste at a centralised surface facility for the next 50 to 100 years.
2. Research into long-term waste management options.

The Central Organization for Radioactive Waste (COVRA) was established as the sole organization in order to carry out the first part of the above-listed policy. At COVRA, all types of Dutch radioactive waste are collected, processed and being stored for at least 100 years in facilities specifically designed for this purpose. In order to ensure long-term safety, the wastes are isolated and well-controlled. While COVRA has been storing LLW and ILW at its site in the Vlissingen-Oost region for many decades, the HLW is separated and stored in a dry vault storage facility (the HABOG facility). This allows for further surface storage, returning spent fuel to the supplier country for reprocessing, and, most importantly, future disposal in a deep geological formation for long-term safety (up to 1,000,000 years) [22].

Regarding the second part of the policy, COVRA is targeting its research on the disposal of the waste in the Dutch host rock. This is a similar approach adopted in many other countries like Belgium, Finland etc. [1]. COVRA also focuses their research on retrievable repository designs in both rock salt and clay formations, as well as extended surface storage [22]. In terms of research budget, 3 times more has been spent on rock salt compared to clay.

HLW includes not just nuclear waste and medical waste, but also spent nuclear fuel components utilized in research reactors (either for test, research or energy generation purposes). There are currently three operational test and research reactors in the Netherlands: two reactors (High and Low Flux) in Petten and one (Hoger Onderwijs Reactor (HOR)) in Delft. The spent research fuel that is the focus of this waste management project is coming from these reactors. Because spent fuel components are no longer usable, they must be removed and replaced with new fuel rods. Spent fuel can also be considered as an asset. In fact, approximately one third of the spent fuel is reprocessed to recover the reusable substances including, isotopes for medical applications, uranium and plutonium, which then results in new fuel and HLW [23]. The waste is still highly radioactive and generates a significant amount of heat, therefore it is usually transferred to a fuel pool for several years. After this period,

it is transferred to a wet or dry storage facility. The canisters containing the HLW are usually stored in air-cooled vaults or casks. In the HABOG facility it is stored using a dry vault storage technology [22]. The exact composition of spent fuel is determined by the fuel type, enrichment (fraction of fissile content), reactor type, and operating conditions [24].

It has been discovered that the best way to ensure long-term safety for spent fuel and HLW is by isolation in deep geological repositories (DGR) [1]. The Dutch geological disposal facility (GDF), planned with this universally adopted approach in mind, can be seen as a schematic in Figure 1.1 below. The facility consists of both underground and surface components. The depth of the underground facilities depends on the envisaged impact by climate change (ice ages). In the North of the Netherlands, these facilities may need to be deeper than in the South of the Netherlands. A minimum depth of 200 metres for isolation purposes is used. A maximum of 1000 metres for acceptable underground working conditions is currently assumed. A point of departure of 500 metres depth was used [1]. The long term safety is provided by both natural and engineered barrier systems. The disposal tunnels, located in the host rock formation, are planned to be separated and optimized for different types of fuels: for high-level wastes, for spent fuel from research reactors, for the disposal of low and intermediate level wastes and depleted uranium [1].

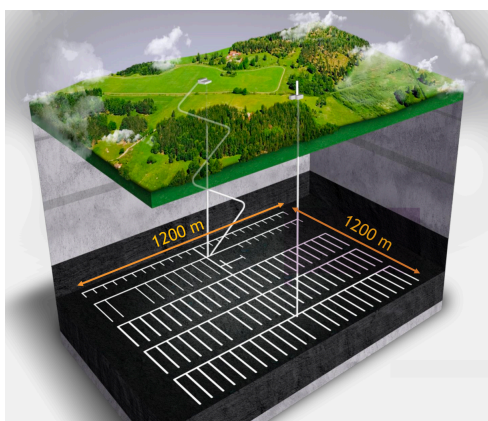


Figure 1.1: Artist's rendition of the planned Dutch Geological Disposal Facility [1]

As it can be seen from the artist's rendition above, in the long-term plan, the nuclear wastes are isolated and the radionuclides within them are contained by multiple barriers. These barriers can be discussed under two categories: natural barrier systems and engineered barrier systems (EBS) in order to maintain safety. A schematic displaying the various layers of the GDF can be found in Figure 1.2 below.

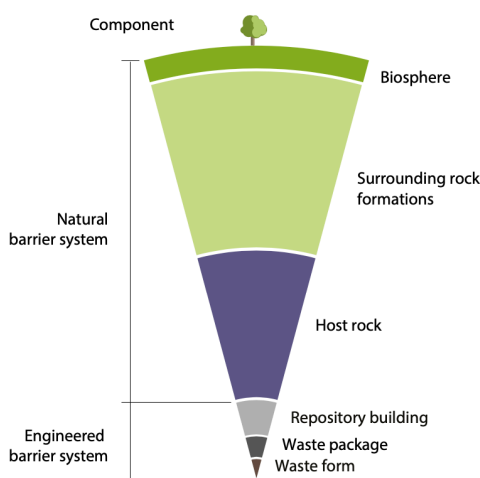


Figure 1.2: Multibarrier approach of the GDF [1]

Natural barriers are made up from the host rock layer found in the site location and the overlaying geological formations. Because the design utilizes naturally found components for the containment, it is highly dependent on the geological environment in which the facility is placed. For Netherlands, clay and rock salt have been determined as the most likely host rock formation [1]. In this report, clay will be taken as the principal natural barrier and will be referred to as Boom Clay, because much knowledge is available about this clay for disposal. All Paleogene clays are considered [25]. Boom Clay provides a stable and low permeability barrier that protects both the EBS and the wastes from the natural processes and any interactions with flowing water. It is also able to hold and slow down the diffusion of radionuclides. The overlying geological formations, denoted in light green in Figure 1.2, are generally mixed layers of sand, silt and clay, and they serve to diffuse and dilute the radionuclides that are able to leave the host rock layer [1].

The engineered barrier system, on the other hand, is made out of many components that provide both physical and chemical containment for the radionuclides in the waste. It is mainly made out of cementitious material along with steel containers for disposal of waste in a GDF hosted in clay. A more detailed explanation on the various components of the EBS can be found in Section 2.1; Overall, each component of the EBS is chosen for their non-overlapping weaknesses to ensure safety over long periods of time. However, despite the geological settings of the Boom Clay and the many layers of the EBS protect the waste from erosion and climate change, there is still a possibility of waste and (pore) water contact. However, the fuel elements (either filled with uranium-aluminide or uranium-silicide) are covered in aluminium cladding. As a result, anaerobic corrosion of either the cladding or the uranium aluminium matrix due to oxygen-free water may occur.

In the present case, it is assumed that the steel canister is already compromised and water has come in contact with the waste. In case of this potential deterioration, extra waste processing/protection barriers are required to limit the hydrogen gas buildup that can form as a result of the aforementioned corrosion. Spent research reactor fuel contains aluminium with a high surface area exacerbating the problem further. For this reason the focus of this study will be on this part of the waste package.

Two main approaches to prevent the formation of the H₂-gas during anaerobic corrosion of aluminium have been demonstrated. An insoluble layer could be formed on the aluminium cladding which would prevent the corrosion, or an engineered barrier which prevents the water from coming into contact with the cladding can be introduced. It has already been discovered that LiNO₃ forms an insoluble layer on the aluminium cladding, preventing the H₂-gas from being formed. However, the availability of lithium is expected to drop in the future due to the increased usage of batteries. Furthermore, it is impossible to ensure that an engineered barrier will remain impermeable to water for elongated periods of times. Consequently, a new solution must be found in order to prevent H₂-gas generation during nuclear waste disposal.

1.1. Scope of the Project

Although the other layers of the engineered barrier system (EBS) are already designed to prevent water from coming into contact with the aluminium, the possibility of corrosion occurring simply due to the extremely long disposal time must still be addressed. Therefore for this study it is assumed that the other barriers have failed and the aluminium is in direct contact with highly alkaline water, which is the main driver of the aluminium corrosion.

The scope of this study is to report on existing options that can be used for preventing the aluminium corrosion. The intention is to present only those options that are feasible now, or expected to be available soon. The main challenges to overcome during this study are data availability regarding gas perturbation in the clay host rock and coating application technologies, as well as uncertainties with the location where the waste will be disposed, thereby predicting the environmental conditions for the next 100,000 years.

The main constraints that are given by COVRA are:

- The criticality: it is the state in which the nuclear chain reactions are able to sustain themselves. The amount of fuel elements and their arrangement have to be considered to prevent criticality.
- The availability of materials: although the use of LiNO_3 is a known solution against Al corrosion, it has low availability hence no lithium containing materials can be included in this study.
- Ease of use: room temperature handling is preferable to minimize hazards and failures.
- No organic materials: since organic materials could act as food source for microbes, they can not be used.
- Strength: Determination of the strength of the material is outside the scope, however any information on this is welcome.

Based on these constraints, a suitable cementitious covering is sought so the aluminium cladding and the inner fuel meat remain stable.

2

Waste Disposal System and Physical Processes

2.1. Physical and chemical components of the disposal cell

Initially, the HABOG facility of COVRA stores the spent research reactor fuel in ECN canisters, which are stainless steel containers that are welded shut after any corrosive gasses and leftover liquids are removed and replaced with helium. Within this stainless steel container rests a framework of steel, which holds the fuel waste elements enriched in fuel particles. These waste elements are enclosed in aluminium cladding, within are the fuel particles used for research reactors [26]. The fuel particles are either; uranium-aluminide (a mixture of UAl_3 and UAl_4) or uranium-silicide (e.g. U_3Si , U_3Si_2 or USi) of a size between 40 and 150 μm . They are dispersed in an aluminium matrix which is metallurgically bonded to aluminium cladding surrounding the whole [4]. Aluminium is chosen due to its low neutron absorption cross section, low cost and good manufacturability [4]. The chance that a neutron reacts is directly proportional to the absorption cross section and must be kept in-check to prevent criticality. Research reactors have previously been running with High Enriched Uranium (HEU 93% ^{235}U), but are now only running on Low Enriched Uranium (LEU 19.75% ^{235}U) due to public security concerns [1, 27] LEU contains U_3Si_2 and HEU a mixture of UAl_3 and UAl_4 with 60wt% and 40wt% [26]. These ECN canisters are supposed to be transported to the underground repository.

As discussed before, the approach chosen for the disposal system by utilizing both the Boom Clay host rock and the EBS is expected to provide the high levels of containment and isolation required. There are two key features of the EBS that needs to be discussed. First is the sheer amount of cementitious material contained in the supercontainers. This is a concept that has been adopted from Belgium in 2010 [1]. In fact, in the HLW tunnels, the waste material only makes up 0.9% of the supercontainer volume, the steel 0.78% and the cementitious material 98.3%. This high volume of concrete and cement translates to an approximately 1.50 meter barrier between the waste and the Boom Clay [1]. The second feature is the extensive number of barriers designed to separate the HLW and the spent fuel from the outside environment. Below is a scaled cross-section of the EBS for spent fuel supercontainers.

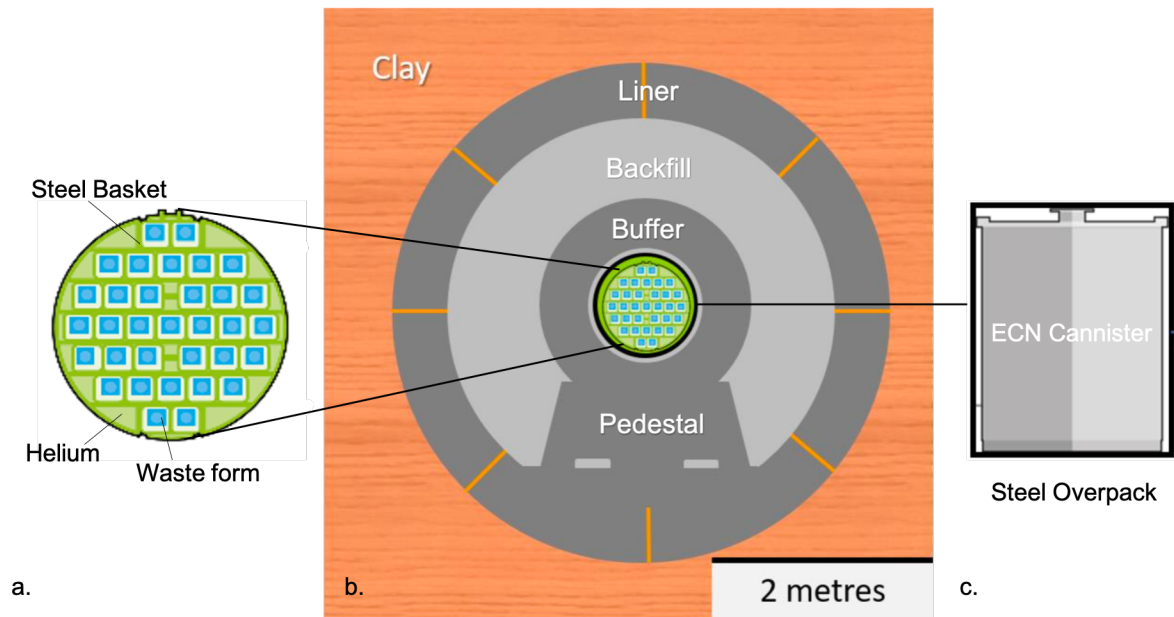


Figure 2.1: Scaled side view cross-section of the EBS

Starting with the innermost layer of the EBS, in Figure 2.1.a the ECN canister can be seen, which is housed in the steel overpack shown in 2.1.c. The blue squares are the waste elements (either LEU or HEU), which are surrounded by the dark green lines and represent a steel basket intended to hold the waste elements in place. The light green in between the steel and waste is helium gas. Within each waste element, the fuel plates housing the material are arranged in a way that can be seen in as top down view in Figure 2.2 below [1].

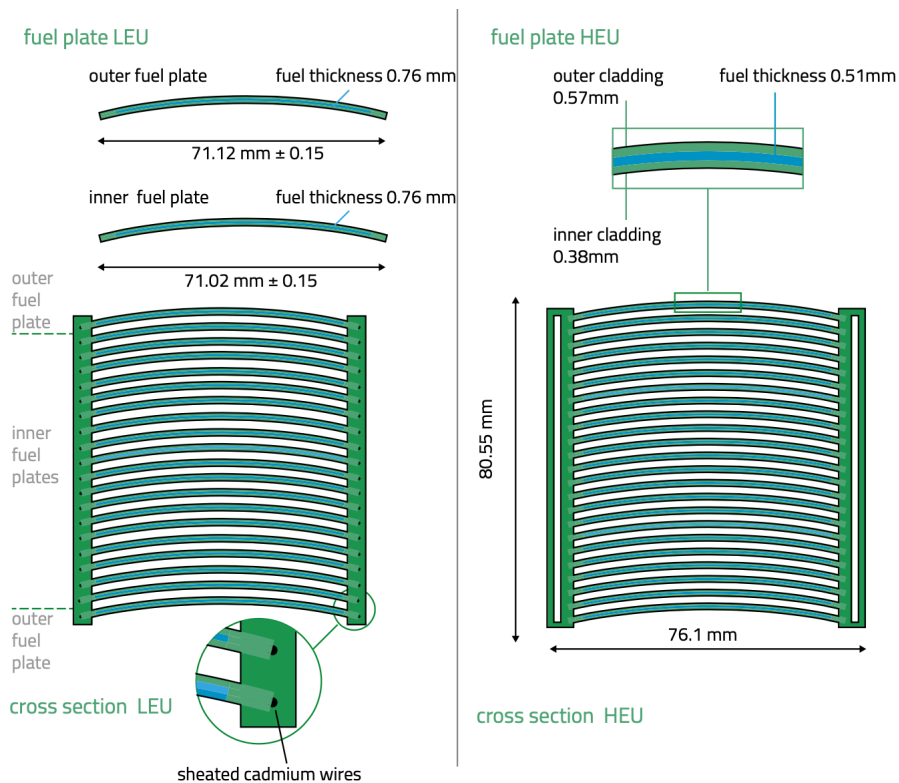


Figure 2.2: Schematic top view of the fuel plates for spent research reactor fuel [1]

The first two barriers separating the fuel elements, helium/cementitious filling and the steel basket from the outside environment are the ECN canister and the steel overpack and they can be seen in Figure 2.1.b. It is assumed that there is no transfer of material after closure of the ECN canister and that any breach of the container can be detected by measuring the helium content during storage. For disposal, the canister are envisaged to be placed in a carbon steel overpack which should prevent the transfer of fluids during the thermal phase where the spent fuel will emit heat due to the decay of the fission products inside the spent fuel.

After the overpack, the cementitious layers that make up most of the EBS begin. These start with the buffer, which is a concrete container with additional hardened concrete. The purpose of these cementitious layers is to provide a high pH environment (at least 10-13,5 pH) and low water permeability which is essential for minimizing the corrosion of the steel overpack [28]. The same cementitious mixture is also poured over the buffer to achieve sufficient shielding thickness and form the pedestal. For simplicity, it can be assumed that the same mortar recipe is used for the buffer, pedestal and the outermost layer- the liner. However, foamed concrete is chosen to serve as the backfill between the buffer and liner. The backfill provides sufficient heat dissipation from the waste to the clay, and the concrete liner is the first line of defence for the EBS as it makes direct contact with the clay.

Above are all the layers currently researched and intended for use in the underground repository [1]. As stated in the scope of the project, it is assumed that at some point all these barriers will fail and water will come into contact with the aluminium cladding of the waste element. Therefore, an additional barrier is proposed to prevent the corrosion of the aluminium cladding of the fuel elements, which can lead to pressure buildup and the creation of hazardous conditions. This additional layer must be located between the steel of the ECN canister and the aluminium of the fuel elements, which corresponds to the light green in 2.1.a. Due to the familiarity COVRA has with cement, a preference has been expressed to consider a cementitious material with corrosion limiting functionality.

It is clear that corrosion must be prevented, there are several avenues to achieve this; passivation by pH control, adsorption inhibitors and film-forming inhibitors [2]. First, the physical processes will be elaborated on, which give a clearer picture of the situation at the cement-aluminium interface.

2.2. Physical processes

The physical processes relevant to the waste container and the surrounding layers are described as follows. First, the ground water must penetrate through the layers surrounding the waste (1), after which contact with the aluminium cladding is realised. At this point, the water and the aluminium cladding will react and form hydrogen gas due to corrosion (2), leading to this hydrogen gas being displaced and transported again through all the layers (3). While all these processes take place, the nuclear waste must also be kept in a sub-critical state (5). The potential for heat generation due to the nuclear reactions is also present (4). A schematic is presented in Figure 2.3

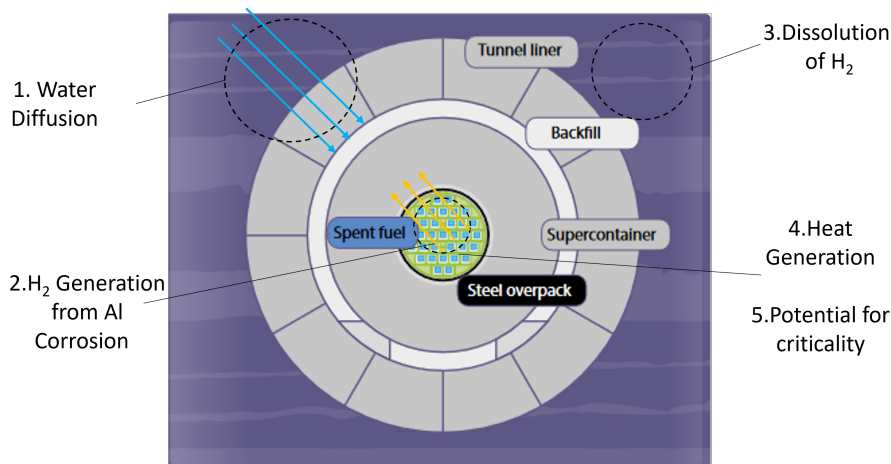


Figure 2.3: Summary of physical processes.

2.2.1. Water diffusion

The COVRA disposal plan for the spent research reactor fuel involves many cementitious components such as the backfill, concrete liner and the supercontainer buffer. These large amounts of hydrated cements are influential in determining the physical and chemical conditions of the system and its performance for the duration of the storage period [4].

It can be expected that the degradation of the EBS along with any changes that occur in the r-region will be driven by the differences in the chemical conditions between the structural cementitious materials and the groundwater infiltrating into this region. Thus, considering our aim to minimize the gas generation through water contamination of the fuel rods, investigating the diffusion of water into the system is an essential part in understanding the parameters involved with our project. The expected diffusion path of the water can be seen in Figure 2.4 below.

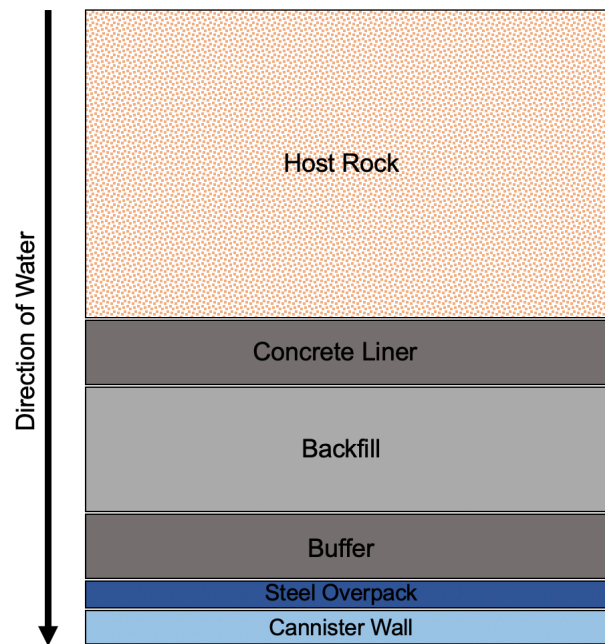


Figure 2.4: Diffusion path of water

Since the reference date for implementing the geological disposal facility in the Netherlands is more than 100 years from today, the exact location of the site, and therefore the exact properties of the host rock along with the pore water, is still unknown. However, the expected overall conditions of the clay can be constrained to a certain degree.

For instance, it can be assumed that the clay will have sufficiently low enough permeability such that pore water is effectively stagnant [1]. This means that the dominant process in which various species (water, hydrogen gas, minerals etc.) will move through the clay and the system is through diffusion driven by concentration gradients.

There are three hydraulic properties that depend on the clay host rock which in turn are related to the performance of the system. The hydraulic conductivity influences the time required for the resaturation of the repository, the mass transport to and from the disposal tunnels and the leaching of the species found in the backfill or the buffer. The porosity and permeability of the host rock affects the gas flow out of the near field and the possible formation of gas phases in the repository. Finally, the pore water composition can affect the chemical conditions of the surrounding area and thus the degradation rates of the cementitious barriers along with the corrosion rate of the metallic waste components [4].

Through modelling done by COVRA, the vertical permeability of the clay at a depth of 500 meters was found to be in between $6 \times 10^{-18} \text{ m}^2$ and $5 \times 10^{-19} \text{ m}^2$ [29]. During the experimental study, the permeability was found to be around $1 \times 10^{-19} \text{ m}^2$ [30]. These values support the assumption of stagnant pore waters and can be used to calculate the hydraulic conductivity with the following equation:

$$k = K(\mu/\rho g) \quad (2.1)$$

where k is permeability (m^2), K is hydraulic conductivity (m/s), μ is the dynamic viscosity of the fluid ($kg/(m \cdot s)$), ρ is the assumed constant density of the pore water ($1020 kg/m^3$) and g is the acceleration due to gravity ($9.81 m/s^2$). Since the main method of transport of species is expected to be through diffusion, the characteristics of the pore water significantly affect diffusion and its consequences in several ways. For instance, different composition of minerals could lead to changes in the concentration gradients between the EBS and the clay which then affect the diffusion rate. The presence of a reactive component could cause unwanted reactions which could damage the EBS, affecting its longevity and modify the diffusion rate. The pH of the groundwater could also induce a gradual lowering of the pH of the cement pore water. In fact, it is expected that a pH value below 10 could be reached in thousands to tens of thousands of years. Through this decrease, corrosion behaviour of the steel overpack and the aluminium cladding will be altered.

After testing three different scenarios, Behrends et al. reported that the pore water samples from the clay from Zeeland suggested a strong seawater signature. The computed composition of the pore water that is expected to be found in the clay near the system is listed in the Table 2.1 below [31].

Table 2.1: Modelled pore water composition for the seawater scenario [15]

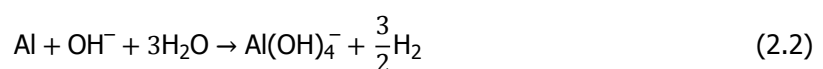
Components / Properties	Computed Values (mmol/kg water)
Al	3.30×10^{-5}
C	7.20
Ca	13.2
Cl	541
Fe	3.10×10^{-6}
K	9.80
Mg	56.1
Na	461
S	28.4
Si	0.30
pH	6.90
pe	-2.80

Although more representative conditions for the pore water composition of the Boom Clay and its hydraulic properties are not available yet, the characteristics described above still allow us to have an overview of the long-time evolutionary pathway of the disposal system [32]. This change that is the result of a continuous interaction between the Boom Clay pore waters and the cementitious materials will include the gradual evolution of the EBS from an unsaturated state to a saturated state and from aerobic (oxygen-present) to anaerobic (oxygen-free) conditions [4].

2.2.2. H_2 generation by the corrosion of aluminium

Because of its light weight and strength, aluminium is widely used for structural purposes. It is also one of the most abundant metals in the earth's crust. With an energy density of around 30 MJ/kg, Al has proven to be a good energy carrier [33]. It has a quite low standard redox potential ($\epsilon = -1.66$ V), making it an excellent reducing agent. This means that when Al comes in contact with water, it produces hydrogen gas, which causes internal stress, that can lead to not only mechanical damage to the cement matrix but also to the formation of a possibly explosive atmosphere. The H_2 gas is formed during the corrosion process in an alkaline or neutral environment. Heat, water vapor, and hydrogen gas are all produced by the Al- H_2O reaction.

There are multiple possible routes for the reaction of Al with H_2O , all of which are thermodynamically favourable. Under room temperature and alkaline conditions, the overall reaction is more favorable to produce $Al(OH)_4^-$, as depicted in Equation 2.2. This reaction is also highly exothermic (With $\Delta H = -413.3$ kJ mol $^{-1}$).



The overall reaction under alkaline conditions, is derived from water reduction (Equation 2.3), as the cathodic reaction balances the anodic aluminium dissolution. However, aluminium can also be

balanced by the oxygen reduction (Equation 2.4).



Lastly, the anodic dissolution of Al can be seen in Equation 2.5



Many metals, including aluminium, when in presence of oxygen, are protected from corrosion by a tightly adhering surface oxide film that prevents oxidizing agents from penetrating deeper layers. The thickness of the protective layer can range between 20 to 100 Å. When the metal comes into contact with oxygen, it forms such Al_2O_3 films. The oxygen influences the corrosion of Al, especially when the dissolved oxygen concentrations are high. As a result of corrosion processes on the aluminium surface, the total thickness of the protective layer increases, but the thickness of the inner layer remains constant. The scheme of the protective layer formation mechanism can be seen in Figure 2.5.

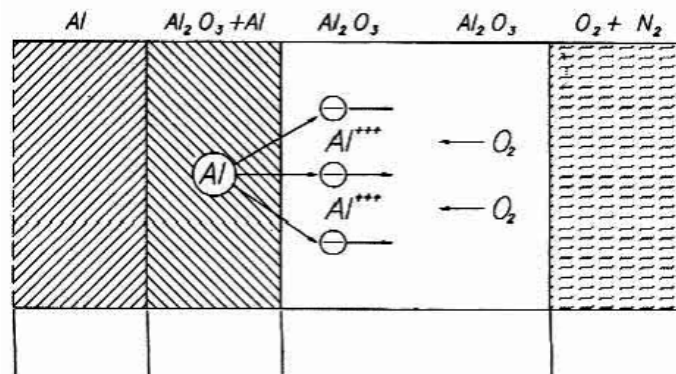
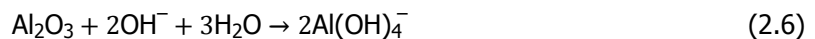


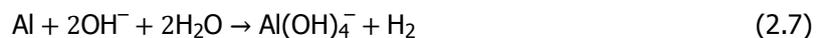
Figure 2.5: Al_2O_3 protective layer formation

Although the oxide films are good electrical insulators, they have a relatively high thermal conductivity [34]. Aluminium alloys can corrode in a variety of ways, so it is critical to understand the corrosion pathway in order to find an appropriate solution. Aluminium is generally stable in neutral water due to the passivated layer of Al_2O_3 , but it is soluble in both strongly acidic (below pH 4) and basic (above pH 9) aqueous solutions. It is unknown what the pH of the supercontainer (buffer) will be when pore water and aluminium come into contact. This moment could last thousands of years or more. However, due to the high alkaline nature of cements that surround the aluminium, it is expected to corrode. The corrosion potential begins during waste processing, when a cementitious fluid with a high pH is poured onto aluminium. Due to the rapid depletion of oxygen, a high rate of H_2 gas is produced during this process (anaerobic corrosion). This means that corrosion is an issue not only thousands of years later, but also during the pouring process.

The mechanism of Al corrosion is displayed in Figure 2.6. Due to the alkaline environment, as can be seen in Equation 2.6, the OH^- ions attack and dissolve the passivated layer and produces soluble hydroxy aluminate ions, which then expose the Al surface.



Then the Al metal surface gets further attacked by the OH^- ions and the water, which then leads to a formation in more soluble hydroxy aluminate ions and hydrogen gas, as shown in Equation 2.7. As the cement surrounding the aluminium hardens, the reaction becomes less active. This is because hydrogen bubbles are unable to form a porous layer around the aluminium.



The final stage of the Al corrosion is the reaction of the hydroxyl aluminate ions ($\text{Al}(\text{OH})_4^-$) with the surrounding cement. This then leads to the decrease of OH^- ions, and as the cement hardens,

the hydroxyl aluminate ions decompose into aluminium hydroxide ($\text{Al}(\text{OH})_3$) phase around the metal surface.

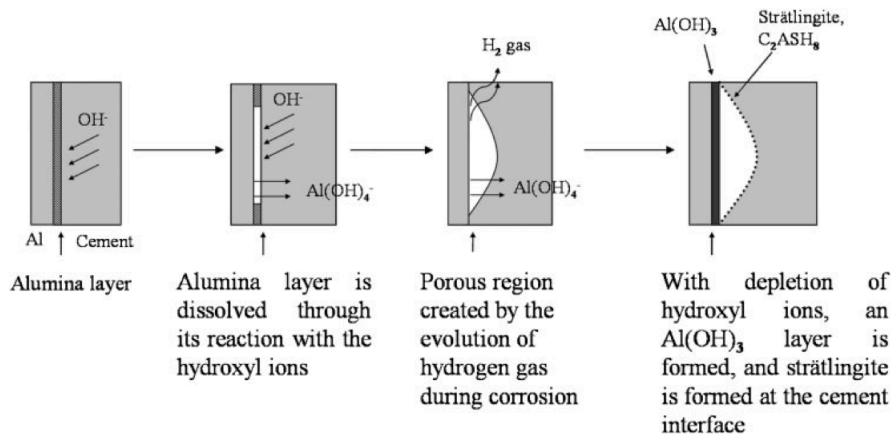


Figure 2.6: Al corrosion in cements [3]

Furthermore, depending on the surrounding pH, different types of Al corrosion can take place. The diagram in Figure 2.7 depicts the total corrosion behavior of aluminium. The two most relevant regions/corrosion types for this study are uniform corrosion and galvanic corrosion due to the cementitious repository conditions. The uniform corrosion happens when there is a continuous shifting of anode and cathode regions which then come in contact with the electrolyte and attack the Al surface. Such corrosion can be limited or even prevented by the use of chemical inhibitors, which are explained further in Section 3. The galvanic corrosion, on the other hand, can occur when the Al comes in contact with seawater. When Al comes into contact with other metals, the salt water acts as an electrolyte, resulting in a highly conductive medium. In this case, the Al corrodes because it serves as an anode. When comparing the two corrosion types, the galvanic corrosion can occur much quicker than uniform corrosion.

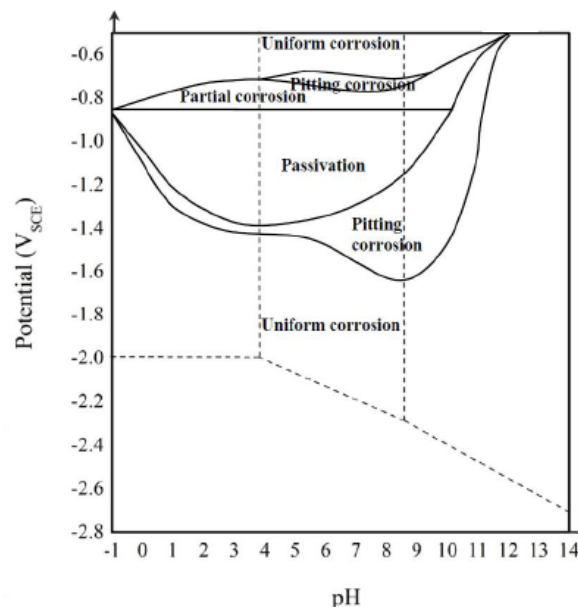
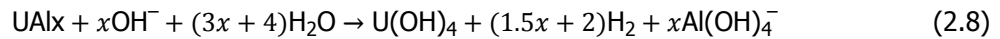


Figure 2.7: Corrosion types that occur at different pH levels [4]

The rate of corrosion of aluminium cladding can be obtained by measuring the H_2 gas production or the formation of an oxide layer. Previous research has revealed that the initial corrosion rates of

the Al cladding (composed of 99.5% Al and 0.5% AlMg) in clay or brine solutions are quite high (over 0.1 mm per year). This is owing to the cladding's impurities, which contain a high concentration of oxidants and anions [4]. This means that after a few years, the cladding deteriorates.

Apart from the corrosion of the Al cladding, the uranium-aluminium (UALx) matrix present in the fuel, must also be addressed when determining the degradation of spent fuel. It has been observed that the corrosion rate of unirradiated UALx at 25°C varies between 1422 and 1524 μm per year at pH 11 and anoxic conditions [4]. Equation 2.8 shows corrosion reaction for such fuel cells in such conditions.



For the fuel containing a significant proportion of the alloy (up to 50 vol%), the corrosion behavior has been proven in multiple studies to be comparable to that of the cladding [4]. The fuel matrix has therefore been calculated to have a limited lifetime until it fully corrodes in 10 years [4]. As the aim for this study is to maintain the lifetime of 100,000 years, inhibition techniques for such aluminium claddings are required.

2.2.3. Dissolution of H₂ into pore waters

During the containment of the spent research reactor fuel, gas will be generated by several mechanisms. Additionally in the processing of waste with highly alkaline cementitious fluid, gas can also be generated due to the depletion of oxygen. After closure of the repository, conditions will become anaerobic, due to oxygen being consumed by initial oxidation. Hereafter, the main gas generation comes from the anaerobic corrosion of metals in the canister. This causes a local pressure build up, which in turn causes a pressure gradient towards the surrounding host rock. Water will fill pores of the surrounding material, leading to some additional transport methods and also a way to partially capture the gas. Depending on the material gas transport through the following processes can be relevant [35].

1. **Gas generation processes:** The rate and amount of gas generation effect the following gas transport due to pressure. The generation is dependant on the species concentration (O₂ and H₂O) needed for corrosion, temperature and pH. When more gas is produced a higher local pressure is build-up. This generation depends on available material and conditions: such as water and oxygen for corrosion, temperature and pH.
2. **Gas consuming reactions:** Adding barriers which can react with the produced gas and through gas sorption reduce the net gas molecules, therefore reducing the pressure.
3. **Dissolution of gaseous molecules:** Present water can dissolve gas to its solubility limits at the situ temperature and pressure. If the solubility is not met, no gas phase can effectively form.
4. **Advection and diffusion in solution:** Advection through water can transport gasses upwards. If no flow is seen, diffusion is the main contribution to transport.
5. **Visco-capillary two-phase flow:** In porous material, when gas displaces water, two phase flow condition can occur, meaning that the gas has overcome the viscous and capillary effects. Whether this is an abundant or totally lacking phenomena, is dependant on the porous material.
6. **Pathway dilation:** In deformable material, two phase visco-capillary flow is difficult, there in gas transport is mainly through pathway dilation. Then displacement of the liquid phase is limited.
7. **Gas fracturing:** In highly deformable material, gas generation can cause pressure build up, which when released creates high local permeability. Depending on the self sealing capability of the material, the permeability is again reduced after sealing.

Considering all these processes, two different sets can be made: one for clay and one for concrete. For concrete it is expected to be harder and relative to clay, quite porous. In the porous holes water will be stored and gas can dissolve into it. The following ways for diffusion will be relevant: 1, 2, 3, 5, and 6. The hydrogen can now be diffused by either the composition gradient or the pressure gradient, referred to as diffusive and bulk migration, respectively [36].

The diffusive migration is driven by a compositional gradient in the stagnant pore water. This migration is dependent on a material specific diffusion coefficient and can change dependant on temperature and the maximum concentration which is governed by both the in-situ temperature, pressure and solvent. The process can be expressed by the Equation 2.9

$$\frac{\delta C}{\delta t} = \frac{\delta}{\delta x} \left[D \frac{\delta C}{\delta x} \right] \quad (2.9)$$

D being the diffusion coefficient in m^2/s , C being the concentration in kg/m^3 and lastly x being the distance in m . Calculations on the extent of diffusion x therefore requires both an approximation of the D and C . Measurements on inter-diffusion of hydrogen and nitrogen in vacuum-dried ordinary Portland Cement mortars showed the following diffusion coefficients with a respective water-cement ratio [36]:

Table 2.2: Diffusion coefficients in water cement mixtures

Diffusion coefficient (m ² /s)	Water-cement ratio
4.8 x 10 ⁻⁷	0.65
1.9 x 10 ⁻⁷	0.50

Later variance to the pressure showed a decrease in diffusion coefficients with increased pressure, this is indicative of Knudsen flow in capillaries with relatively small width to length ratio's [36]. This means that the molecules hit the sides of the walls more often while flowing, halting the diffusion rate. This behaviour is expected in all similarly structured cements.

2.2.4. Criticality

A potential problem for nuclear waste storage is criticality. Criticality means that more neutrons are produced than consumed during the nuclear chain reactions. While a typical nuclear reactor operates at a steady state, for nuclear waste storage and disposal the system must be subcritical. The change of the number of neutrons between two subsequent time intervals is called k_{eff} .

1. $k_{eff} > 1$ Supercritical state
2. $k_{eff} = 1$ Critical state
3. $k_{eff} < 1$ Subcritical state

In the following text the neutron transport equation will be derived. Then the k_{eff} multiplication factor will be introduced and the way in which it can be calculated will be outlined.

The number of neutrons about a position \mathbf{r} in a region of space R with energies between $E1$ and $E2$, traveling in the direction $\boldsymbol{\Omega}$ and with an angle $d\boldsymbol{\Omega}$ equals:

$$n(t) = \int_{E1}^{E2} \int_{4\pi} \int_R N(\mathbf{r}, \boldsymbol{\Omega}, E, t) dV d\boldsymbol{\Omega} dE \quad (2.10)$$

where $N(\mathbf{r}, \boldsymbol{\Omega}, E, t)$ is the number density of neutrons in the 6-D phase space defined by $\mathbf{r}, \boldsymbol{\Omega}, E$, with units of $cm^{-3} Mev^{-1}$.

The number of neutrons that pass through a surface dS in the direction of $\boldsymbol{\Omega}$ is in a time period dt equals:

$$N(\mathbf{r}, \boldsymbol{\Omega}, E, t) dV d\boldsymbol{\Omega} dE = (\boldsymbol{\Omega} \cdot \mathbf{n}) v N(\mathbf{r}, \boldsymbol{\Omega}, E, t) dS d\boldsymbol{\Omega} dE dt \quad (2.11)$$

where v the neutron speed and \mathbf{n} the unit vector perpendicular to surface S . The angular flux ψ equals:

$$\psi(\mathbf{r}, \boldsymbol{\Omega}, E, t) = v N(\mathbf{r}, \boldsymbol{\Omega}, E, t) \quad (2.12)$$

The total net number of neutrons hat leak through a surface S is defined as:

$$J = \int_0^\infty \int_{4\pi} \int_S (\boldsymbol{\Omega} \cdot \mathbf{n}) \psi(\mathbf{r}, \boldsymbol{\Omega}, E, t) dS d\Omega dE \quad (2.13)$$

By using the divergence theorem which states that for a vector field \mathbf{F} the following relation holds:

$$\int \int (\mathbf{F} \cdot \mathbf{n}) dS = \int \int \int (\nabla \cdot \mathbf{F}) dV \quad (2.14)$$

By applying this theorem to the total flux J the following relationship is obtained:

$$J = \int_0^\infty \int_{4\pi} \int_V \nabla \cdot \boldsymbol{\Omega} \psi(\mathbf{r}, \boldsymbol{\Omega}, E, t) dV d\Omega dE = \int_0^\infty \int_{4\pi} \int_V \boldsymbol{\Omega} \cdot \nabla \psi(\mathbf{r}, \boldsymbol{\Omega}, E, t) dV d\Omega dE \quad (2.15)$$

The neutron balance for a volume dV in R can be written as follows:

$$\frac{1}{v} \frac{\partial \psi(\mathbf{r}, \boldsymbol{\Omega}, E, t)}{\partial t} d\Omega dE dV = \text{Rate of Gain} - \text{Rate of Loss} \quad (2.16)$$

The neutron losses can be caused by either collisions or leakage. The leakage term can be calculated by the surface integral of the flux as it was demonstrated in Equation 2.16. When neutrons collide with a nucleus they can either scatter (elastically or inelastically), initiate fission or be captured. Each fission event produces approximately 200 Mev. The probability that a neutron hits a surface dS and react with another nucleus is:

$$dP = \sigma n_s / S \quad (2.17)$$

where σ is the area of a nucleus and n_s the number of nuclei at the surface A . However,

$$n = NSd\omega \quad (2.18)$$

where N is the nucleus density and $d\omega$ a direction differential length towards $\boldsymbol{\Omega}$. Consequently the probability is now equal to:

$$dp = \sigma(E)Nd\omega = \Sigma_t(E)d\omega \quad (2.19)$$

where Σ_t is the material cross section (cm^{-1}) and E the energy of the neutron. For a mixture of nuclei the total cross section is additive. Also each event (absorption, fission etc) can have its own cross section, which when added would total Σ_t .

From 2.19 the rate of neutron-neutron collisions that happen in a the 6-D phase space $dVd\Omega dE$ equals:

$$r_c = \frac{\Sigma_t d\omega N(\mathbf{r}, \boldsymbol{\Omega}, E, t) dV d\Omega dE}{dt} = \Sigma_t v N(\mathbf{r}, \boldsymbol{\Omega}, E, t) dV d\Omega dE = \Sigma_t \psi(\mathbf{r}, \boldsymbol{\Omega}, E, t) dV d\Omega dE \quad (2.20)$$

Consequently,

$$\text{Rate of Loss} = [\Sigma_t \psi(\mathbf{r}, \boldsymbol{\Omega}, E, t) + \boldsymbol{\Omega} \cdot \nabla \psi(\mathbf{r}, \boldsymbol{\Omega}, E, t)] dV d\Omega dE \quad (2.21)$$

The rate of gain in neutrons for in the volume $dVdEd\Omega$ can be caused by either neutron scattering or from fission. During scattering, neutrons from a different direction $\boldsymbol{\Omega}'$ and energy E' change to a direction $\boldsymbol{\Omega}$ and energy E . The new direction depends only on the angle $\boldsymbol{\Omega}'\boldsymbol{\Omega}$. Consequently, neutrons travel in a cone after scattering as seen in Figure 2.8.

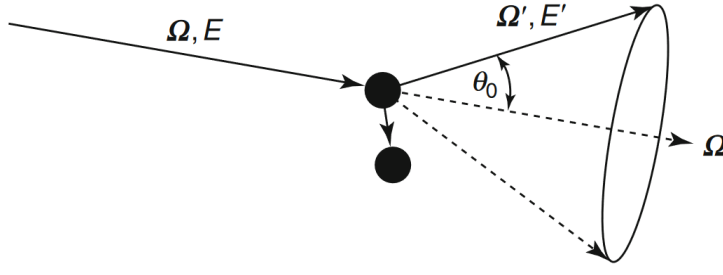


Figure 2.8: Neutrons scattering from direction Ω and energy E to direction Ω' and energy E' [5].

If the probability that a neutron traveling a distance $d\omega$ is scattered in a direction Ω and energy E is defined as follows:

$$dP = \Sigma_s(E')p(\Omega', \Omega, E' \rightarrow E) d\omega d\Omega dE \quad (2.22)$$

where p is the probability distribution. The macroscopic differential scattering cross section is defined as:

$$\Sigma_s(\Omega', \Omega, E' \rightarrow E) = \Sigma_s(E')p(\Omega', \Omega, E' \rightarrow E) \quad (2.23)$$

According to equations 2.22, 2.23 the rate of gain due to scattering to energy E and direction Ω can be defined as:

$$r_s = \frac{\int_0^\infty \int_{4\pi} [N(\mathbf{r}, \Omega', E', t) \Sigma_s(\Omega', \Omega, E' \rightarrow E) d\Omega' dE'] d\omega d\Omega dE dV}{dt} \quad (2.24)$$

which also equals,

$$r_s = \int_0^\infty \int_{4\pi} \Sigma_s(\Omega', \Omega, E' \rightarrow E) \psi(\mathbf{r}, \Omega', E', t) d\Omega' dE' d\Omega dE dV \quad (2.25)$$

If a neutron with energy E' collides with matter the number of neutrons that are emitted after a collision is $\nu(E')$. The probability that one of the emitted neutrons has energy of E is defined as:

$$dP = \chi(E)dE \quad (2.26)$$

The gain of neutrons due to fission equals in $dVdEd\Omega$ is:

$$r_f = \int_0^\infty \int_{4\pi} \frac{\chi(E)}{4\pi} \Sigma_f(E') \nu(E) \psi(\mathbf{r}, \Omega', E', t) d\Omega' dE' d\Omega dE dV \quad (2.27)$$

By combining the above equations the neutron transport equation can be defined:

$$\frac{1}{v} \frac{\partial \psi(\mathbf{r}, \Omega, E, t)}{\partial t} = \int_0^\infty \int_{4\pi} \frac{\chi(E)}{4\pi} \Sigma_f(E') \nu(E) \psi(\mathbf{r}, \Omega', E', t) + \Sigma_s(\Omega', \Omega, E' \rightarrow E) \psi(\mathbf{r}, \Omega', E', t) d\Omega' dE' - \Sigma_t \psi(\mathbf{r}, \Omega, E, t) - \Omega \cdot \nabla \psi(\mathbf{r}, \Omega, E, t) \quad (2.28)$$

After having defined the neutron transport equation it is now possible to define the k_{eff} multiplication factor. The first step is dividing the fission term in equation 2.28 by k_{eff} for a steady state.

$$\int_0^\infty \int_{4\pi} \frac{\chi(E)}{k_{eff} 4\pi} \Sigma_f(E') \nu(E) \psi(\mathbf{r}, \Omega', E', t) + \Sigma_s(\Omega', \Omega, E' \rightarrow E) \psi(\mathbf{r}, \Omega', E', t) d\Omega' dE' = \Sigma_t \psi(\mathbf{r}, \Omega, E, t) + \Omega \cdot \nabla \psi(\mathbf{r}, \Omega, E, t) \quad (2.29)$$

Then k_{eff} is defined as the largest possible value for which a non zero solution for ψ exists. This means that if $k_{eff} < 1$ then more neutrons leak out than are produced inside the boundaries of the geometry. The opposite is true for $k_{eff} > 1$ [5].

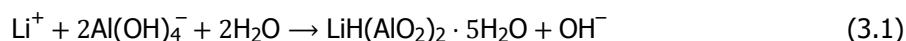
3

Product concepts and selection

3.1. Preexisting Solution: Lithium Nitrate

One solution that has already been found in multiple studies is the use of lithium nitrate to form an insoluble layer. The problem with this solution is the use of lithium, as this element is extensively used in batteries. Therefore a new solution has to be found. In this chapter, it will be explained why and how lithium nitrate can inhibit the corrosion of aluminium. Then, this information can be used as motivation for a new solution.

It is reported that when lithium-nitrate is added to cement, the Li-ions can act as a corrosion inhibitor for Al in alkaline environments. The lithium ions react with aluminium to form a thin layer of 5–10 μm of lithium aluminate ($\text{LiH}(\text{AlO}_2)_2 \cdot 5\text{H}_2\text{O}$ or Li–Al) [37–40]. This layer is significantly less soluble in alkaline environments than the Al_2O_3 layer, allowing it to inhibit corrosion. Matsuo et al. added 1.5 wt% of LiNO_3 to their cement mixture, and found that this reduced the corrosion rate to less than $10^{-5}\text{m}/1000\text{hr}$ [39].



Matsuo et al. also looked at the use of other alkali metals as corrosion inhibitor, namely sodium and potassium [38]. They compared their results to the use of lithium. They found that only lithium is able to form an insoluble layer in alkaline conditions. They suggest that this is the result of a difference in binding strength, which originates from the ratio of ionic radii of the alkali metals and Al. They described two conditions that should be fulfilled to inhibit the corrosion successfully:

1. It should form an insoluble salt by the reaction with aluminate ions in the alkaline solution; i.e. preservation film formed on aluminium surface must be insoluble.
2. It should dissolve readily and greatly in alkaline solutions (the concentration should be 0.1 M, because the pH of cement paste is about 13, i.e. the concentration of OH^- , is 0.1 M, and it is easily anticipated that the formation reaction of the preservation film will not succeed with a lower concentration of the corrosion inhibitor than that of OH^-).

They also mentioned that for example Mg^{2+} and Ca^{2+} do fulfill the first, but not the second condition. Only alkali metals fulfill this condition [38].

3.2. Product concepts

Two approaches to corrosion inhibition (H_2 gas formation) are discussed in this chapter. The first method involves altering the environment so that the passivating aluminium oxide layer no longer dissolves. This translates into studies involving the use of low pH cements. The other option is to form another passivating layer, which is discussed further in the Section 3.2.2.

3.2.1. Low pH Cements

The previous mentioned solution with lithium nitrate, and the experiments with the other alkali metals sodium and potassium, were both based on the use of cement. Cementitious media have a high potential for a uniform coverage around the aluminium cladding and solidify at room temperature; For this reason, their use is highly preferred as their application is very simple. However, a blended cement between Portland and Blast Furnace slag (CEM III/B) that's typically used in COVRA has high pH which causes the aluminium embedded in it to corrode. Therefore, it is worthwhile to investigate the possibility of lowering the pH of the pore water in these cementitious media into the passivation range ($4 < \text{pH} < 9$) to inhibit hydrogen generation.

According to Coumes et al., cements with pore water pH in the passivation range include magnesium phosphate cements, calcium phosphate (apatite and brushite) cements, sorel cements and plaster [3]. Plaster cements are not resistant to water making them unsuitable for our purpose. Sorel cement is suggested as a possible solution for lowering the pH level to 8/10, which could result in the formation of protective Al_2O_3 and thus significantly reduced corrosion rates [6]. These type of cements are made by combining magnesium oxide and concentrated magnesium chloride. Water resistance can be increased by adding additives such as phosphates, borax, and calcium sulfate-silicate mixtures. This is accomplished by converting hydroxychloride hydrates to insoluble carbonates [41]. However, chloride salts can cause corrosion, and because the study's goal was to avoid a chlorine-rich environment, this alternative will not be pursued further. As for apatitic cements while having a near neutral pH, they exhibit very high porosity (more than 50 % of the volume), and high reactant cost due to the elevated temperatures needed for their manufacture [3].

Table 3.1: H_2 gas generation comparison between cements with pore water pH inside the passivation range compared to Portland cement.

Cement Type	pH	H_2 Gas Generation ($\text{L}/\text{m}^2\text{y}$)
Portland Cement	13	4700
Magnesium Phosphate Cements	5	0.026
Calcium Phosphate Cement (Brushite)	7	7.000
Sorel Cement	8/10	-
Plaster	7	-

The choice of cement is based on a multitude of characteristics, concerning the initial application of the cement in the fuel container and the functionality in its hardened state. In the initial flowing state, a wide coverage of the aluminium cladding is necessary, leading to a minimum viscosity of the cement. Additionally, the solubility of the functional corrosion inhibitor is important. Firstly in the hardened state, the situational pH of the cement and pore water has an effect on the corrosion, either an inhibiting or promoting effect. Secondly, when it pertains to gas and liquid transport, an appropriate diffusion coefficient must be met. Therefore, in the case of hydrogen generation the gas has to be transported out and in the case of water, has to be limited in the permeability into the canister. The following options for cement were explored.

Magnesium phosphate cements

Magnesium phosphate cements (MPCs) are a class of cements that are formed by an acid-base reaction between a soluble acid such as ammonium or potassium oxide and magnesium oxide in the presence of water.



The resulting salt from this reaction has cementitious properties [6]. The main advantages of this material relevant to our application include: Neutral pH, high strength, high binding strength with rock and no shrinkage during hydration, low setting temperature.

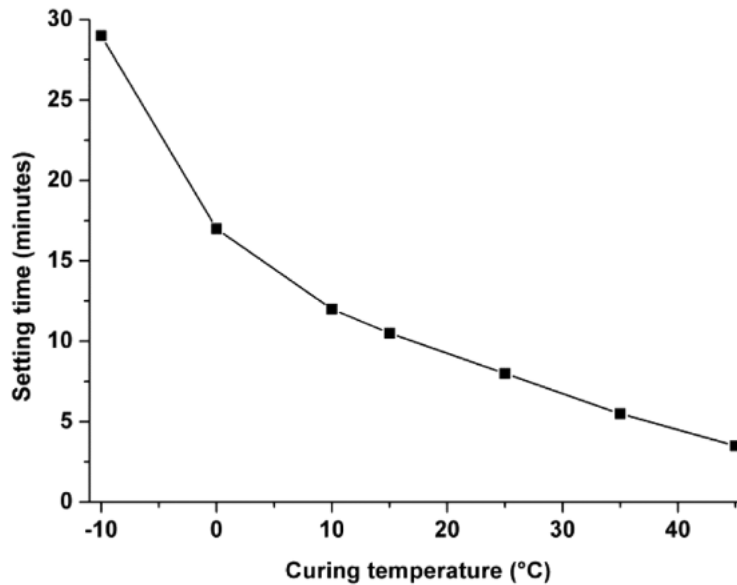
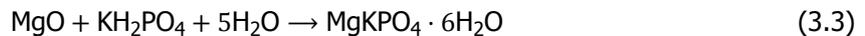


Figure 3.1: Setting time with respect to temperature[6].

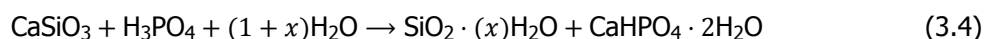
These types of cements exhibit a very fast setting time. To mitigate that, retardants that contain boron are used [42]. In our case the extra cost of these is not a negative because boron is also a known neutron absorber. This means that the potential for criticality is reduced and thus allowing more rods to be placed in a canister. Finally, during the setting process of MPCs a significant amount of heat is generated. However the use of KH_2PO_4 can mitigate those problems. By using this acid instead the following cementitious salt is formed (3.3).



Cements using the above acid are called MKPC cements. Finally, these types of acid base phosphate cements are already being used for road quick repairs of roads [6]. This means that it is not necessary to develop a completely new process in order to deploy this technology.

Calcium phosphate cements (brushite)

Calcium phosphate cements (CPC) with a brushite crystal structure are produced by the following reaction.



Since they are also acidic cements such as MPC they also exhibit low pH mixtures. More specifically, during the setting process the pH goes from 1 and stabilises at a value around 6. Another similarity between these two cements is their need for retardation due to heat generation. Boric acid can also be used in this case as well. Their setting time can range from 8-22 minutes at room temperature. Moreover, hydrated CaHPO_4 has a pK_{sp} value of 6.9, making it slightly soluble in water. This could potentially cause leaching, especially in a very large time horizon as the one for our purposes. These cements are already widely used as bone replacement, so they are already available for purchase [3].

3.2.2. Conversion coatings

Conversion coatings are coatings that are used as with the main purpose to inhibit corrosion of all sorts of metals. The most precise definition is a process which turns the metal oxide layer (e.g. Al_2O_3) into a coating with different properties with incorporation of the metal cations. [43, 44]

In Table 3.2, different conversion coating types are displayed with some of their characteristics. A more detailed exploration on the different conversion coatings listed below can be found in Appendix A.

Table 3.2: Different types of conversion coatings and their characteristics

Coating type	Formula	Inhibiting efficiency	Toxicity	Availability	Ref.
Chromate hydroxide	CrOOH	Chromate coatings display excellent corrosion inhibition due to their low equilibrium pH of 6.57	Chromates are highly toxic. They are carcinogenic, mutagenic and teratogenic	Chromium is the 21st most abundant element in Earth's crust, thus quite available.	[14]
Cerium hydroxide	Ce(OH) ₃	Cerium hydroxides have a comparable corrosion inhibition efficiency to chromates	Cerium is often named as a replacement of the toxic chromate coatings, as its toxicity is very low to negligible	Despite being a rare-earth metal, cerium is the 25th most abundant element in Earth's crust, and thus not rare at all	[45–48]
Zinc Phosphate	Zn(HPO ₄) ₂	The inhibiting efficiency of phosphates is less than cerium- and chromate-coatings	Phosphates are food additives, so in low levels they aren't toxic	Phosphates are intensively used in fertilizers and their occurrence is limited.	[43, 44]
Aluminium molybdate	Al ₂ (MoO ₄) ₃	Aluminium molybdate shows comparable inhibiting efficiency to chromate coatings	Molybdenum is also compared to chromates, as their mechanism seems to be comparable but their toxicity is way less	Molybdenum is the 58th most abundant element in the Earth's crust, making it relatively rare.	[49, 50]

The application methods of all of these coatings are quite comparable. The aluminium surface would have to be submerged into a number of different solutions to rinse and clean the surface, and to form the coating. Dipping the fuel assemblies into water would cause dangerous situations. This is due to the radiolysis of water which is the decomposition of water into several compounds such as radicals, ions and hydrogen gas by alpha-radiation. The amount of hydrogen produced could cause dangerous work environments for the operators applying the coatings [51].

Some of the coatings could also be applied by spray coating. The problem with this would be to achieve a high surface coverage, as it would be hard to spray between the aluminium plates [52].

3.3. Product selection

To make a final selection from the above options, a Pugh matrix was used to consider the criteria and come to a final conclusion. A Pugh matrix is a criteria-based decision matrix, which is used to select the best option from multiple potential options. The potential solutions are compared to an already existing solution. A scale is chosen which indicates if a potential solution performs better or worse at that specific criterion [53].

Different criteria were chosen and assigned a weight between 1-5. Portland Cement(PC) with added LiNO₃ was taken as the standard, from there MPC, CPC and PC with different conversion coatings were considered and rated on how they deviate from this standard on a scale between -2 and 2, with -2 being poor and 2 being good. Corrosion protection is obviously given the highest importance. LiNO₃ coatings offer the highest corrosion protection. When combined with MPC cement the generated gas was below the detection limit of the measuring device (10⁻⁴ L/m²s) [3]. Phosphate cements had much better performance than plain Portland cements but not as good as that of LiNO₃ coatings.

The safety of application is also rated with the highest weight. As far as nuclear waste are concerned no compromises on safety can be made. There is not much margin for flexibility in the application process due to the existing facilities. It would be difficult and dangerous to move the fuel assembly. Consequently, putting it in a bath, as required for conversion coatings, is not an advantageous proposition. For this reason the application of conversion coatings is problematic. On the other hand filling the canister with a liquid that solidifies on site is both easier and safer. The same reasoning applies for the ease of application as well, which was however weighted slightly lower than safety.

After these criteria, the cost and durability follow with a weight of 3. The cost is quite important, as the main problem with the use of lithium nitrate was the price. The price LiNO₃ has been found to range between 50 to 200 \$ [54]. Durability is also significant, as the product needs to be reliable for long time periods. Due to the intrinsic porosity, CPC shows slightly higher results than the rest [55].

Toxicity could potentially be dangerous if the product dissolves in the ground waters. However, it is assumed that this chance is quite low, which explains the relatively low weight of 2. Only conversion coatings use toxic compounds like chromate but as other alternatives have been introduced this factor is not very important. The maximum contaminant level for Chromium in drinking water is 0.1 mg/L [56].

The resource availability also was rated with a weight of 2. This is because of the fact that not large volumes of material are required compared to other industry sectors. Lithium is the only material included in our selection that is anticipated to be in short supply in the future.

The reason CPC are rated slightly lower on safety and corrosion protection than MPC cements is their initial very low pH of 1, which is below the passivation range of aluminum. This causes gas generation during the application and setting processes.

Table 3.3: Pugh Matrix

Criteria	Weight	PC(+LiNO ₃)	MPC	CPC	PC+Conversion coatings
Ease of Application	4	0	0	0	-2
Safety of Application	5	0	0	-1	-1
Corrosion Protection	5	0	-1	-2	1
Toxicity	2	0	0	0	0
Cost	3	0	2	1	1
Durability	3	0	0	1	0
Resource Availability	2	0	1	2	1
Total		0	3	-7	-3

When analysing the Pugh matrix, it can be seen that the conversion coatings score low, mainly due to the difficulty of application and danger they pose to the staff handling the waste. Therefore, the choice was made to focus only on the different options of cements, since they don't present these problems. Here MPC was identified as our best option of the two cements, mainly due to its availability and low cost.

4

Concept stage

4.1. Market Analysis

4.1.1. Quantity of product required

The amount of research reactor waste that needs to be disposed in 2130 according to the OPERA Safety Case is 104 m^3 [1]. This is the volume of the total amount of ECN canisters. These canisters have a height of 1.236 m and a diameter of 0.73 m [1], meaning that they have a volume of 0.517 m^3 . This means that ≈ 201 canisters need to be disposed. After the amount of canisters that is needed is known, the next step is to find how much of the volume of those canisters needs to be filled with the product. Assuming 33 fuel assemblies per canister, the empty volume fraction can be calculated. It is found to be 52 % [26]. The ECN-canisters that are used, have an inner diameter of 0.74 m and an inner height of 0.94 m [1]. The volume is thus $\approx 0.404 \text{ m}^3$. Using the empty volume fraction of 52 %, which means that $\approx 0.21 \text{ m}^3$ needs to be filled with the product.

4.1.2. Competitor activities

It is internationally agreed upon the fact that Al-containing nuclear fuel and Al-cladded fuel is not suitable for direct disposal, due to the anticipated hazards that corrosion may bring [57]. The R1 reactor in Sweden is an example of this. The fuel that was used in this reactor contained a cladding of aluminium. After the closure of this reactor in 1970, the waste was temporarily stored. Over time, it was noticed that gas was leaking from the storage containers. Further investigation revealed that water was leaking inside, causing corrosion [57].

Another example is the storage of aluminium cladded fuel at the Savannah River Site in the United States. Parts of this waste showed severe corrosion after only 7 years of storage, while at other storage sites sometimes little or no corrosion occurred. As a result, the Department of Energy (DOE) initiated a major investigation into corrosion damage to more than 1700 Al-clad fuel elements. This revealed that in 7 percent of cases, the corrosion was so severe that it had penetrated the entire cladding [57].

However, while corrosion is known to cause problems for long-term geologic storage, it is difficult to identify what these countries plan to do to inhibit corrosion. The paper by Bennett et al. mentions a few approaches that are taken [57]. For example, the Radioactive Waste Management Strategic Plan investigates multiple different routes. They investigate decladding of the fuel assemblies in dry and wet conditions. HALOX is a dry decladding technique, which reacts chlorine gas at high temperatures to convert the materials into volatile components. In wet decladding they dissolve the fuel plates in 1M sodium hydroxide [57]. Thus, these techniques take a very different approach from this report. They aim to remove the cladding, instead of protecting it from corrosion.

4.1.3. Collaborations

The first step in collaborative efforts is to share acquired knowledge internationally. This could significantly accelerate research and final disposal. This is already being done by COVRA, at European but also at global level [25]. Countries like Finland, Sweden are the first that will actually start building the repositories, so good tracking of their progress could be of value when it comes to building the repositories. However, these countries only will dispose nuclear power fuel, which is composed of UO_2

and a Zircaloy cladding, which are both almost nonreactive towards water [1]. In literature, nothing can be found on the disposal of spent research reactor fuel in these countries, which shows that COVRA is currently the leading party in this area.

Belgium is also researching the geological disposal of their nuclear waste. COVRA is already collaborating closely with the Belgian agency for disposal of nuclear waste (ONDRAF/NIRAS). Since the host rock and many elements of the GDF are very similar for both countries, close cooperation with Belgium is hugely beneficial for efficiency of the research, and to avoid duplication of work [1].

In addition to all countries that plan to build their own repositories, there are also the countries with smaller amounts of nuclear waste. For these countries the construction of a national repository is a real challenge. The European Repository Development Organisation (ERDO) is there to support these countries, and explores the opportunities to build shared disposal facility [25]. Another solution to this problem that might also be considered is to take over the waste from these countries in return for payment, for example. Since the amounts of waste produced by these countries are not significantly high, this could be efficient for both parties [25]. Another option that could potentially be a collaborative opportunity is fuel exchange, proposed in the paper by Bennett [57]. In this case, the waste could be exchanged between countries if that would be beneficial for both countries. [57] In this scenario, waste could be exchanged with other countries for waste that contains Al-U fuel or Al-cladding. This would expand the market for the product.

4.2. Product Design

4.2.1. MKPC Cement

As determined above, MKPC is a promising substitute for Portland cement, which creates a high pH environment in which Al corrodes easily. The potential of using MKPC's in radioactive waste encapsulation technologies inhibiting corrosion has been demonstrated by numerous studies. Gardener et al. [12] used a mixture of MKPC cement and other additives that more than halved the amount of gas generated by uranium corrosion compared with OPC cement. The period of the study reached 700 days [12]. McCague et al. also examined the corrosion behaviour of aluminium in different cement mixtures. Aluminium embedded in an MPC mixture exhibited a negligible corrosion rate compared to OPC which reached a corrosion rate of 1.5mm/yr. Even though the cement reached a pH of 9.6, which is above the passivation range of aluminium, the corrosion rate remained negligible [17].

Other important aspects regarding cement properties are hydration behaviour and its products, which are directly related to the molar ratio between the MgO and KH_2PO_4 , the activity of the water and the overall pH. The possible hydration products at constant reaction conditions at 25 °C and 0.1 MPa are reported and displayed in Table 4.1 [16]. Zhang et al. determined the steps of the hydration process of MKPC cements by KDP using thermodynamic modeling [16]:

1. Water addition to the mixture of MgO and KDP causes the KDP to dissolve first due to its higher solubility. The dissolution of KDP causes a reduction of the solution pH producing an acidic solution according to the following reaction:



2. MgO particles dissolve into the solution at a much slower pace. The Mg_2^+ concentration and pH value of solution start to increase during this stage. $\text{MgHPO}_4 \cdot 3\text{H}_2\text{O}$ precipitates from the solution only after its saturation index is met.
3. The precipitation of only $\text{MgHPO}_4 \cdot 3\text{H}_2\text{O}$ occurs when the M/P molar ratio is lower than 0.64, with a corresponding pH precipitation interval from 4.3 to 7.5. When M/P ratio ranges between 0.64-0.67, both $\text{MgHPO}_4 \cdot 3\text{H}_2\text{O}$ and $\text{Mg}_2\text{KH}(\text{PO}_4)_2 \cdot 15\text{H}_2\text{O}$ are formed. The pH value interval in this cases is around 7.5-7.8. When M/P ratio is higher than 0.67, $\text{MgHPO}_4 \cdot 3\text{H}_2\text{O}$ exist only during intermediate stages of the setting process.
4. Next the precipitation of $\text{Mg}_2\text{KH}(\text{PO}_4)_2 \cdot 15\text{H}_2\text{O}$ causes further increase of pH value of the solution since H_2PO_4^- transforms into HPO_4^{2-} and PO_4^{3-} . $\text{Mg}_2\text{KH}(\text{PO}_4)_2 \cdot 15\text{H}_2\text{O}$ also starts to precipitate

when the solubility products of the above ions meet its value. Pure $\text{Mg}_2\text{KH}(\text{PO}_4)_2 \cdot 15\text{H}_2\text{O}$ precipitates for M/P molar ratios and pH intervals ranging from 0.64-0.67 and 7.5-10.3 respectively. For an M/P molar ratio between 0.67 and 1.00, $\text{Mg}_2\text{KH}(\text{PO}_4)_2 \cdot 15\text{H}_2\text{O}$ and $\text{KMgPO}_4 \cdot 6\text{H}_2\text{O}$ both coexist for pH values ranging from 7.8-10.3.

5. The Precipitation of $\text{KMgPO}_4 \cdot 6\text{H}_2\text{O}$ also further increases the pH. For this reason, the concentration of the PO_4^{-3} ions also increases. $\text{KMgPO}_4 \cdot 6\text{H}_2\text{O}$ then, starts precipitating only after solubility products of PO_4^{-3} , K^+ , and Mg^{2+} match that of $\text{KMgPO}_4 \cdot 6\text{H}_2\text{O}$. $\text{KMgPO}_4 \cdot 6\text{H}_2\text{O}$ precipitates from the solution when the M/P molar ratio is higher than 0.64. Moreover, when pH value exceeds 10.3, it can also exist stably in solution.
6. In an MKPC system, Mg_2^+ and OH^- ions can transform to trace amounts of $\text{Mg}(\text{OH})_2$. Even if the amount is small the presence of $\text{Mg}(\text{OH})_2$ can influence the pH value of the solution.

Table 4.1: Hydration products of MKPCs [16]

M/P ratio	Final hydration products	pH value
<0.64	$\text{MgHPO}_4 \cdot 3\text{H}_2\text{O}$	4.5–7.4
0.64–0.67	$\text{MgHPO}_4 \cdot 3\text{H}_2\text{O} + \text{Mg}_2\text{KH}(\text{PO}_4)_2 \cdot 15\text{H}_2\text{O}$	7.4–9.0
0.67–1.00	$\text{Mg}_2\text{KH}(\text{PO}_4)_2 \cdot 15\text{H}_2\text{O} + \text{KMgPO}_4 \cdot 6\text{H}_2\text{O}$	9.0–11.7
>1.00	$\text{KMgPO}_4 \cdot 6\text{H}_2\text{O} + \text{Residual MgO}$	12.1

Aluminium corrosion in cementitious matrices based on three types of cements (ordinary portland cement, magnesium phosphate cement with or without LiNO_3) has been analysed with respect to dihydrogen release. The electroanalysis uses Open Circuit Potential (OCP) as a corrosion indicator. All of the measurements showed that for the Al electrode the OCP is close to the cathodic limit of water. This, therefore, indicates that the major corrosion of aluminium is aqueous corrosion with H_2 generation [7].

OCP reaches $-0.9 \text{ V} / \text{Pt}$ in the magnesium phosphate cement paste with and without LiNO_3 in about 15 days indicating that Al can be protected against corrosion when using this type of cement. Figure 4.1 represents the measured OCP values on an Al electrode. aluminium is initially covered by an aluminium oxide layer. Due to the pH range of MKP pore water, the solubility of aluminium oxide is low. As a result, MKP is better at preserving the oxide layer and thus at limiting aluminium corrosion [7].

The results from this study also show that time plays an essential role with respect to increasing OCP to a value of -1.3 V/Pt for Portland cement encapsulations. The difference between H_2 production observed in the two MKP matrices (with and without LiNO_3) occurs only at the early stage of corrosion. Later, H_2 production reaches a constant value corresponding to a steady state for both matrices. This delay between MKP and MKP- LiNO_3 is explained by the different nature of the protective layer. This difference is caused by the kinetics of formation of these layers [7].

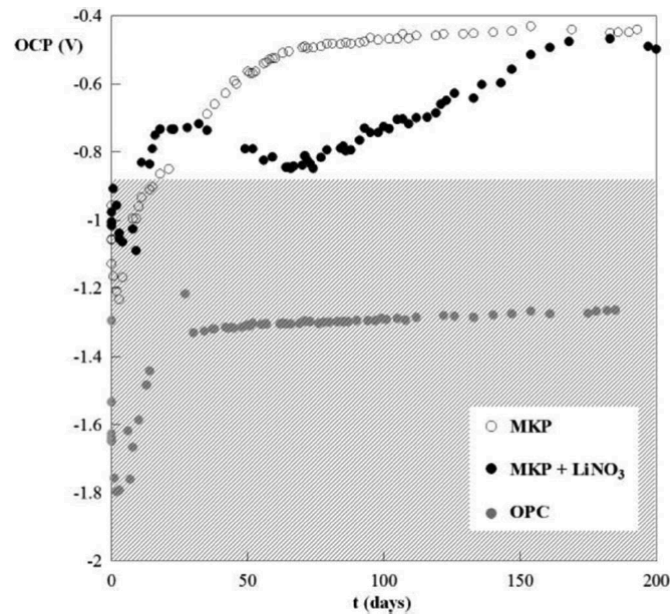


Figure 4.1: OCP measurements on aluminium electrode as a function of time [7].

4.2.2. House of Quality

The first step in determining the product specifications is to translate the demands of the customer into technical requirements. For this reason the house of quality methodology will be employed. The customer requirements that arose during our discussions with COVRA are as follows:

1. Workability: Ease of application of the cement. More concretely, the cement must be mixed, placed, compacted and applied without separation of its components.
2. Corrosion Resistance: As stated before, corrosion must be prevented so as to prevent hydrogen generation.
3. Criticality Prevention: The fuel rods in a canister could cause criticality to occur. For this reason the filling material should not exacerbate the problem.
4. Fuel Plate Coverage: The filling material should completely fill and cover the fuel rods.
5. Durability: The cement should be able to resist the high underground pressure and the water for long stretches of time.
6. Safe Application: As the application of this cement happens on top of the radioactive fuel assembly the application process should be safe.

Table 4.2: House of quality

	Viscosity	Neutron Absorbance	Setting Time	Heat Generation	Aggregate Size	Leakage	Compressive Strength	Pore water pH	Volume Change
Workability			+	-					-
Safe Application				-				-	
Corrosion Resistance								-	-
Criticality Prevention		+							
Fuel Plate Coverage	-				-				-
Durability						-	+		-

The above requirements are translated into the following technical requirements.

1. Pore water pH: As previously stated, corrosion of aluminium is prevented at pH values ranging from approximately 4 to 9. pH is of vital importance to corrosion prevention so the cement pore water must remain at this passivation range.
2. Neutron absorbance cross section(cm^{-1}): To avoid criticality from occurring neutron absorbing materials with high absorption cross-sections could be used. However criticality can also be controlled by the amount of rods placed in the canister so this factor is not so important in determining the final cement formulation.
3. Setting time(min): A reasonable setting time is significant for the workability of cement. It should not be so low (in the order of minutes) that the application process cannot be completed fast enough. It is also important in corrosion prevention, since the entire surface of the assembly must be covered, which will be impossible if the cement hardens too fast. It is preferred that the setting time approaches 1 day in order to reduce the risk of machine malfunction.
4. Heat generation(kW): During the setting process a lot of heat is generated. This can cause safety issues. This can also be exacerbated by the already heat generating nuclear waste.
5. Leakage: Leakage is the amount of cement that dissolves in water causing erosion of the material. For long term waste disposal, this amount must be very small.
6. Viscosity(Pa*s): The cementitious fluid must have low viscosity to ensure ease of application and full coverage.
7. Volume Change: The volume change for Reaction 3.3 has been reported to increase by 105%. This means that for MKPC cements the volume change is quite significant.
8. Compressive Strength(MPa): The cement must endure at high depths in an underground environment for large tracts of time. Consequently it must be able to withstand elevated pressures.

4.2.3. Cement Mixture Parameters

Type of Phosphate

MPCs were initially made with phosphoric acid. The problem with this were the very short setting time and the highly exothermic setting reaction, which limited the applications [6, 58]. This caused a search for another phosphate that could do this reaction. One of the phosphates that was found is $NH_4H_2PO_4$. It showed a relatively low reaction rate and high early strength. The problem with the use of $NH_4H_2PO_4$, is the release of NH_3 -gas, which is highly toxic [6, 58]. Because of this issue, another ammonium-free MPC is required. As a result, cement derived from KH_2PO_4 and MgO was chosen for this study. Because this compound has weaker acid properties than phosphoric acid, it has a slower reaction time. This

slower reaction rate also addresses the high heat release during the reaction [6, 58]. Furthermore, at the early stages, these magnesium potassium phosphate cements (MKPC) have low water demand, low drying shrinkage, and higher compressive strength.

MgO to KH_2PO_4 ratio (M/P)

The M/P ratio is a significant parameter for MKPC cement mixtures, affecting multiple properties. The theoretical M/P molar ratio for complete MgO reaction is 1 according to Reaction 3.3. However an excess of magnesium is usually used. The reason is that the crystallisation of K-Struvite, ($\text{MgKPO}_4 \cdot 6\text{H}_2\text{O}$), (main component of MKPC cements), can only take place in a saturated solution.

Wang et al. studied the pH of the pore water of MKPC cements with different M/P ratios. The results are presented in Figure 4.2. The pore water pH increases with increasing M/P ratios. These results were obtained for a mixture with 0.22 W/C and 0.15 borax weight ratios respectively [8]. More studies with different mixtures have also been conducted, as seen in Table 4.3. Most results are either in or near the passivation range. Exceptions include, the suspensions with W/C ratios of 5 and another mixture with pH of 12.8. All these three mixtures have not any type of retardants mentioned in the studies. A possible explanation is that retardants are usually acidic in nature.

Table 4.3: Summary of MKPC pore water pH studies

M/P	W/C	Retardant (%w/w)	Retardant Type	Sampling time (d)	pH	Source
10	0.11	8.8 %	borax	28	9.3	[59]
10	0.11	8.8 %	borax	60	9.8	[60]
2.7	5	-	-	-	11.2	[61]
8	5	-	-	-	11.5	[61]
8	0.5	-	-	28	12.8	[62]
1	1	0 %	boric acid	0.4	8.5	[63]
1	1	2.58 %	boric acid	1.6	7.6	[63]

The volume deformation ($E = \Delta L(\text{mm})/2.5$) of MKPC after 42 days of curing under air curing for the M/P ratios of 3, 4 and 5 has been reported to be $-9.5 \cdot 10^{-4}$, $-1.52 \cdot 10^{-4}$, and $-1.94 \cdot 10^{-4}$, respectively. The volume of MKPC is reduced under air-curing conditions. Expansion can be caused by different hydration products, while, by evaporation and water diffusion into the surrounding air. Under air curing conditions the shrinkage effect dominates [11].

The M/P ratio affects both the strength of the cements and its setting time, as seen in Figure 4.2. The M/P ratio has not a significant effect on the setting time. For the strength of the cement the effect is more pronounced. The strength increases until a peak and then decreases. This peak is at around 14 M/P ratio. These results were obtained for a mixture with 0.1 W/C and 0.05 borax weight ratios respectively [9]. The strength of MPC, even for low M/P ratios (35 MPa), is comparable to that of fabricated waste package mortar made at COVRA (48-55 MPa) [64].

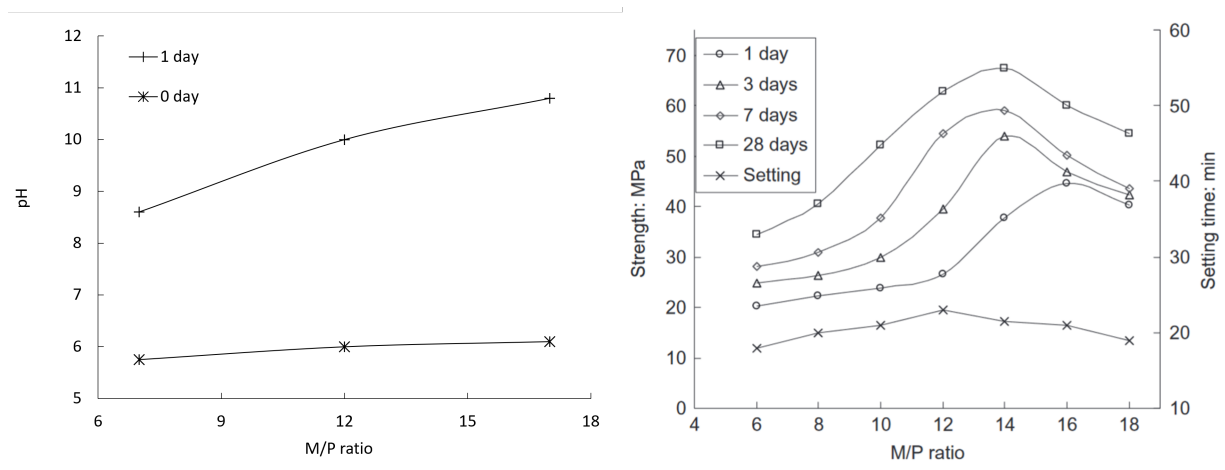


Figure 4.2: Effect of the M/P ratio, on the pore water pH (left)[8] & on the setting time and and strength of the cement mixture (right)[9].

Retarder

Retarders are used to decrease the reaction rate, and therefore increase the workability of the cement by prolonging the setting time. It also controls the release of heat during the reaction. Retarders that are generally used are sodium-tripolyphosphate ($\text{NaP}_3\text{O}_{10}$ or STP), borax ($\text{NaB}_4\text{O}_7 \cdot 6\text{H}_2\text{O}$) and boric acid (H_3BO_3).

STP is reported to increase the pH of the pore-waters in the cement. Shijian and Bing found that the addition of STP increased the strength of the cement, until the fraction surpassed 2wt%. The use of STP is however limited by the solubility in the acid phosphate solution [6, 42]. Therefore, it is able to increase the setting time to about 15 minutes, which is still quite limited [65].

Borax is able to raise the setting time even higher, up to around 1 h [42]. It also is very effective and therefore only has to be added in small quantities [6]. There are different theories about the mechanism of this phenomenon. Sugama and Kukacka [66] suggested that tetraborate ions ($\text{B}_4\text{O}_7^{2-}$) react with the dissolved Mg^{2+} to precipitate around the magnesia. Hall et al. disagreed with this and suggested that $\text{B}(\text{OH})_3$ or $\text{B}(\text{OH})_4^-$ form a protective layer around the magnesia [42]. The disadvantage of the use of borax, is that it could decrease the strength of the cement [58]. The effect of borax is shown in more detail in Figure 4.3. Borax, as stated before decreases the strength of the cement but mainly on the first two days of curing. Moreover, the setting time of the cement sharply increases with increased borax content. These results were obtained for a mixture with 0.1 % W/C 5 % M/P weight ratios [9]. Also, the use of borax is becoming restricted in European countries, because of its reproductive toxicity [6].

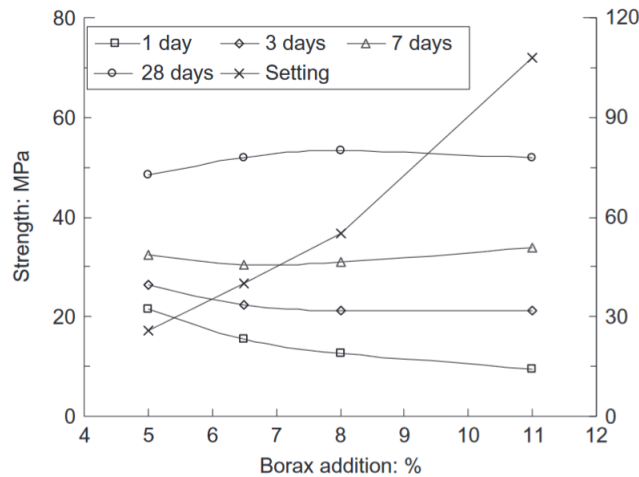
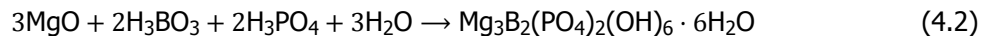


Figure 4.3: setting time and cement strength with respect to borax content [9].

Boric acid (H_3BO_3) can also be used to retard the cement. Hall et al. found that its retardation effect is comparable to borax [42]. However, the amount of borax needed to achieve the same retardation effect is 1.55 higher than for boric acid. It also led to an increase of the final strength of the cement. It is suggested by Wagh that the boric acid forms a coating on the MgO that slows its dissolution and therefore the reaction rate [67]. The coating that is formed is Lunebergite and is formed through reaction 4.2



According to Walling, boric acid is also becoming restricted in European countries [6].

Additives

There are also other additives that can be added to the cement to influence its properties. These generally include fly ash and silica fume. In most of the literature, these compounds are considered inert, but there are reports that disagree and state that there is actually a chemical reaction taking place that brings about the changes in properties of the cement [6]. Fly ash (FA) is the coal-combustion product, which is also used a lot in regular Portland-cement. When added to MPC, it is able to double setting times, although this requires 50wt% of FA [6]. At the same time, it also increases the flow ability of the cement [6, 18]. It also increases the final strength and lowers the cost [18]. Li and Bing [10] reported that FA increases the water resistance of their MPC. However, FA could become less available in the future, as the burning of coal will become less common. When Silica Fume (SF) is added to MPC, it is reported to improve the water resistance, reducing porosity and increase the early strength. Some researches also state that it reduces the expansion, which is sometimes problematic [18].

Water to cement ratio

Another ratio that is fairly important for the properties of the cement is the water to cement ratio (W/C). That is, strength decreases with increasing w/c. [6] Walling and Provis even stated that a higher w/c ratio would make the cement unable to set [6]. Li and Bing [10] found increased the setting time of their cement past to 25 minutes with a w/c of 0.20. They also found that the compressive strength of their paste had an inverse relationship with w/c. This is because of the increased number of pores that are formed by higher water content.

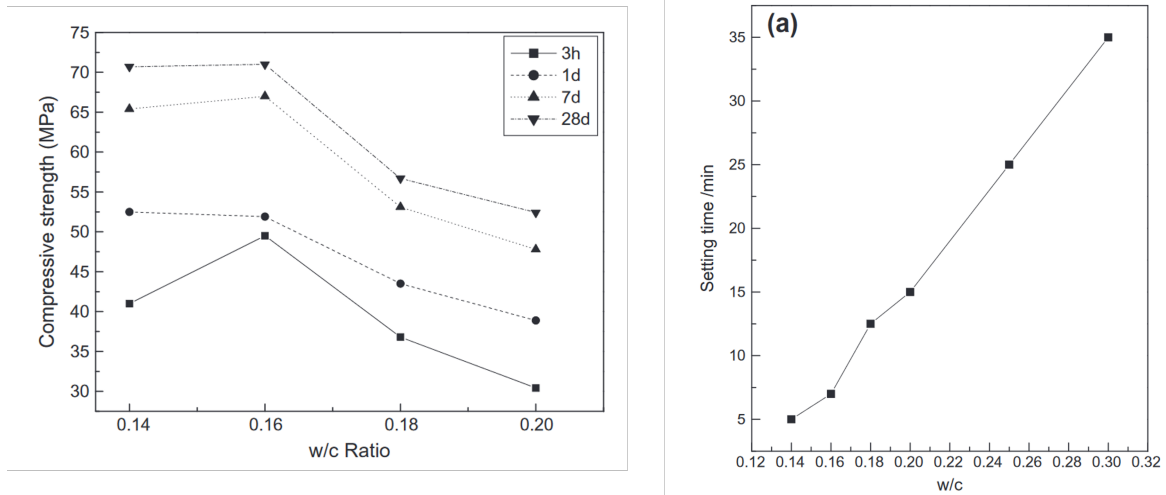


Figure 4.4: Compressive strength and setting time with respect to W/C ratio [10].

As stated before the theoretical M/P molar ratio is 1 for a complete reaction. However dead burnt magnesia does not react completely with KDP. Moreover, the amount of different hydration products also changes with the M/P ratio. For this reason the W/C ratio is not constant. On the other hand the ratio of KDP to water, P/W mass ratio remains constant at 0.661 for a fully reacted MKPC mixture. The theoretical W/C mass ratio with respect to the M/P one is presented in Figure 4.5.

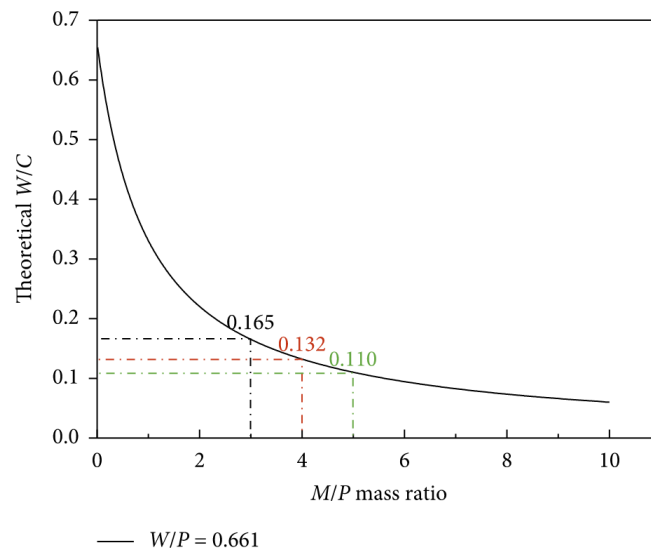


Figure 4.5: Theoretical W/C mass ratio with respect to the M/P ratio [11]

Gardner et al. [12] also examined the the fluidity of MKPC cement pastes containing fly ash and blast furnace slag. They found that as expected the fluidity of cement increases with the water content. For a mixture containing fly ash at least a W/C mass ratio of 0.24 is required to achieve the same results as Portland cement. The results for mixtures containing the above additives at 50 % weight(excluding water) are presented in Figure 4.6.

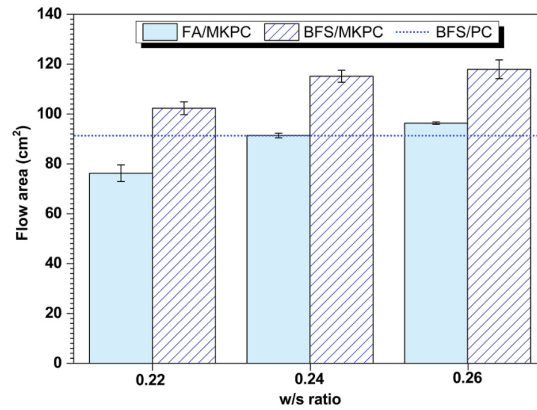


Figure 4.6: Compressive strength and setting time with respect to W/C ratio [12].

The maximum heat flow of heat generated by the previous cement mixtures are shown in Table 4.4. The addition of additives more than halves the peak amount of heat produced. When using FA the maximum amount of heat is increased when the water content is also increased. Burned slag on the other hand is not affected by the water content. For Portland cement this amount is around 0.002 W/g [17].

Table 4.4: Peak Heat Flow (W/g)[17]

W/C	MKPC	MKPC/FA	MKPC/BFS
0.22	-	0.004	0.005
0.24	0.015	0.007	0.006
0.26	-	0.010	0.005

4.3. Final formulation

The final formulation of the MPC proposed, requires consideration of all the previous mentioned parameters in section 4.2.3. The issue of which phosphate would be most suitable for use seems fairly simple to solve. Phosphoric acid is ruled out because the setting time of this cement would be way too fast. $\text{NH}_4\text{H}_2\text{PO}_4$ could be fairly harmful to the employees that need to pour the cement due to the formation of NH_3 -gas, this one is also ruled out. This only leaves KH_2PO_4 as option.

As it can be seen in Figure 4.2 the value of the pore water pH drops for lower M/P ratios. For this reason a slight excess of M/P ratio of 1.5 is selected. This mixture has also worked in the study of McCague et al [17]. The selection of M/P ratio was made primarily with the pH in mind, since the strength of the material is not as important.

As for the choice of retarder, boric acid or borax are considered. As boric acid seems to be more effective, the choice is made for this material. A 15 % w/w is suggested to maximise the setting time. Longer setting time means not only increased workability, but also slower heat generation. In our case the use of additives could be beneficial by reducing the price of the mixture and improving some of its properties. However not enough is known about the effect of the additives on the pore water pH. For this reason their use is avoided. Several papers used W/C ratios between 0.16 and 0.24 [10, 12]. Therefore it was decided to take the middle of this range, which holds a W/C ratio of 0.2.

Table 4.5: Mass fractions of raw materials in final product

Material	Mass fraction
MgO	0.218
KH_2PO_4	0.490
Boric acid	0.125
H_2O	0.167

5

Manufacturing of the product

Generally, the manufacturing process for cements can be divided in six stages. The first 5 correspond mainly to the primary product production, while the last step is purely cooling and final grinding and mixing with water. First, the raw ingredients are milled and crushed. Then in stage 2 they are mixed with additives and further grinded in a homogeneous mixture. In stage 3 the mixture is pre-heated to reduce the energy consumption before it enters the kiln phase during which calcination takes place. This stage is extremely important to ensure the cement mechanical properties. After exiting the kiln, the mixture is rapidly cooled, and some additives can be added. To save energy, the heat generated by the clinker is returned to the kiln. Grinding is the final stage of cement production. The cementitious powder is smoothed and uniformed using rotating drums fitted with steel balls. The powder is then loaded into silos and packaged in 20-40 kg bags, or it is mixed directly with water.

As mentioned, the majority of MPC products are represented by $Mg(X_2PO_4)_2 \cdot nH_2O$ or $MgXPO_4 \cdot nH_2O$, where X denotes hydrogen, ammonium, or any other alkali metal. However, the $Mg(X_2PO_4)_2 \cdot nH_2O$ products are soluble in water, and therefore form the more stable $MgXPO_4 \cdot nH_2O$ in the presence of an additional MgO. This means that an excess of MgO is required in the production of MPC in order to meet the product specifications mentioned in previous chapters. When comparing the ceramics formed by NH_4 , Al, or K ions, K is employed the most due to the highest pH in acidic range and the least amount of heat is generated during formation of KH_2PO_4 [67]. Then, the MgO and the KH_2PO_4 are mixed together until a uniform product is obtained. The mixture is further poured into a mold and stirred with water in a ratio (1:5) for approx. 30 minutes. The liquid mixture is then ready to be poured into the canister and is expected to solidify completely within a few hours.

5.1. Production of magnesium oxide

Magnesium oxide or magnesia (MgO) can be produced in two different ways: a dry and a wet route.[6, 18] The dry route involves the calcination of crushed magnesite ($MgCO_3$) according to reaction 5.1. Depending on the application of the magnesium oxide produced, the temperature in the calcination process can be varied.[6] The temperature has to be at least the thermal decomposition temperature, which is defined as the temperature at which the standard Gibbs free energy of reaction for Reaction 5.1 is 0. For magnesium this temperature is $\approx 393.5^\circ C$. Increasing the temperature also increases the size of the magnesium oxide crystals that are formed, and therefore decreases the surface area of the product [6]. This decrease in surface area has a linear relationship with the reactivity due to sintering [6]. Therefore, different calcination temperatures yield different grades of magnesium oxide. The general classification used is presented in Table 5.1. The type of magnesia that is used for production of MPC is dead burned.



The wet method involves precipitating $Mg(OH)_2$ from a magnesium-rich solution such as seawater. This solution is reacted with $Ca(OH)_2$ or $CaMg(OH)_4$ to form $Mg(OH)_2$ according to reactions 5.2 and 5.3. The produced $Mg(OH)_2$ is then filtered, washed and eventually calcined to form MgO. [6].

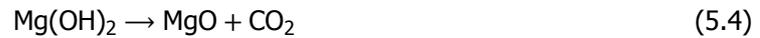
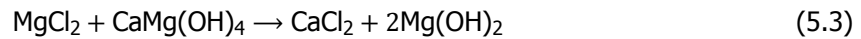
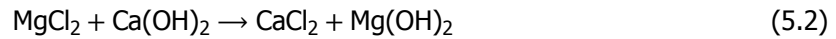


Table 5.1: Classification of type of magnesia according to their calcination temperature [6, 18]

Type of magnesia	Reactivity	Calcination temperature ($^{\circ}\text{C}$)
Caustic-calcined	High	650-1000
Middle-burned	Intermediate	1000-1500
Dead burned	Low	1500-2000
Fused	Very low	>2000

Due to the higher energy cost of the wet route, most of MgO worldwide is produced through the dry route [18]. As stated before, the grade of magnesia required for production of MPC is dead-burned magnesia (DBM), which requires calcination temperatures of 1500 – 2000 $^{\circ}\text{C}$. DBM is mostly produced in rotary kilns or shaft kilns [18]. A rotary kiln is a cylindrical-shaped reactor, which is placed in a slightly inclined position (generally 1.5 – 5%) [68]. As the name implies, the kiln is rotated at a low speed, usually between 0.2 and 2 rpm. MgCO_3 is supplied to the high side, and by gravity and rotational motion moves to the low side where it is discharged [68]. Before the MgCO_3 enters the kiln, it is preheated to $\approx 700^{\circ}\text{C}$ [18]. Then the raw material enters the kiln, where it is heated further to the desired temperature. This is mostly done by counter-current heat exchange with a hot gas [13]. This hot gas is produced either by a heater outside the kiln, or with a flame directly in the kiln.[18] The MgO is discharged at the end, where it is cooled to $\approx 200^{\circ}\text{C}$ [18]. This heat and the heat of the exhaust gas CO_2 can be used to feed the pre-heater to save energy.

A simple schematic of the production of the magnesia can be found in Figure 5.2.

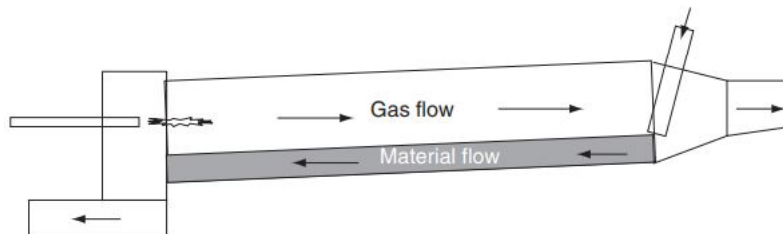


Figure 5.1: Simple schematic of a countercurrent flow rotary kiln [13]

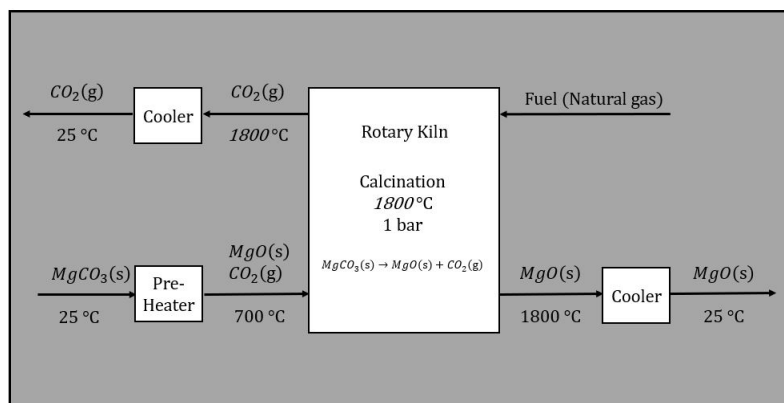


Figure 5.2: Schematic of MgO production

5.2. Production of monopotassium phosphate

Monopotassium phosphate (MKP) is widely produced through the neutralization reaction of potassium hydroxide (KOH) and phosphoric acid (H_3PO_4) as illustrated in the Equation 5.5. The KOH can also be replaced with the less expensive KCl. In this case, an organic solvent is required and hydrochloric acid is produced. Although, there are several methods for removing the produced hydrogen chloride, the overall economics of this process are higher than when KOH is used.



Because of the exothermic nature of the reaction, crystal precipitation may occur as a result of pre-drying, which may cause clogging in the atomizer during spray drying. One solution for this problem is to dilute the mixture with water already during the first stage. However, this increases drying time and costs. The reported reagent concentrations for phosphoric acid range between 70 and 85%, while potassium hydroxide concentrations range between 40 and 50% [69].

Figure 5.3 depicts the MKP manufacturing process, which is fairly simple. The reagents are first added or pumped into the reaction vessel. Pumping rates of 2 gallons per minute for 5 minutes for H_3PO_4 and 2 gallons per minute for KOH have been reported [69]. It has also been reported that a molar ratio of 1:1 at 50 °C obtains satisfactory monopotassium phosphate crystal size and reasonable yields [70]. The mixture can then be diluted with water to retain it slurry-like. After that, depending on the particle size required, the mixture is stirred for 10 to 120 minutes. Agitators in the reaction vessel are the most prevalent way of mixing.

The products are then transferred to a storage tank to cool and crystallize MKP (usually at temperatures between 50 and 60 °C). The mixture then is pumped to a homogenizer and then pumped to a spray dryer with an inlet temperature approximately 400 °C and outlet temperature approx. 100 °C [69]. This results in a fine, free flowing powder. The air/powder stream is then separated in a cyclone, where the remaining powder is discharged at the bottom. In the case of high air temperatures, the powder product is usually cooled using chilled water.

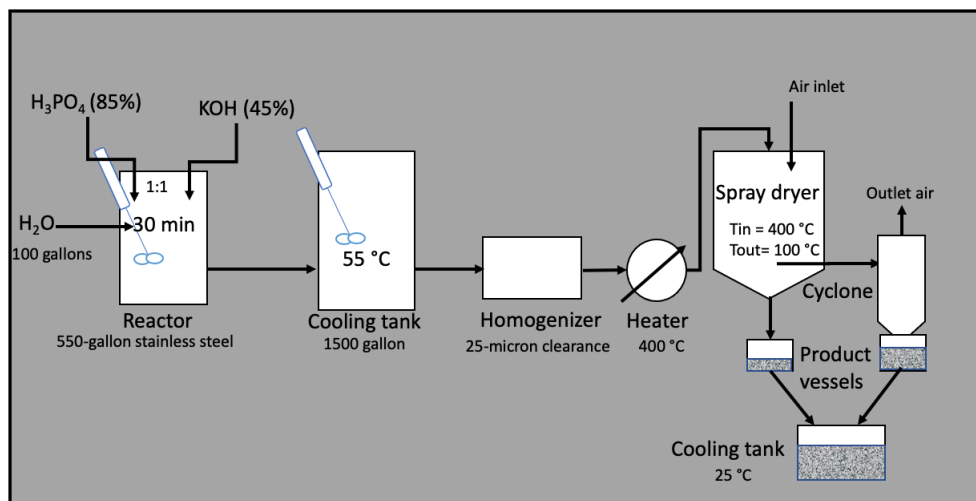


Figure 5.3: Schematic of KH_2PO_4 manufacturing

After the production of the MgO- and KH_2PO_4 -powder, the powders need to be mixed, together with the additives. As all of these are powders, this is done in a ball mill mixing unit. The final powder that is obtained needs to be stored dry in a cement silo to prevent it from hardening before application. In order to produce cement with the specifications mentioned in Section 4.3, the powders first are mixed with a M/P molar ratio of 1.5 and a W/C ratio of 0.2.

6

Process control

In this chapter, the main parameters that need to be controlled in the production process are identified. Manufacturing objectives include keeping the process as short as possible, using as little energy as possible, and producing items of the highest possible quality and purity.

6.1. MgO-production

6.1.1. Calcination temperature

A key parameter in the calcination process is the temperature at which the magnesia is produced. As explained before in section 5.1, different temperatures yield very different types of magnesia when it comes to reactivity. (Table 5.1) When the temperature during the calcination process becomes too low, the reactivity of the produced magnesia will increase. This increase in reactivity would result in a faster reaction with the potassium-phosphate, which would decrease the setting time. To avoid these inconveniences, the temperature of the calcination reaction should be controlled.

As the temperature range for DBM is quite large (1500 – 2000°C), there is some tolerance in a deviation of temperature. The choice for a temperature of 1800°C was made so that deviations of temperature would keep it in the desired range. However, in this range, the reactivity of the DBM also differs, so to produce cement with the uniform properties, it is important to keep the temperature within the limits.

To control the temperature, it should be monitored continuously. A jacket with heat transfer fluid could be installed around the reactor, to react to sudden temperature changes with immediate heating or cooling [71].

6.1.2. Air for combustion of natural gas

To minimize the amount of natural gas required to provide sufficient heat to the rotary kiln, incomplete combustion should be avoided. This is done by controlling the amount of air supplied to the kiln. In theory a stoichiometric amount of air should be enough, but in practice often an excess of about 1-3 % of air is used in the combustion [18].

6.1.3. Hot spots monitoring

If the steel shell on the outside of the kiln are exposed to the high temperatures inside the kiln due to refractory failure, this shell can weaken and cause mechanical failure [72]. This could result in product loss, costly repairs and also further refractory damage due to the thermal shock [72].

To prevent this from happening, the kiln should be monitored continuously with thermal imaging methods to find potential hot spots. These hot spots on the shell then can be cooled locally or the settings of the kiln can be altered to prevent failure [72].

6.2. MKP production

The quality of the primary reactants is critical for producing pure MKP. As a result, phosphoric acid produced through wet processes is preferred. This implies that the molar ratio of KOH to H₃PO₄ is 1:1.

The required concentrations are approximately 80 and 45 percent, respectively.

After the mixing of KOH and H_3PO_4 , the reaction mixture must be cooled to precipitate the monobasic potassium phosphate crystals. Knowing that the reaction is exothermic, and that the excess water begins to evaporate above $60\text{ }^\circ C$, the reaction mixture is cooled at temperatures below $60\text{ }^\circ C$.

As mentioned in Chapter 5, the mixture prior to entering the spray dryer is prone to pre-drying, so its moisture must be controlled to avoid clogging. One option is to dilute the mixture with water. To reduce the solids by 25%, the water ratio in the subsequent drying operation is increased by 284%. This simply implies that the spray drying process is being prolonged, and hence the costs are increasing.

One parameter that must be monitored very closely is the water/cement ratio. However this parameter lays outside of the production process, but is part of the application procedure. Therefore it is more of importance for the employees that will apply the cement to the canisters. This parameter has a major impact on the final properties of the cement, like setting time and strength, and should therefore be carefully monitored.

7

Balances and Utility requirements

7.1. Plant capacity

To create the mass and energy balances, first the plant capacity should be defined. In Section 4.1.1 it was already stated that $104m^3$ needs to be filled for 52%. This means that $\approx 54.08m^3$ of product needs to be produced.

To convert this in mass, the density of the final cement is needed. As the product has a very specific composition, it is hard to find an estimate for the density of the cement. Therefore, a very simple estimate is made, by taking the mass fractions of the components and multiplying them by their density. With this method a density of $2289kg/m^3$ was found. When comparing this value to values found by Qin et al. [73], it seems to be a reasonable number. They found values between 2100 and $2300kg/m^3$. Although their cements have compositions that are quite different from this report, it is assumed that the calculated density is in the acceptable range.

In Table 7.1, the assumptions made concerning the production capacity are presented. Using these in combination with the calculated density and the required volume results in a production rate of $173.36kg/hr$ is found.

Table 7.1: Assumptions made concerning the production capacity

	Assumption	Justification
Production window	3 months	The production window is taken this short, because the required quantity of product is so low.
Downtime	1 week	It is expected that one week of downtime is needed to clean the ball mill before and after the use.
Hours/day	8	As there is no need to work around the clock due to the low quantity, regular working hours are assumed.

7.2. Assumptions

For the production of MgO, the conversion for $MgCO_3$ is assumed to be 100 %. This assumption is made because there is no mention in the literature of the separation of unreacted $MgCO_3$. Also, the calcination temperature of $1800^\circ C$ is far above the calculated decomposition temperature of $MgCO_3$.

For the synthesis of KH_2PO_4 the same reasoning is used as with the MgO production. As no information was found on the separation of unreacted reactants, a conversion of 100% is assumed.

It is assumed that all of the $MgCO_3$ is already converted into MgO and CO_2 during the preheating, as the outlet temperature of $700^\circ C$ is way higher than the decomposition temperature of $393.5^\circ C$.

When using a spray dryer, some of the solid product will remain in the gas stream. This is separated by a cyclone, where after it will be combined with the solid product of the spray dryer. Since the particle distribution is not known, it is assumed that the majority of the solid will already be separated in the spray dryer. Only 20w% of the solid entering the spray dryer will remain in the gas stream.

The water used in MKP production to make the solid easier to process, can all be recycled. As there is also water in the solutions of H_3PO_4 and KOH, and there is also some water formed in the reaction,

this water needs to be purged.

7.3. Mass balances

In Table 7.2 the stream summaries for the production of MgO and KH_2PO_4 can be found. The flow diagram can be found in Figure 7.1. Note that the utility flows (e.g. air, cooling water, natural gas) are displayed in the diagram, but their streams are not numbered. This is because they do not really participate in the mass balances. Also, stream 22 and 23 only contain the CO_2 generated by the calcination, and not the CO_2 and H_2O that is formed by the combustion of the natural gas.

In Table 7.3, the differences between in- and outgoing mass for both processes can be found. They are in the order of 10^{-4} and 10^{-3} and can therefore be neglected.

Table 7.2: Stream summary

Stream	Temperature(°C)	Pressure(bar)	Mole flow(Mol/hr)	Mass flow(kg/hr)
F1	25	1	5043.77	90.86
F2	25	1	4204.14	109.06
F3	25	1	1714.32	100.84
F4	25	1	1312.04	110.62
F5	25	1	490.70	30.34
1	50	1	150363.99	2708.85
2	50	1	4204.14	109.06
3	50	1	1714.32	100.84
4	62.5	1	151238.68	2827.88
5	55	1	151238.68	2827.88
6	55	1	151238.68	2827.88
7	400	1	151238.68	2827.88
8	400	1	151238.68	2827.88
9	100	1	699.76	95.23
10	100	1	150538,93	2732,66
11	100	1	150538,93	2732,66
12	100	1	174.94	23.81
13	100	1	150363.99	2708.85
14	100	1	699.76	95.23
15	100	1	174.94	23.81
16	25	1	150363.99	2708.85
17	25	1	150363.99	2708.85
18	25	1	874.69	119.03
19	25	1	145320.22	2617.98
20	25	1	150363.99	2708.85
21	700	1	1312.04	110.62
22	1800	1	1312.04	57.74
23	25	1	1312.04	57.74
24	1800	1	1312.04	52.88
25	25	1	1312.04	52.88
E1	25	1	1312.04	57.74
E2	25	1	5043.77	90.86
E3	25	1	-	272.40

Table 7.3: Errors in overall mass balances of both production processes

Process	Absolute difference(kg)
MgO	$1.3 * 10^{-4}$
KH_2PO_4	$1.5 * 10^{-3}$

7.4. Energy balances

7.4.1. MgO production

The production of MgO requires a lot of energy to achieve the required temperature for the calcination to DBM. The MgCO_3 needs to be heated to 700°C before it enters the kiln, after which the temperature is further raised to 1800°C in the kiln with the burning of natural gas. Next to this, the calcination reaction is an endothermic reaction ($\Delta H_{rx} = 116.59\text{kJ/mol}$), which means that even more heat needs to be delivered. After the calcination the products are cooled to room temperature. These heating and cooling requirements need to be combined to reduce the utility requirements.

The heating and cooling requirements are summarized in Tables 7.4 and 7.5. The 'Pre-heating' duty includes the heating of MgCO_3 to its decomposition temperature ($\approx 393^\circ\text{C}$), the heat of reaction, and the heating of MgO to 700°C . The 'Kiln' includes the heating to the required temperature for DBM (1800°C). The cooling includes the cooling of the MgO- and CO_2 -product to 25°C .

Table 7.4: Heating requirements for the MgO production

Stream	Duty(kW)
Pre-heating	66.91
Kiln	44.82
Total	111.73

Table 7.5: Cooling requirements for the MgO production

Stream	Duty(kW)
Cooling of MgO	33.06
Cooling of CO_2	34.94
Total	68.00

7.4.2. KH_2PO_4 production

The production of MKP requires some preheating of the reactants before they enter the reactor. All of the heat that is produced in the reactor is transferred into the products, causing the product mixture to warm up to $\approx 62.5^\circ\text{C}$. This mixture is then cooled to 55°C in the cooling tank. Before it enters the spray dryer, the mixture is heated up to 400°C . Then all of the water is assumed to be evaporated in the spray dryer, and both the solid MKP product and the water vapor is assumed to leave at 100°C . After the spray dryer, the MKP product is cooled to 25°C . The water is also condensed and cooled to 25°C .

The heating and cooling requirements are summarized in Tables 7.6 and 7.7. The heat capacity for MKP is assumed to be constant over the whole temperature range, as the only heat capacity that could be found was the C_p at 298K.

Table 7.6: Heating requirements for the KH_2PO_4 production

Heating	Duty(kW)
Pre-heating	79.76
Before spraydryer	593.40
Spraydryer	1237.12
Total	1910.28

Table 7.7: Cooling requirements for the KH_2PO_4 production

Cooling	Duty(kW)
Cooling tank	23.58
KH_2PO_4 final	2.12
Water final	1923.03
Total	1948.73

The overall energy balances were also calculated over the separated processes. The differences that were found between the in- and outgoing energy can be seen in Table 7.8. These differences seem like significantly big numbers, but when compared to all the energy that is entering the process they seem negligible (0.24% and 0.0089% of incoming energies). These could for example be explained by inaccuracy of the thermodynamic data used. For example, the assumption that the heat capacity of KH_2PO_4 is constant over a temperature interval of $25^\circ\text{C} - 400^\circ\text{C}$ is a pretty rough one and an almost certainly wrong assumption. The same is true for the enthalpy of the formation of KH_2PO_4 , which is also thought to have a small uncertainty. By making small changes to these numbers, it is able to make the margin of error go to zero.

All the thermodynamic data that is used can be found in Appendix ??.

Table 7.8: Errors in overall energy balances of both production processes

Process	Absolute difference(kJ)
MgO	4446
KH_2PO_4	3187

7.5. Utility requirements

The utility requirements will be presented here. In Tables 7.15-7.18, the choices for the utilities are explained.

7.5.1. Hot utilities

Natural gas will be used to deliver the required heat for both processes. A heating value of 37445 kJ/m^3 is used, which is the mean of the LHV and HHV of natural gas according to [74]. Tables 7.9 and 7.10 show the amount of utilities needed for both processes.

Table 7.9: Hot utility requirements for the production of MgO

Heating	Natural gas (m^3/hr)
Pre-heater	6.43
Kiln	4.31
Total	10.74

Table 7.10: Hot utility requirements for the production of MKP

Heating	Natural gas (m^3/hr)
Pre-heating	7.67
Heating before spraydryer	57.05
Spraydryer	118.94
Total	183.66

7.5.2. Cold utilities

For the cooling of the MgO after the rotary kiln, chilled air is used. The temperature change for this air is assumed to be 30 degrees. For the cooling of the CO_2 chilled water is used, with an assumed temperature change of 20 degrees [74].

For the cooling requirements of the cooling tank in the MKP-production, cooling water is used. The temperature change of the water is assumed to be 19 degrees [74]. The C_p of the cooling water is assumed to be constant over this temperature interval, with a value of $4167,46 \text{ kJ}/(\text{m}^3 * \text{K})$.

For the cooling requirements after the spray dryer, again chilled water is used, with an assumed temperature change of 20 degrees [74]. Tables 7.11 and 7.12 show the amount of utilities needed per kg of product for both processes.

Table 7.11: Cold utility requirements for the production of MgO

Cooling	Chilled air(m^3/hr)
Cooling of MgO	0.00086
	Chilled water(m^3/hr)
Cooling of CO_2	0.00042

Table 7.12: Cold utility requirements for the production of MKP

Cooling	Cooling water(m^3/hr)
Cooling tank	1.07
	Chilled water(m^3/hr)
KH_2PO_4 final	0.092
Water final	83.06

7.6. Heat integration

Since performing a heat integration is not required for product groups, the full analysis is not done. However, there are some chances in saving energy in the process. The main opportunities lie in the MgO-production. The rotary kiln needs a lot of energy to warm up the reactants, and afterwards they are cooled back to room temperature. It would be a waste of energy to not use that energy to warm up the reactants. As the recovery of this amount of heat could have a significant impact on the price of the product, it is worthwhile to make a rough estimate of this. To do this, it is important to keep in mind the minimum temperature difference that needs to be kept to achieve efficient heat exchange. A minimum temperature difference of 20 degrees is used in these calculations.

When maintaining this temperature difference, the resulting heat integration that can be done in the MgO-production is shown in Table 7.14. A large part of the cooling of the MgO and CO_2 is used to heat the reactants in the preheater, and to deliver the reaction heat.

In the MKP-production, there are less chances of energy saving, despite there are large heat flows involved. This is due to the fact that large amounts of the heating and cooling that is needed is latent

heat by the vaporization and condensation of water. Also the temperature differences are not big enough to exchange large amounts of heat efficiently.

Table 7.13: Hot and cold streams in the MgO-process suitable for heat integration

Stream	Type	Supply temperature (°C)	Target temperature (°C)	Duty (kW)
Pre-heating	Cold	25	700	66.91
MgO-cooling	Hot	1800	25	33.06
CO ₂ -cooling	Hot	1800	25	34.94

Table 7.14: Reduction in duties by heat integration in MgO-process

Stream	Type	Former duty(kW)	New duty(kW)	Reduction (%)
Pre-Heating	Heating	66.91	11.51	82.8
MgO-cooling	Cooling	33.06	4.33	86.9
CO ₂ -cooling	Cooling	34.94	8.18	76.6

Table 7.15: Natural gas utility review

	Justification
Reason for selection	Natural gas seems to be the most commonly used fuel for rotary kilns [18].
Major users	The spraydryer and the auxiliary preheater
Other options	Petroleum coke, fuel oil and sometimes even waste [13, 18].
Possibilities for future reduction	The heat that is recovered by cooling of the products of the rotary kiln could be used to reduce the demand for natural gas [13, 18].

Table 7.16: Cooling water utility review

	Justification
Reason for selection	Cooling water is a cheap option for the cooling in the temperature range of the cooling tank [74].
Major users	Cooling tank in MKP production
Other options	Air cooling
Possibilities for future reduction	As the cooling duty is fairly low, the cooling could be done in a cooling tank that is able to lose its heat to the surroundings

Table 7.17: Chilled water utility review

	Justification
Reason for selection	Cooling water alone is not able to cool to room temperature efficiently.
Major users	Water cooling and condensation in the MKP process
Other options	Refrigerants or brines.
Possibilities for future reduction	In the present case, the cooling of the CO ₂ is done with only chilled water. Much of the cooling could also be done with ordinary cooling water, only the cooling in the lower temperature range should be done with chilled water.

Table 7.18: Chilled air cooling utility review

	Justification
Reason for selection	Rotary coolers use air as the refrigerant, and these units seem to be generally used for this purpose [75]. Also, air can be used in direct-contact heat exchange. The reason that the air is chilled is because the MgO needs to be cooled to room temperature.
Major users	Cooling of the products of the rotary kiln
Other options	Chilled water, refrigerants or brines.
Possibilities for future reduction	The cooling could be used in heat integration to deliver heat to the preheater of the kiln to reduce air demand.

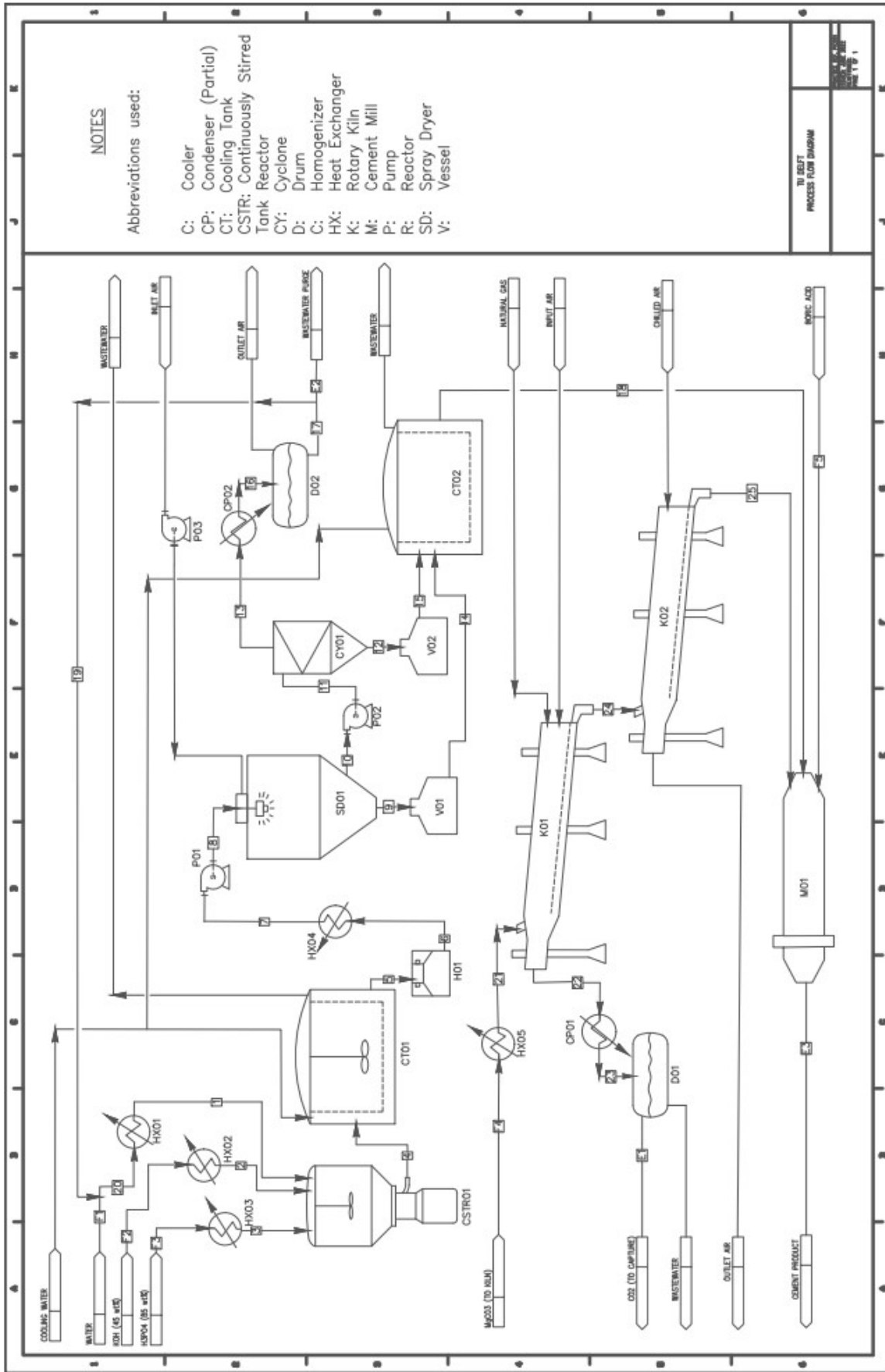


Figure 7.1: Flow diagram of the whole process

8

Equipment List and Unit Design

8.1. MgO-production

For the production of MgO the major piece of equipment is the rotary kiln, connected with some heaters and coolers.

The outside of the rotary kiln is a shell made of steel plates [68]. As these plates will not be able to withstand the high temperatures required in the kiln, the inside is lined with a refractory material. Refractory materials are used for this purpose, as they can assure mechanical integrity in these high temperatures [13, 68]. This refractory material can be for example magnesium aluminate spinel, which has a melting point of 2135°C [76]. Around the kiln shell, there are riding rings that are placed on steel rollers that allow the kiln to rotate as frictionless as possible. Two thrust rolls are there to prevent the kiln from moving off the support rollers. The kiln is rotated by a gear ring. If the rotation of the kiln is malfunctioning, mostly there are internal-combustion motors that will keep it slowly rotating, to prevent overheating at one side, causing damage to the shell and refractory materials [13, 68].

For the cooling of the MgO-product, a similar reactor as the rotary kiln is used: a rotary cooler. It operates in almost the exact same way, apart from the fact that the heat transfer is now reversed. Ambient or chilled air is used to cool the solid product to the desired temperature. Rotary coolers are able to handle high temperatures that are reached in the calcination process. It also has a steel shell, with a refractory material on the inside to ensure mechanical integrity. The heat recovered here can be for example be used to heat the reactants in the preheater of the rotary kiln.

8.2. KH_2PO_4 -production

Due to the presence of very acidic H_3PO_4 and alkaline KOH, a corrosion-resistant material, such as stainless steel, for the reactor vessel is required. Moreover, it is reported that a 550 gallon stainless steel tank with a Cowles Dissolver agitator as part of the mixing equipment for such reaction [69]. As stated in Chapter 5, the reacted mixture must then be chilled to roughly 50°C . This indicates that the product can crystallize with the help of a water cooling tank. The crystallized mixture must then be homogenized. To achieve quick and efficient mixing times, a high shear mixer can be used. According to the patent, an IMPEX High Shear Mill homogenizer with a 25 micron clearance between the rotor and stator can achieve a uniform/homogenized slurry mixture [69]. Spray drying is the final step in the MKP powder production process, in which the slurry mixture is atomized into a spray and then dried to obtain a fine powder. Spray dryers typically include a feed pump, an atomizer, an air heater, an air disperser, a drying chamber, and exhaust air cleaning and powder recovery systems [69]. Any conventional spray dryer can be used to efficiently convert the slurry to powder. A cyclone is then used to separate the air with the remaining powder. Since the product outlet temperature is still high, a cooling unit capable of lowering the temperature to 25°C can be employed. As a result, water can be obtained, which can then be partially purged and recycled back into the system.

8.3. Mixing of solids

After the production of the MgO and KH_2PO_4 they need to be mixed. Also, the boric acid needs to be added. All of this is done in a Ball mill. The rotation speed must be lower than the critical speed (the speed at which the centrifugal force is equal to the gravitational force). This keeps the balls from clinging to the mill surface and allows for more efficient grinding of the mixture. The speed is therefore chosen to be 80% of the critical speed. The ball mill mixing system consists of two chambers both with different size steel alloy balls. The diameter of the balls in first chamber is around 90 mm, and mill liners are intended to elevate the media as the mill rotates, so crushing dominates the milling process in the first chamber [77]. The balls in the second chamber are smaller with a size between 15 to 60 mm [77]. In the second chamber water and air flow is added to provide cooling and steady cement flow. Since such grinding processes require a lot of energy, the cement is removed right before it gets over-grinded. The coarse fraction is then returned back to the mill inlet.

9

Safety, Health, Environment and Sustainability

According to the Euratom Waste Directive, each country is required to create and implement a framework and program for the responsible and safe management of spent fuel and radioactive waste [78]. This means that it is critical to encapsulate the waste in a corrosion-resistant and mechanically stable container that will provide isolation for an appropriate period of time. Regarding this study it is important to note that the waste is disposed deep underground for thousands of years, which means that relocation of the spent fuel casks, or pressure control system is not possible, hence all safety precautions have to be considered before the waste enters the permanent disposal facility. This also includes, that it is required to evaluate the unforeseeable events such as fire, flooding or other natural or human caused occurrences.

9.1. Safety analysis

9.1.1. Bow-Tie for the Disposal System

As stated in the introduction, the main risk in this case is the production of hydrogen gas, which can cause a pressure buildup in the underground disposal facility, as well as the containment of radioactive waste, which may emit radiation that poses serious risks to human health and the environment. This, therefore, means that the main event that causes the hazard to lose control is foreign materials coming into contact with the canister.

The environment around the disposed waste is the primary factor that can influence the occurrence of a hazardous event. If the disposal site is near a seaside, corrosive species, particularly chlorides, can be carried to the canister surface and react with water to form a local area for corrosion. Furthermore, water in an alkaline environment can corrode the aluminium canister, so an additional layer or coating is required to prevent such threats from occurring.

The potential consequences have already been mentioned: Al corrosion, hydrogen gas production leading to pressure buildup, radionuclide diffusion, and a significant increase in criticality. To avoid this, the pH of the surrounding area can be maintained, a protective layer around the Al can be implemented, the amount of fissile material can be reduced, and the geometry of the canisters can be adjusted.

The visual representation for the safety assessment can be seen in Figure 9.1.

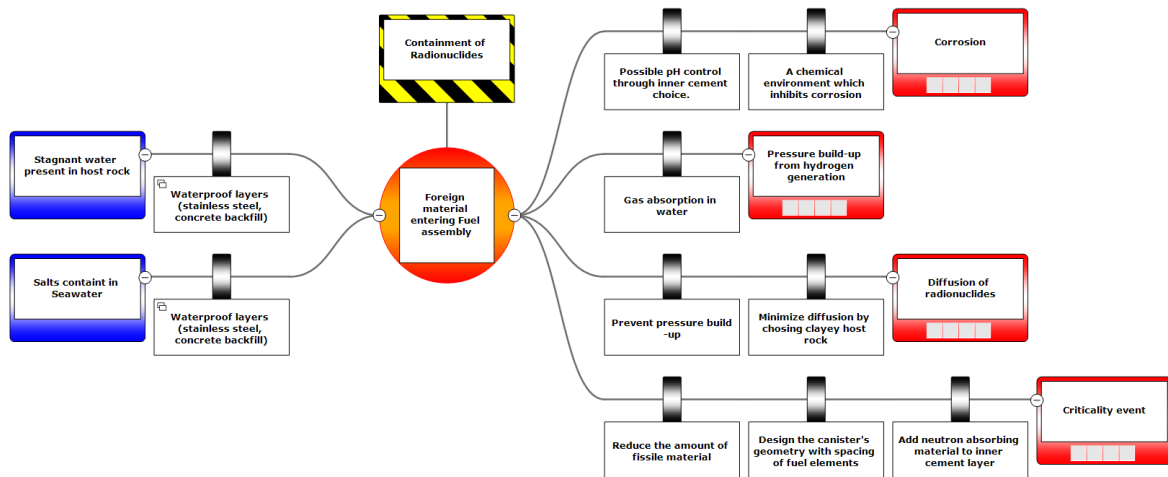


Figure 9.1: Bow-tie analysis: Foreign material entering fuel assembly

9.1.2. MPC Manufacturing safety analysis

Magnesium Phosphate cements, as earlier indicated, have a high potential for covering a uniform layer around the canister media. Since the manufacturing process of such cementitious media is investigated, safety concerns must be addressed.

Due to the high temperatures and pressures involved, the MPC manufacturing process can be described as intrinsically unsafe [79]. Addressing this issue requires the implementation of prevention measures such as minimizing hazardous equipment and materials as well as establishing good operating practices.

Starting from the materials, an overview of the potential hazardous properties of all the compounds involved in the process can be found in Table 9.1 below.

Table 9.1: Hazard(s) identification information of materials involved in MPC manufacturing [19]

Compounds	Hazard(s) Identification
KOH	Acute toxicity (oral). Skin corrosion/irritation. Hazardous to the aquatic environment - Acute
H ₃ PO ₄	Skin corrosion/irritation. Serious eye damage/eye.
KH ₂ PO ₄	Not considered hazardous by the 2012 OSHA Hazard Communication Standard.
CO ₂	Contains gas under pressure; may explode if heated. May displace oxygen and cause rapid suffocation. May increase respiration and heart rate.
MgCO ₃	May be harmful if swallowed.
MgO	May cause irritation of eyes, skin or nasal passages. May cause irritation of the upper respiratory passages.
H ₂ O	Not applicable.

Although some of the materials could lead to some serious issues and injuries, these can be alleviated by providing written instructions for the use of the hazardous substances and the risks involved, implementation of protective clothing and adequate training of the personnel. Given that COVRA is familiar with the complex handling of nuclear wastes, we are confident that carrying out these precautions will be attainable.

In terms of the production line itself, the manufacturing process includes two pieces of equipment that need to be investigated with a more careful eye. The first is the spray dryer due to the potential

clogging and over-pressurizing issues and the second is the rotary kiln because it reaches temperatures up to 1800°C degrees.

To address these issues, a limited Hazard and Operability studies (HAZOP) can be completed for both.

Table 9.2: Hazard & Operability Analysis (HAZOP) for the Spray Dryer

Guide Word	Deviation	Causes	Consequences	Action
No	No air flow	Pump turned off or clogged, residue buildup	Material not sprayed properly leading to improper drying	Consider flow indicator to ensure proper air flow, regular checks for residue
No	No product flow	Pump turned off or clogged, residue buildup, not enough material	Overpressurizing in the system, not enough yield	Ensure correct slurry consistency, regular checks for residue
Less	Too little product collected	Clogging at the output channels	Not enough yield, spray dryer capacity decrease, material buildup inside	Consider prepping the surface to minimize clogging, regular checks for residue
Early	Material added too early	Residue buildup, improper operational sequence	Slurry clogs the spray nozzle	Ensure airflow is turned on prior to the slurry flow, implement standardized procedural instructions
More	Too much pressure in dryer	Pump setting are off, air output is clogged	Possible explosion	Implement pressure detectors and isolation extinguishers to mitigate explosion propagation, regular checks for residue
More	Too high temperature	Heat exchanger is overworking, foreign particles enter the dryer and ignite	Possible explosion, unsafe working conditions	Implement temperature indicators and system that shuts down the process automatically if the temperature gets too high

Table 9.3: Hazard & Operability Analysis (HAZOP) for the Rotary Kiln

Guide Word	Deviation	Causes	Consequences	Action
No	No air flow	Pump turned off or clogged, residue buildup	Reaction doesn't progress, reduction in yield, wasted fuel	Regular checks for residue, implementation of standard operation procedures
No	No rotation	Gears blocked, residue buildup	Uneven mixing, reduction in yield, malfunctioning equipment	Regular checks for residue
Less	Too little product collected	Blockage, low temperature	Reduction in yield and capacity	Implementation of temperature indicators, regular checks for residue
Less	Not enough temperature achieved	Too little fuel	Reduction in yield, impure product	Implementation of flow meters to check the natural gas input
More	Too much flame	Foreign particles igniting	Damage to the equipment, explosion	Ensure reactant purity by buying from trusted sources
More	Too much pressure	Malfunctioning pump, blockage	Explosion, damage to the equipment	Implement pressure indicators

Although the rotary kiln reaches temperatures up to 1800°C degrees, an additional Dow's Fire and Explosion Index has not been performed as it requires the preparation of a full Piping and Instrumentation diagram as well as an idea for the layout of the processing plant.

As it can be seen from the process flow diagram of the manufacturing process in Figure 7.1 for the MPC, there are two main direct waste products: CO₂ and waste water. Knowing the contribution that CO₂ emissions have on climate change, we have incorporated a suggestion for CO₂ capture in the plan. Additionally, to minimize the use of clean water, we have decided to recycle the water coming out of the spray dryer back into the tank reactor.

Due to the nature of the product being part of a long-term nuclear waste management system with timelines reaching 1,000,000 years, an end-of-life analysis as part of a life cycle assessment (LCA) was deemed not applicable for this project. Additionally, since the plans for the GDF doesn't yet include a site location, the effects of transportation and manufacturer choice cannot be calculated within the scope of this report. However, given COVRA's experience with certified cement manufacturing, it can be assumed that the transportation costs related to MPC manufacturing will not play a huge role in the LCA done when more data is available.

9.2. Criticality

An important aspect of the safe disposal of nuclear waste is to prevent the waste from going critical. More concretely, the multiplication factor k_{eff} for the waste inside the ECN canister must not exceed 1. Factors that affect criticality include the amount of waste inside the canister, how closely is the material packed and the materials inside the canister. The materials affect the speed and the absorption of neutrons. For example, water slows down neutrons, allowing nuclear reactions to occur while, boron typically absorbs neutrons preventing the chain nuclear reactions from continuing.

In order to ensure the safe disposal of nuclear waste for extended periods of time the main factor that is going to be considered is the amount of fissile material. The reason for this is that this factor is the only one that can be controlled for the long time periods that are relevant in nuclear waste disposal. The fuel assemblies can be compressed during geological disposal. Consequently, the initial spacing is subject o change over time. Moreover, the water content of the cementitious fluid inside the canister can be increased due to ingress from the surrounding rock. Additionally, part of the cement can be leached away after long periods of time. This will result in increasing the criticality of the canister due to the moderating effect of the water.

The geometry and the materials of the problem is depicted in Figure 9.2. The geometry was made according to the one presented by Verhoef et al. [26]. The host rock can either be Kaolonite, Phlogopite, or a Salt Rock formation [22]. For the cementitious fluid MKPC cement will be used. Moreover it will also be replaced by water to model the additional safety cases. The steel plate will be either boron free or contain 1 % w/w boron. Because dimensions where not available for the steel basket by Verhoef et al. the thickness of the boron plates is assumed to be 2.5 mm around the fuel assemblies. For the circular outer steel plate the thickness is assumed to be 5 mm. The fuel assemblies 9.2 (right) consist of aluminum(pure Al) cladding and the fuel plates. Each plate contains a total amount of 7.7 g U-235 per plate. The thickness of the rectangular cladding surrounding the plates is not given by Verhoef et al. and is assumed to be 2.5 mm [26]. The exact Serpent code that was used to generate the geometry is given in Appendix C.

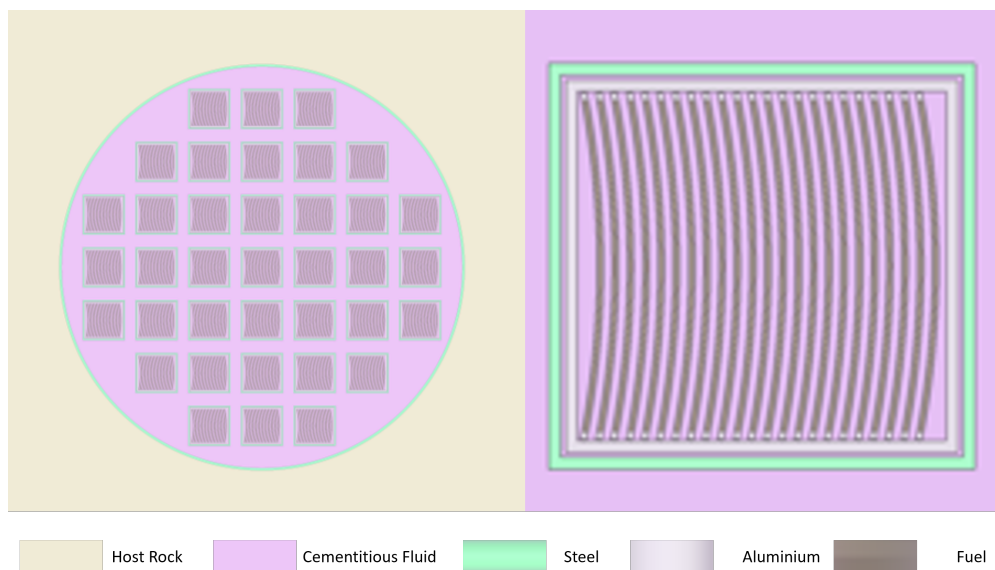


Figure 9.2: ECN canister Geometry and materials

As stated before total flooding is the worst case scenario. For this reason two different scenarios of total flooding will be examined. For the first one the surrounding host rock is assumed to be pure Kaolonite ($Al_4Si_4O_{10}(OH)_8$). The spacing between the the assemblies(the distance between the centers of the fuel rods) will be reduced until they are in contact with each other. The number of fuel rods ranges from 37 to 25. The use of borated steel (1% w/w) will also be examined as a medium for reducing criticality. The other scenario examines the effect of water ingress in salt rock formations (modelled as pure NaCl). The use of borated steel will again be be studied. This scenario is ran for 37 rods.

From the results in Figure 9.3(left) It can be determined that for pure steel plates the max amount that can be stored is 25 assemblies per canister. When borated steel is used on the other hand, the margin of safety is so large that more assemblies, can be stored safely. In 9.3(right) the effect of the salt concentration is apparent. As the salt concentration is increased the criticality drops significantly. Consequently the disposal of nuclear wast in salt formations seems to be safer as far as the criticality is concerned.

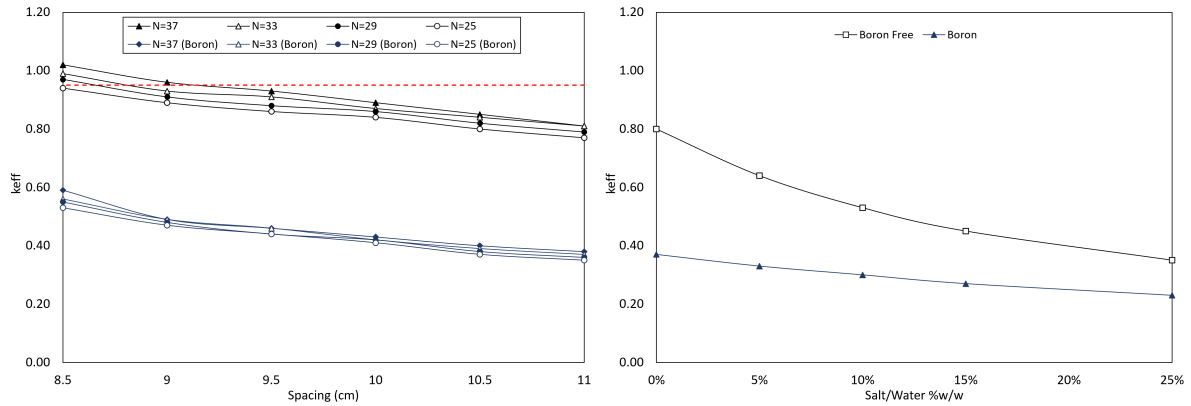


Figure 9.3: The multiplication factor k with respect to the spacing for different number of fuel rods (left) and with respect to salt content of water % w/w(right).

Finally, a base case scenario is run for a canister filled with MKPC developed in this study. It will be modeled as pure K-Sturvite ($\text{KMgPO}_4 \cdot 6\text{H}_2\text{O}$). For this case the canister is filled with 37 fuel rods. The effect of pure water ingress when the canister is disposed in Kaolinite ($\text{Al}_2\text{Si}_2\text{O}_5(\text{OH})_4$) and Phlogopite ($\text{KMg}_3(\text{AlSi}_3)\text{O}_{10}(\text{OH})_2$) will be examined. Finally, the effect of borated still will also be measured. The distance between the centers of two fuel assemblies is 11 cm.

From Figure 9.4 it is apparent that water ingress increases the criticality of the container. However the effect is not pronounced. The type of clay is insignificant for waste storage according to these calculations. The initial geometry with a spacing of 11cm is deemed safe for disposal, especially when borated steel is used. However in order to avoid criticality at all eventualities the maximum amount of rods that can be placed in a canister is 25 according to the first scenario(without borated steel plates).

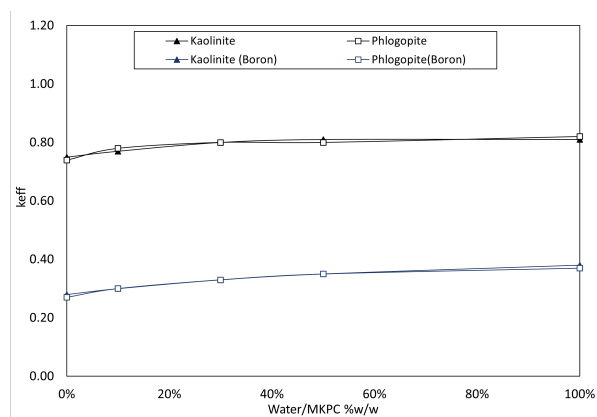


Figure 9.4: The multiplication factor k with respect to water content(from ingress by the surrounding rock) of MKPC cement % w/w.

The k_{eff} factor can not be determined analytically for complex geometries. For this reason the Serpent Monte Carlo code is used to determine the criticality multiplication factor. This code does not make any assumptions about the physics underlying the problem [80]. The boundary condition at the edges of the geometry was assumed to be the absorption of the neutrons when they reach the boundary of the domain. The cross-sections Σ were accessed from a data repository in TU Delft Servers. The data was available for 70 energy levels.

10

Economics

Since the product isn't for sale, there will be no cash flow or income, therefore we focused on the additional cost COVRA could theoretically expect. It has been reported that the overall waste to be treated at COVRA facilities are 104 m^3 and the free volume that can be filled with the cementitious media is 0.52 of the whole waste [1]. This leads to the required product volume of 54.08 m^3 or 123,779 kg. Assuming that the production of such amount of cement is split throughout 1/4 year, the required production rate is then 242.70 kg/hr. In other words, by knowing the mass fractions of the reacting powders (0.218, 0.490, 0.125 for MgO, KH_2PO_4 and H_3BO_3 respectively), the total volumetric rate of 86.5 l/hr is expected for the ball mill grinding device. From the information available on the internet, a ball mill of size 300L can be used with a rotary speed of approx 35 rpm [81]. The diameter of the mill (d) can be then determined from the critical speed (N_c) (reported to be 70-80% of the mill speed) by using the Equation 10.1 and 10.2 [82].

$$N_c = 42.29 * \sqrt{d} = 0.75 * 35 = 26.25 \text{rpm} \quad (10.1)$$

$$d = \left(\frac{42.29}{26.25}\right)^2 = 2.60 \text{m} = 8.52 \text{ft} \quad (10.2)$$

When using this diameter value in mache.com (the cost information for educational content website), the approximate cost for the ball mill is 832,800 USD in 2014, which is approx. 786,847 EUR (exchange rate on June 22,2022). This means that the cost of such a ball mill in 2022 is around 1,001,000 USD (946,000 EUR) [83]. However, when compared to data available on the internet, the ball mill prices appear to be significantly lower. As an example, a ball mill for cement grinding has been found at a price below 60,000 USD (56,700 EUR) [84]. Furthermore, because COVRA is already involved in cement mixing, it would be interesting to investigate the feasibility of using the equipment (forced mixer) they already have, given the small amount of product. As the ball mill price appears relatively high and the equipment is required for only 1/4 year, an alternative solution can be using another company for mixing/ grinding the cementitious powder.

Furthermore, because the production of cement requires a lot of equipment, and the required amount of the final product is relatively small (124,000 kg), it was decided to buy MgO, KH_2PO_4 and H_3BO_3 rather than produce them. Table 10.1 presents the amounts of raw materials that are needed for a production of 1 kg of final product. The price of water is taken from the 'Cost Sheet' from the course PPD. It can be seen that the total costs of the product is 0.76 EUR/kg. The price of water is only $5.86 * 10^{-05}$ €/kg. Compared to the prices of the other materials, this can be neglected.

Table 10.1: Material requirements for the production of 1 kg of final product

Raw material	kg of raw material/kg of product	Price (€/kg of raw material)	Price (€/kg of product)	Source
MgO	0.218	0.3	0.07	[85]
KH ₂ PO ₄	0.490	1.22	0.60	[86]
H ₃ BO ₃	0.125	0.75	0.09	[87]
H ₂ O	0.167	0.00035	0.00	
Total			0.76	

This leads to the raw material costs of 94,000 EUR for the desired MPC cement. In contrast, the Portland Cement and LiNO₃ blend of 1.50 wt% for the same volume would cost around 165,400 EUR (data from [54], and [39]), which is significantly higher. Furthermore, due to the widespread use of lithium in batteries, the availability of lithium nitrate is expected to become more limited, raising the price significantly. Thus, not only are the properties of MPC advantageous, but the economics of using such cement are also justified.

The only operation that is considered here, is the mixing in the ball mill. Therefore, 3 operators are needed per 4 hour shift in a 5 day work week with 8 hour days [74]. Resulting in 10950 hours needed to be covered. The equation for total labor-related operations O is dependant on 5 terms: direct wages and benefits (DW&B) for technical assistance, direct salaries and benefits for operators (DS&B), operating supplies and services (OS&S), technical assistance (TA) and lastly control laboratory (CL) [74].

$$O = DW\&B + DS\&B + OS\&S + TA + CL \quad (10.3)$$

Here DS&B and OS&S are both a percentage of DW&B, 15% and 6% respectively. DW&B can be calculated as seen in 10.4.

$$DW\&B = \frac{\text{operators}}{\text{shift}} * (\text{shifts}) * \frac{\text{hr}}{(\text{yr} * \text{operators})} * (\text{€/hr}) \quad (10.4)$$

TA and CL are a function of operators per shift as seen in 10.5 and 10.6.

$$TA = \$60000 / \left(\frac{\text{operators}}{\text{shift}} \right) = \text{€}56755 / \left(\frac{\text{operators}}{\text{shift}} \right) \quad (10.5)$$

$$CL = \$65000 / \left(\frac{\text{operators}}{\text{shift}} \right) = \text{€}61485 / \left(\frac{\text{operators}}{\text{shift}} \right) \quad (10.6)$$

An average of 21 €/hr for chemical plant operators taken [88]/ This gives the following values.

Term	Cost(k€)
DW&B	76.7
DS&B	11.5
OS&S	4.6
TA	6.3
CL	6.8
Total	105.8

Table 10.2: Manual labor cost

Maintenance costs are calculated as a percentage of the depreciable capital (C_{TDC}), a downtime of 1 week for maintenance is accounted for. Maintenance cost is the sum of wages and benefits (MW&B), salaries and benefits (S&B), materials and services (M&S) and maintenance overhead (MO) as seen in table 10.3 [74]. C_{TDC} is only the price of the ball mill, which was 56689 EUR.

Term	% of value x	Cost(€)
MW&B	4.5% of C_{TDC}	2551
S&B	25% of MW&B	637.75
M&S	100% of MW&B	2551
MO	5% of MW&B	127.55
Total		5752.30

Table 10.3: Maintenance cost

The overhead cost is taken as 22.8% of salary, wages, and benefits for maintenance and labor-related operation (M&O-SW&B), which is the sum of DW&B, DS&B, MW&B and S&B. Summing these values from 10.2 and 10.3 gives €91336.25.

Overall, assuming a 10-year lifetime for the ball mill, the annual costs, including labor and maintenance, are around 206,000 EUR when taking the most expensive equipment option into consideration (worst case scenario). Since a mixing process is required for any type of cementitious media, a thorough examination of possible alternatives for powder/cement mixing is required.

11

Creativity and Group Process Tools

Coming up with a successful solution or an approach to an engineering problem is a task deeply rooted in creativity just as much as it is on technical knowledge. Knowing this, we were challenged to figure out the most effective way to utilize creativity to come up with a novel approach to prevent aluminum corrosion for long-term spent nuclear fuel storage. Aside from our inclusion of the creativity methods that will be described below, our work also benefited from the group process tools that allowed us to use each of our strengths. In this chapter the creativity and group process tools utilized by our group will be discussed.

11.1. Creativity Tools

At the start of the project we were aware that we were given a very specific task for a problem to solve in an industry where not that familiar with. Actually, there are many aspects of the long-term storage strategy of COVRA for spent nuclear fuels that can be improved and approached with creativity tools. However not only were we to only focus on only one aspect but also our ideas were mostly constrained by the current scientific literature available.

Therefore, before we set out to do any brainstorming we tasked ourselves with reading as much of the available literature as we can. We all made sure to prepare a list of each of our ideas, so during the discussion each member was able to contribute. Our goal was to establish a more proactive creativity session where we would be less likely to feel stuck. Then we set up a brainstorming session to come up with several ideas to the limit aluminum corrosion that we could present our principal such as low pH cements, silica-based additives, etc. Upon talking to her we learned that many of the ideas we came up with were actually being investigated by COVRA or the other countries involved with long-term nuclear waste management. This was a very rewarding information to learn as it inspired us to not be afraid of connecting the papers we were reading with the project at hand.

In fact, we can even say that it triggered our creativity because we ended up combining ideas found in different studies to come up with novel approaches such as adding two levels of protection against the corrosion: both an inhibition layer onto the cladding and filled in gaps with reinforced cement material. In the upcoming stages of our project we will be continuing to use creativity and will be including the techniques utilized in our final report.

11.2. Group Process Tools

We had started exploring our group dynamic for the PPD course in the previous quarter by making our group profile and filling out the team role inventory test. The profile and the test results can be found in Appendix B. The results of the profile indicated that we would be strong with systematic thinking, domain knowledge and being persistent with problem situations which proved to be very useful when we were doing the literature study trying to come up with a suitable material. The profile also showed our potential weaknesses in creativity, economics, making the right choices, accuracy and coordination. Knowing these potential weaknesses influenced us to be more communicative, set internal check points that allow us to stick to the plans and keep in mind our differences when we get

tired and idea generation through brainstorming becomes fruitless. Keeping in mind our weaknesses and strengths we also assigned each member of the group some general responsibilities to keep us in track. These assigned roles can be found in the table below.

Table 11.1: Team Member Responsibilities

Names	Responsibilities
Agneta Meikšāne	Arranging meeting rooms, contacting people outside the group.
Alexandros Mantzanas	Assessing if ideas are realistic and finding literature that backs that up.
Deniz Erkan	Generates ideas and initiates group work, as well as finalizing the final report.
Jakob Bregman	Quality controller, who checks that objectives are met and aligned.
Kevin Koets	Coordinates meetings/discussions, to make sure that results are achieved within the time that is available.

Additionally, we decided to implement the use of the task manager in Microsoft Teams whenever we assigned new tasks for everyone to see each other's internal deadlines and make sure the work is divided evenly. Along this line we also made sure to ask our questions or communicate doubts with our supervisors in a timely manner. For this purpose and some added accountability, we had weekly meetings with our group coach to focus on our target deliverables for the week and our progress from the last week. These meetings allowed us to be better team players as it made us understand each person's contributions and concerns. During this quarter we also worked more on group integration. Even though because many of us lived far from campus working together every day was not an option, we made sure to have lunch together every time we were on campus. It was also a bonding experience to travel to the COVRA facilities together as it allowed us to get to know each other a little bit better and get a better understanding of our backgrounds.

Conclusion and further recommendations

11.3. Conclusion

As stated before, the scope of this project was to find a suitable material that could be added to the hardening fluid to cover the aluminium cladding around the UAl_x fuel in spent research reactor fuel. This is needed to inhibit the formation of hydrogen gas by corrosion of the cladding and the fuel meat, since this would most likely jeopardize the integrity of the barriers. The product that is chosen is a magnesium phosphate cement. This type of cement has a lower pH than ordinary Portland cement, which prevents the alkaline corrosion of the aluminium cladding. This product meets the requirements set at the start of the project. It can be handled at room temperature, which eases the application procedure. However the setting time is steel faster than OPC which could complicate the application process. The product does not contain any rare elements such as lithium. Also, no organic materials are included in the cement. Finally, it is suggested that the effect of $LiNO_3$ is temporary and that at longer time periods the H_2 generation of MKPC pastes with our without $LiNO_3$ converge.

Due to the low quantity needed, it was found that designing the described production process would not be feasible for this purpose. The investment costs would be way too high. Therefore it was decided to analyze the costs of the product only based on the mixing of the raw materials with a ball mill. The MPC raw material costs proved to be significantly lower (almost 2 times) instead of the before proposed Portland cement and $LiNO_3$ blend when taking the same free volume for canisters.

Moreover, criticality calculations were done to asses the ability of the spent fuel to sustain the nuclear chain reactions. Steel plates containing boron were found to be able to deal with all potential scenarios and prevent the fuel from exceeding the criticality limit.

One of the problems that arose during this project was the difficulty to compare the results between different literature. As every scientific paper uses their own very specific formulation of their cement, it is hard to predict the properties of the specific formulation that was made for this purpose. Also, it was not possible to verify this with experiments.

11.4. Recommendations

During this project, some simplifications or assumptions had to be made due to lack of time or resources. Therefore, some recommendations are made here on how to continue and improve the project.

11.4.1. Experimental work

Experiments could give a huge boost to this project when it comes to choosing the exact composition of the cement. As mentioned earlier, the literature was not sufficient to determine the exact properties (pH of pore waters, setting time, strength) of the final composition. Experiments could be used to determine the trends that determine the properties of the cement, while also investigating the relationship between adding different components at the same time. Moreover, studies with a longer time frame regarding the setting time are required in order to more accurately predict corrosion rate of Al embedded in cement. Another problem that requires further experimental work is the pH of MKPC cements surrounded by multiple engineered barriers made of OPC. The alkaline environment of the OPC cement could affect the near neutral pH of the MKPC paste.

11.4.2. Addition of additives

The addition of additives such as fly ash and silica was discussed in this report but not further pursued. This was done due to the fact that there was limited literature on the influence of these additives on the pore water pH of the cement. Despite this, it seems that these additives can have a significantly positive influence on the properties and/or price of the cement. Therefore, it would be interesting to further research the influence of these additives.

11.4.3. External production

Since the quantity of product required is not very large, one might consider cooperating with an outside company that already produces this type of cement. It does not make sense to make such a large investment in a production process for only a small quantity of product. One should investigate the possibility of having exact formulations of the cement produced by the company in question.

Reference list

- [1] E. Verhoef, E. Neeft, N. Chapman, and C. McCombie, *OPERA SAFETY CASE* www.covra.nl, Tech. Rep. (COVRA, 2017).
- [2] E. McCafferty, *Introduction to Corrosion Science* (Springer New York, 2010) pp. 357–402.
- [3] C. Cau Dit Coumes, D. Lambertin, H. Lahalle, P. Antonucci, C. Cannes, and S. Delpech, *Selection of a mineral binder with potentialities for the stabilization/solidification of aluminum metal*, *Journal of Nuclear Materials* **453**, 31 (2014).
- [4] G. Deissmann, K. Haneke, A. Filby, and R. Wieggers, *Corrosion behaviour of spent research reactor fuel under OPERA repository conditions*, (2016).
- [5] A. K. Prinja and E. W. Larsen, *General Principles of Neutron Transport*, *Handbook of Nuclear Engineering*, 427 (2010).
- [6] S. A. Walling and J. L. Provis, *Magnesia-Based Cements: A Journey of 150 Years, and Cements for the Future?* *Chemical Reviews* **116**, 4170 (2016).
- [7] S. Delpech, C. Cannes, N. Barré, Q. T. Tran, C. Sanchez, H. Lahalle, D. Lambertin, S. Gauffinet, and C. C. D. Coumes, *Kinetic Model of Aluminum Behavior in Cement-Based Matrices Analyzed by Impedance Spectroscopy*, *Journal of The Electrochemical Society* **164**, C717 (2017).
- [8] D. Wang, Y. Yue, T. Mi, S. Yang, C. McCague, J. Qian, and Y. Bai, *Effect of magnesia-to-phosphate ratio on the passivation of mild steel in magnesium potassium phosphate cement*, *Corrosion Science* **174**, 108848 (2020).
- [9] F. Qiao, C. K. Chau, and Z. Li, *Setting and strength development of magnesium phosphate cement paste*, *Advances in Cement Research* **21**, 175 (2009).
- [10] Y. Li and B. Chen, *Factors that affect the properties of magnesium phosphate cement*, *Construction and Building Materials* **47**, 977 (2013).
- [11] J. Wu, Z. Lai, Q. Deng, and M. Liu, *Effects of Various Curing Conditions on Volume Stability of Magnesium Phosphate Cement*, *Advances in Materials Science and Engineering* **2021** (2021), [10.1155/2021/6652363](https://doi.org/10.1155/2021/6652363).
- [12] L. J. Gardner, C. L. Corkhill, S. A. Walling, J. E. Vigor, C. A. Murray, C. C. Tang, J. L. Provis, and N. C. Hyatt, *Early age hydration and application of blended magnesium potassium phosphate cements for reduced corrosion of reactive metals*, *Cement and Concrete Research* **143**, 106375 (2021).
- [13] A. A. Boateng, *Rotary Kilns Transport Phenomena and Transport Processes*, 2nd ed. (Butterworth-Heinemann, Oxford, 2016).
- [14] H. A. Katzman, G. M. Malouf, R. Bauer, and G. W. Stupian, *Corrosion-protective chromate coatings on aluminum*, *Applications of Surface Science* **2**, 416 (1979).
- [15] J. Griffioen, M. Koenen, H. Meeussen, P. Cornelissen, L. Peters, and S. Jansen, *Geochemical interactions and groundwater transport in the Rupel Clay. A generic model analysis*, Tech. Rep. (2017).
- [16] T. Zhang, H. Chen, X. Li, and Z. Zhu, *Hydration behavior of magnesium potassium phosphate cement and stability analysis of its hydration products through thermodynamic modeling*, *Cement and Concrete Research* **98**, 101 (2017).

- [17] L. Wang, Y. Bai, P. A. Muhammed Basheer, C. Mccague, L. Wang, and Y. Bai, *Magnesium phosphate cement as a potential alternative for encapsulation of nuclear wastes containing aluminium* *Rational design of low-CO2 alkali-activated concretes for eco-efficiency and durability* View project *Rational design of low-CO2 alkali-activated*, (2011).
- [18] F. Schorcht, I. Kourti, B. M. Scalet, S. Roudier, and L. D. Sancho, *Best Available Techniques (BAT) Reference Document for the Production of Cement, Lime and Magnesium Oxide*, Tech. Rep. (Joint Research Centre, 2013).
- [19] *Safety Data Sheets | Free SDS Database | Chemical Safety*, .
- [20] M. Chase, *NIST-JANAF Thermochemical Tables*, 4th ed. (American Institute of Physics, Gaithersburg, 1998).
- [21] *Nuclear Energy Agency (NEA) - Radioactive waste management*, .
- [22] D. H. Dodd, J. B. Grupa, M. Houkema, J. B. M. De Haas, T. Van Der Kaa, and A. C. Veltkamp, *Direct Disposal of Spent Fuel from Test and Research Reactors in the Netherlands*, (2000).
- [23] N. Watson, *Global Overview of Radioactive Waste and Spent Fuel Management | IAEA*, (2022).
- [24] IAEA, *IAEA Nuclear Energy Series*, Tech. Rep. (International Atomic Energy Agency, 2018).
- [25] N. Chapman, E. Neeft, A. Buitenhuis, C. McCombie, J. Bartol, G. Van Der Veen, and M. Vuorio, *Long-term research programme for disposal of radioactive waste*, Tech. Rep. November (COVRA, Nieuwdorp, 2020).
- [26] E. V. Verhoef, E. A. C. Neeft, G. Deissmann, A. Filby, R. B. Wieggers, and D. A. Kers, *OPERA-PG-COV023 Waste families in OPERA*, Tech. Rep. (COVRA, 2016).
- [27] L. Gil, *Countries move towards low enriched uranium to fuel their research reactors*, .
- [28] B. Kursten, E. Smailos, I. Azkarate, L. Werme, N. Smart, and G. Santarini, *EUROPEAN COMMISSION 5th EURATOM FRAMEWORK PROGRAMME 1998-2002 KEY ACTION : NUCLEAR FISSION COBECOMA State-of-the-art document on the CORrosion BEhaviour of CONtainer MATerials CONTRACT N° FIKW-CT-20014-20138 FINAL REPORT*, Tech. Rep. (European Commission, 2001).
- [29] H. Verweij and S. Nelskamp, *Definition of the present boundary conditions for the near-field model_1*, Tech. Rep. (2016).
- [30] J. F. Harrington, R. J. Cuss, A. C. Wiseall, K. A. Daniels, C. C. Graham, and E. Tamayo-Mas, *Scoping study examining the behaviour of Boom Clay at disposal depths investigated in OPERA*, Tech. Rep. (COVRA, 2017).
- [31] T. Behrends, I. Van Der Veen, A. Hoving, and J. Griffioen, *Geochemical characterization of Rupel (Boom) clay material: pore water composition, reactive minerals and cation exchange capacity*, Tech. Rep. (COVRA, 2015).
- [32] S. Seetharam and D. Jacques, *Potential Degradation Processes of the Cementitious EBS Components, their Potential Implications on Safety Functions and Conceptual Models for Quantitative Assessment*, Tech. Rep. (COVRA, 2015).
- [33] A. M. Olivares-Ramírez, de Jesús, O. Jiménez-Sandoval, and R. C. Pless, *Hydrogen Generation by Treatment of Aluminium Metal with Aqueous Solutions: Procedures and Uses*, in *Hydrogen Energy*, edited by D. Minic (IntechOpen, Rijeka, 2012) Chap. 3.
- [34] N. Connor, *What is Thermal Conductivity of Materials and Chemical Elements - Definition*, (2019).
- [35] W. J, P. Norris, and S. Sillen, *DELIVERABLE 6.1: Initial State of the Art on Gas Transport in Clayey Materials Project Title European Joint Programme on Radioactive Waste Management Work Package Title Mechanistic understanding of gas transport in clay materials Deliverable Title Initial*, Tech. Rep. (European Joint Programme on Radioactive Waste Management, 2021).

- [36] A. W. Harris, A. Atkinson, and P. A. Claisse, *TRANSPORT OF GASES IN CONCRETE BARRIERS, WASTE MANAGEMENT* **12**, 155 (1992).
- [37] M. Murmu, S. K. Saha, N. C. Murmu, and P. Banerjee, *Inorganic Anticorrosive Materials* (Elsevier Science, 2022) pp. 269–296.
- [38] T. Matsuo, K. Kobayashi, and K. Tago, *Estimation of the Solubility Dependence of Aluminate Salts of Alkali Metals on Ion Radii of Alkali Metals by LDF Molecular Orbital Calculations*, *The Journal of Physical Chemistry* **100**, 6531 (1996).
- [39] T. Matsuo, T. Izumida, M. Hironaga, Y. Horikawa, and T. Shiomi, *LiNO₃ effect on corrosion prevention of aluminum with complex shapes*, *Journal of Nuclear Science and Technology* **34**, 823 (1997).
- [40] M. Nicu, L. Ionascu, C. Turcanu, and F. Dragolici, *USE OF LITHIUM NITRATE AS A POTENTIALLY CORROSION INHIBITOR FOR RADIOACTIVE ALUMINIUM IN CEMENTING SYSTEMS*, *Romanian Journal of Physics* **60**, 1193–1202 (2014).
- [41] Ashok Santra, Christopher L. Gordon, Daniel L. Bour, Keith D. Pewitt, and Dwain King, *SOREL CEMENTS AND METHODS OF MAKING AND USING SAME*, (2008).
- [42] D. A. Hall, R. Stevens, and B. El-Jazairi, *The effect of retarders on the microstructure and mechanical properties of magnesia-phosphate cement mortar*, *Cement and Concrete Research* **31**, 455 (2001).
- [43] T. S. Narayanan, *Surface pretreatment by phosphate conversion coatings - A review*, *Reviews on Advanced Materials Science* **9**, 130 (2005).
- [44] C. Vargel, *Corrosion of aluminium*, 2nd ed. (Elsevier, Amsterdam, 2020).
- [45] M. A. Arenas, A. Conde, and J. J. De Damborenea, *Cerium: A suitable green corrosion inhibitor for tinplate*, *Corrosion Science* **44**, 511 (2002).
- [46] M. Dabalà, L. Armelao, A. Buchberger, and I. Calliari, *Cerium-based conversion layers on aluminium alloys*, *Applied Surface Science* **172**, 312 (2001).
- [47] M. Gobara, A. Baraka, R. Akid, and M. Zorainy, *Corrosion protection mechanism of Ce⁴⁺/organic inhibitor for AA2024 in 3.5% NaCl*, *RSC Advances* **10**, 2227 (2020).
- [48] K. Wandelt, *Encyclopedia of Interfacial Chemistry* (Elsevier, 2018).
- [49] D. Wang, M. Wu, J. Ming, and J. Shi, *Inhibitive effect of sodium molybdate on corrosion behaviour of AA6061 aluminium alloy in simulated concrete pore solutions*, *Construction and Building Materials* **270**, 121463 (2021).
- [50] Y. Huang, S. Mu, Q. Guan, and J. Du, *Corrosion Resistance and Formation Analysis of a Molybdate Conversion Coating Prepared by Alkaline Treatment on Aluminum Alloy 6063*, *Journal of The Electrochemical Society* **166**, C224 (2019).
- [51] D. Féron, *Overview of nuclear materials and nuclear corrosion science and engineering*, *Nuclear Corrosion Science and Engineering*, **31** (2012).
- [52] J. H. Osborne, *Observations on chromate conversion coatings from a sol–gel perspective*, *Progress in Organic Coatings* **41**, 280 (2001).
- [53] C. Adams, *What is a Pugh Matrix?* .
- [54] *Factory Supply Lowest Price 99% Lithium Nitrate Lino3 Cas:7790-69-4 - Buy Nitrate,Fertilizer,Lithium Nitrate Product on Alibaba.com*, .
- [55] M. Espanol, R. Perez, E. Montufar, C. Marichal, A. Sacco, and M. Ginebra, *Intrinsic porosity of calcium phosphate cements and its significance for drug delivery and tissue engineering applications*, *Acta Biomaterialia* **5**, 2752 (2009).

- [56] National Center for Biotechnology Information, [Chromium trihydroxide | CrH6O3 - PubChem](#), .
- [57] P. Bennett, *RECOMMENDATIONS FOR THE CONDITIONING OF SPENT METALLIC URANIUM FUEL AND ALUMINIUM CLAD FUEL FOR INTERIM STORAGE AND DISPOSAL*, Tech. Rep. (Nærings- og handelsdepartementet, Halden, 2010).
- [58] S. Fan and B. Chen, *Experimental study of phosphate salts influencing properties of magnesium phosphate cement*, [Construction and Building Materials](#) **65**, 480 (2014).
- [59] L. Chong, C. Shi, J. Yang, and H. Jia, *Effect of limestone powder on the water stability of magnesium phosphate cement-based materials*, [Construction and Building Materials](#) **148**, 590 (2017).
- [60] L. Chong, J. Yang, and C. Shi, *Effect of curing regime on water resistance of magnesium-potassium phosphate cement*, [Construction and Building Materials](#) **151**, 43 (2017).
- [61] B. Xu, F. Winnefeld, J. Kaufmann, and B. Lothenbach, *Influence of magnesium-to-phosphate ratio and water-to-cement ratio on hydration and properties of magnesium potassium phosphate cements*, [Cement and Concrete Research](#) **123**, 105781 (2019).
- [62] B. Xu, B. Lothenbach, A. Leemann, and F. Winnefeld, *Reaction mechanism of magnesium potassium phosphate cement with high magnesium-to-phosphate ratio*, [Cement and Concrete Research](#) **108**, 140 (2018).
- [63] H. Lahalle, C. Cau Dit Coumes, C. Mercier, D. Lambertin, C. Cannes, S. Delpéch, and S. Gauffinet, *Influence of the w/c ratio on the hydration process of a magnesium phosphate cement and on its retardation by boric acid*, [Cement and Concrete Research](#) **109**, 159 (2018).
- [64] [Cement CEM III/A 42,5N - CEMMAC](#), .
- [65] M. A. Haque and B. Chen, *Research progresses on magnesium phosphate cement: A review*, [Construction and Building Materials](#) **211**, 885 (2019).
- [66] T. Sugama and L. Kukacka, *Magnesium Monophosphate Cements Derived From Diammonium Phosphate Solutions*, [Cement and Concrete Research](#) **13**, 407 (1983).
- [67] A. Wagh, *Chemically Bonded Phosphate Ceramics Twenty-First Century Materials with Diverse Applications* (Elsevier Science, 2005) p. 304.
- [68] J. Grzella and A. Lurgi, *Metallurgical Furnaces*, [Nature](#) **112**, 755 (1923).
- [69] J. Iannicelli and J. Pectin, [PROCESS FOR THE MANUFACTURE OF MONOBASIC POTASSIUM PHOSPHATE](#), (2009).
- [70] S. Klaib, *Production of Mono-Potassium Phosphate*, (2015).
- [71] Delta T Systems, [Reactor Temperature Control](#), .
- [72] HGH Infrared Systems, [Continuous thermal monitoring of rotary kiln](#), .
- [73] J. Qin, F. Dai, H. Ma, X. Dai, Z. Li, X. Jia, and J. Qian, *Development and characterization of magnesium phosphate cement based ultra-high performance concrete*, [Composites Part B: Engineering](#) **234**, 109694 (2022).
- [74] W. Seider, D. Lewin, J. Seader, S. Widagdo, R. Gani, and K. Ng, *Product and Process Design Principles*, 4th ed. (John Wiley & Sons, 2016).
- [75] FLSmidth, [Rotary Cooler - Direct](#), .
- [76] D. Schmidtmeier, G. Büchel, and A. Buhr, *Magnesium aluminate spinel raw materials for high performance refractories for steel ladles*, [Ceramic Materials](#) **61**, 223 (2009).
- [77] P. del Strother, *2 - Manufacture of Portland Cement*, in [Lea's Chemistry of Cement and Concrete \(Fifth Edition\)](#), edited by P. C. Hewlett and M. Liska (Butterworth-Heinemann, 2019) fifth edit ed., pp. 31–56.

- [78] NEA Radioactive Waste Management Committee, *Radioactive Waste Management Moving Forward with Geological Disposal of Radioactive Waste. A Collective Statement by the NEA Radioactive Waste Management Committee (RWMC)*, , 23 (2008).
- [79] R. K. Sinnott, *Coulson & Richardson's CHEMICAL ENGINEERING*, Vol. 6 (Elsevier Butterworth-Heinemann, 2005) pp. 360–660.
- [80] J. Leppänen, M. Pusa, T. Viitanen, V. Valtavirta, and T. Kaltiaisenaho, *The Serpent Monte Carlo code: Status, development and applications in 2013*, *Annals of Nuclear Energy* **82**, 142 (2015).
- [81] Tmax battery Equipments, *Lab Light Roll Ball Mill Machine suppliers,manufacturers,for sale*, .
- [82] Dylan Moore, *Cement Kilns: Size Reduction and Grinding*, (2021).
- [83] *Dollar Euro » Exchange rate Dollar to Euro*, .
- [84] *Small Size Quartz Batch Magnetite Ore Mill,Ball Mill For Cement Factory,Ball Mill Cost - Buy Small Size Magnetite Ore Mill,Ball Mill For Cement Factory,Ball Mill Cost Product on Alibaba.com*, .
- [85] *Dead Burnt Magnesite, Packaging: 25 kg, Packaging Type: Packet*, .
- [86] *Industrial Potassium Phosphate Monobasic MKP Chemical Formula KH₂PO₄*, .
- [87] *Top Quality Boric acid chemical product powder*, .
- [88] *Chemical Plant Operator Average Salary in Netherlands 2022 - The Complete Guide*, .
- [89] *Properties of substance: potassium dihydrogen phosphate*, .

Appendices contents

A	Appendix A	1
A.1	Chromate Hydroxide Coating	1
A.2	Cerium salts	2
A.3	Phosphate conversion coating	2
A.4	Molybdate Coating	2
B	Appendix B	4
B.1	Thermodynamic data	4
	B.1.1 Heat capacities	4
	B.1.2 Standard Enthalpies of formation	4
B.2	General energy balance	5
B.3	Mass fractions of streams	6
C	Appendix E	7
C.1	Serpent code used for the criticality calculations	7

A

Appendix A

A.1. Chromate Hydroxide Coating

The first step in applying a chromate coating is the removal of the AlO_2 layer. This can be done either in an HF solution (pH=1.5) or with a hydroxide solution with (pH=11). After the oxide layer is removed the dichromate ion reacts with the aluminum surface with the following reaction,



HF also dissolves the aluminium hydroxide leaving a layer of only chromate hydroxide coating the aluminium. This means that the acid plays an important role during the coating application process[14]. The complete mechanism of the formation of the chromate coating is depicted in Figure A.1

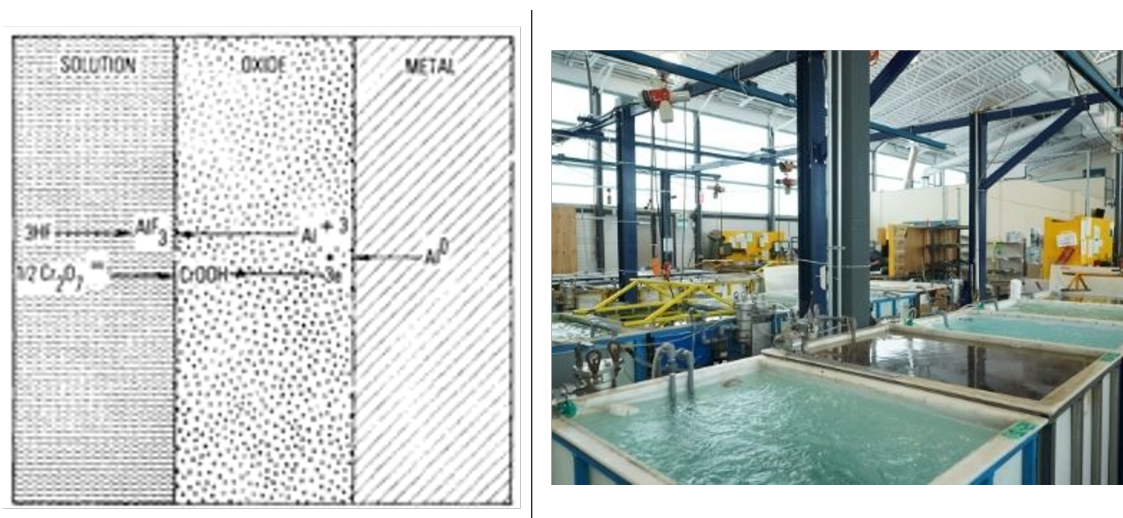


Figure A.1: Layer formation mechanism [14](left) and application process(right)

An excess of unreacted Cr remains in the film, which means that the film can have self-healing properties. The reason the chromium ion binds so well with the aluminium surface is their similar ionic radii. The chromium oxide hydroxide layer is insoluble and impervious, thus providing excellent corrosion resistance properties. This can be seen by the much lower equilibrium pH of chromate coating compared to the aluminium hydroxide one as seen in table A.1.

Table A.1: K_{sp} and equilibrium pH in pure water of hydroxide compounds

Hydroxide	K_{sp}	pH
Al(OH) ₃	$1.8 * 10^{-5}$	12.93
Cr(OH) ₃	$6.3 * 10^{-5}$	6.57

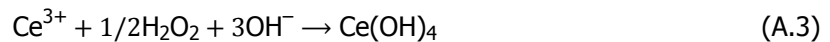
As stated before the coating solution must also be acidic for the coating mechanism to work. This means that it cannot be directly incorporated in the cement mixture as COVRA envisions. Instead, these coatings are usually applied by dipping the aluminum in a series of baths as depicted in Figure A.1.

A.2. Cerium salts

Cerium(III)-salts are widely used as cathodic corrosion inhibitors. They are often named as a replacement of the toxic chromate coatings. They are able to form insoluble oxide layers which precipitate at the cathodic sites, inhibiting the corrosion process. This takes place according to reaction A.2. If hydrogen peroxide is also present, it can oxidize Cerium(III) to Cerium(IV). After that it can also form an even less soluble layer according to reaction A.3.

The formation of the cerium coating is done by immersing the aluminium in a solution of a cerium salt. Before and after the actual formation of the coating, there are several other steps which include rinsing and cleaning of the surface. Cerium chloride (CeCl₃) is considered to be the most effective salt. The formation process is rather slow, but there are multiple ways to speed this up, like for example thermal activation at 50°C.

Cerium salts seem to be a promising solution, as they show comparable inhibition to chromate coatings, but aren't toxic. Their application has to be done by immersing in solution, which implies that the fuel assemblies have to be taken out of the ECN-canister. Also, cerium is a quite abundant element.

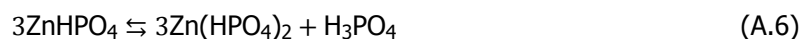
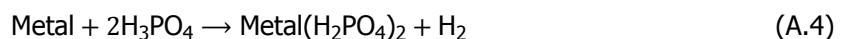


A.3. Phosphate conversion coating

Phosphates are widely used for corrosion inhibition of steel, but is also increasingly being investigated for its application to aluminium. A metal such as steel or aluminium, is dipped into a bath of phosphoric acid and a metal phosphate such as Zinc-, Manganese- or Iron phosphate. The phosphoric acid attacks the metal surface according to Reaction A.4. The consumption of protons in vicinity of the surface increases the pH locally. When the pH becomes high enough, the phosphate ions of the metal phosphate become insoluble, and eventually precipitate on the surface according to reactions A.5 and A.6.

The steps in phosphating a metal surface are the following: cleaning of the surface, rinsing, activation with for example a titanium phosphate, phosphating and rinsing. As the formed phosphate layer is still quite porous, the surface is usually treated with chromic acid, which reduces the porosity with ≈ 50%. As the formation of this layer is in practice very slow, different accelerators can be used to speed up the process, such as sodium-nitrite.

The coatings made with phosphates seem to be less corrosion-resistant than other coatings, such as chromate- and cerium-coatings. Phosphates are also widely used in fertilizers and their occurrence is limited. This makes their use less attractive.



A.4. Molybdate Coating

The molybdate ion (MoO₄²⁻) is a widely used corrosion inhibitor for a variety of metals. In contrast to the high toxicity and carcinogenic nature of many potential inhibitors for aluminium in alkaline conditions,

MoO_4^{2-} ion provides an environmentally friendly alternative with low toxicity that proves to be effective in a variety of conditions.

While studying the inhibitive effect of sodium molybdate on the corrosion behaviour of AA6061 aluminum alloy in various concentrations, Wang et. al suggested that the mechanism for the corrosion can be assumed to initiate with the adsorption of Mo species on the surface of the metal. In moderate MoO_4^{2-} concentrations (10mM), optimum corrosion efficiency is achieved and a uniform oxide layer forms. Below is the illustration of the corrosion mechanism for this moderate MoO_4^{2-} concentration (10mM) case in simulated concrete pore solutions.

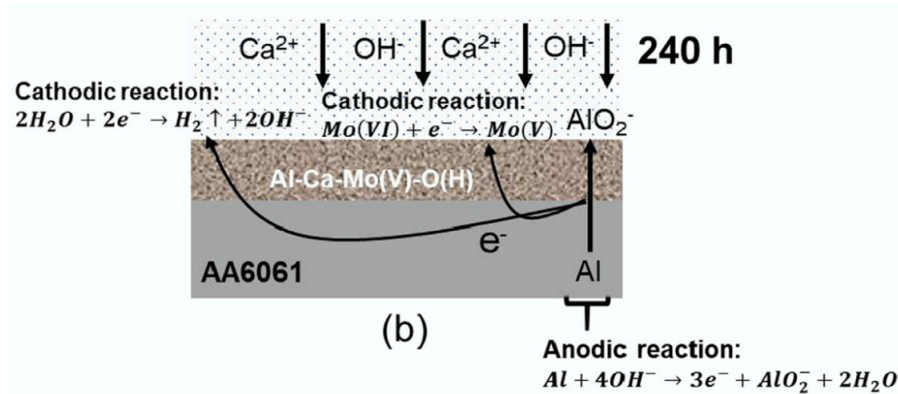


Figure A.2: Schematic illustration of the inhibition mechanism for aluminium corrosion in 10mM MoO_4^{2-} concentration in concrete pore solutions

It should be noted that the mechanism shown above varies in different pH conditions due to molybdenum's changing oxidation capacity with increased pH conditions. As described before we are concerned with highly alkaline conditions at enhanced temperatures in this project and it was reported that the protective layer formed would be $\text{Al}_2(\text{MoO}_4)_3$ and Al_2O_3 .

B

Appendix B

B.1. Thermodynamic data

B.1.1. Heat capacities

The heat capacities that were used for the energy balances were calculated according to the Shomate equation, which is displayed in Equation B.1. This equation calculates the heat capacity in $J/(mol \cdot K)$. The variable t is the temperature in Kelvin, divided by 1000. The constants for this formula for every compound can be found in Table B.1. The heat capacity constants for KH_2PO_4 could not be found, so for this compound a constant heat capacity of $116.57 kJ/mol \cdot K$ was used (C_p at 298K). [89]

$$C_p = A + B \cdot t + C \cdot t^2 + D \cdot t^3 + E/t^2 \quad (B.1)$$

Table B.1: Heat capacities constants that were used for the energy balances. All of this data is retrieved from the 'NIST-JANAF Thermochemical Tables' [20]

Compound	Temperature range (K)	A	B	C	D	E
CO ₂	298-1200	24.99735	55.18696	-33.69137	7.948387	-0.136638
CO ₂	1200-6000	58.16639	2.720074	-0.492289	0.038844	-6.447293
MgCO ₃	298-1000	44.937	149.7085	-74.18274	11.97670	-0.629261
MgO	298-3105	47.25995	5.681621	-0.872665	0.104300	-1.053955
-	-	-	-	-	-	-
H ₂ O(l)	298-500	-203.6060	1523.290	-3196.413	2474.455	3.855326
H ₂ O(g)	500-1700	30.09200	6.832514	6.793435	-2.534480	0.082139
H ₃ PO ₄ (s)	298-315.5	15.48331	303.7442	-0.968190	0.386907	0.007645
H ₃ PO ₄ (l)	315.5-1000	55.20955	301.3204	-0.095194	0.042310	0.000512
KOH	298-516	80.78258	-112.2329	301.1543	-147.9923	-0.468867

B.1.2. Standard Enthalpies of formation

Table B.2: Standard enthalpies of formation of the used chemicals

Chemical	H _f ⁰ (kJ/mol)	Reference
H ₃ PO ₄	-1271,66	[20]
KOH	-425,8	[20]
KH ₂ PO ₄	-1573,6024	[89]
H ₂ O(l)	-285,83	[20]
H ₂ O(g)	-241,83	[20]
MgCO ₃	-1111,69	[20]
MgO	-601,6	[20]
CO ₂	-393,5	[20]

B.2. General energy balance

Table B.3: Energy flows in the MgO-process

Stream	Mole flow (mole/hr)	H_0 (kJ/mol)	H(kJ/hr)
In			
MgCO ₃	1312.04	-1111.69	-1,458,584
Heating	-	-	402,221
Total			-1,056,363
Out			
MgO	1312.04	-601.6	-789,325
CO ₂	1312.04	-393.5	-516,289
Cooling	-	-	244,804
Total			-1,060,810

Table B.4: Energy flows in the KH₂PO₄-process

Stream	Mole flow (mole/hr)	H_0 (kJ/mol)	H(kJ/hr)
In			
H ₃ PO ₄	874.69	-1271.66	-1,112,315
KOH	874.69	-425.8	-372,445
H ₂ O	149489.30	-285.83	-42,728,526
Heating	-	-	8,500,105
Total			35,713,181
Out			
KH ₂ PO ₄	874.69	-1573.6024	-1,376,422
H ₂ O	150363.99	-285.83	-42,978,540
Cooling	-	-	8,638,595
Total			35,716,367

B.3. Mass fractions of streams

Table B.5: Fraction table

Stream	MgCO ₃	MgO	CO ₂	KOH	H ₃ PO ₄	H ₂ O	KH ₂ PO ₄	H ₃ BO ₃
F1	-	-	-	-	-	1	-	-
F2	-	-	-	0.45	-	0.55	-	-
F3	-	-	-	-	0.85	0.15	-	-
F4	1	-	-	-	-	-	-	-
F5	-	-	-	-	-	-	-	1
1	-	-	-	-	-	1	-	-
2	-	-	-	0.45	-	0.55	-	-
3	-	-	-	-	0.85	0.15	-	-
4	-	-	-	-	-	0.96	0.04	-
5	-	-	-	-	-	0.96	0.04	-
6	-	-	-	-	-	0.96	0.04	-
7	-	-	-	-	-	0.96	0.04	-
8	-	-	-	-	-	0.96	0.04	-
9	-	-	-	-	-	-	1	-
10	-	-	-	-	-	0.991	0.009	-
11	-	-	-	-	-	0.991	0.009	-
12	-	-	-	-	-	-	1	-
13	-	-	-	-	-	1	-	-
14	-	-	-	-	-	-	1	-
15	-	-	-	-	-	-	1	-
16	-	-	-	-	-	1	-	-
17	-	-	-	-	-	1	-	-
18	-	-	-	-	-	-	1	-
19	-	-	-	-	-	1	-	-
20	-	-	-	-	-	1	-	-
21	1	-	-	-	-	-	-	-
22	-	-	1	-	-	-	-	-
23	-	-	1	-	-	-	-	-
24	-	1	-	-	-	-	-	-
25	-	1	-	-	-	-	-	-
E1	-	-	1	-	-	-	-	-
E2	-	-	-	-	-	1	-	-
E3	-	0.218	-	-	-	0.167	0.49	0.125

C

Appendix E

C.1. Serpent code used for the criticality calculations

```
set title "can"  
——define surfaces——  
surf 1 pad -21.95 0 18.606 18.657 -10.484 10.484  
surf 2 pad -21.64 0 18.606 18.657 -10.484 10.484  
surf 3 pad -21.33 0 18.606 18.657 -10.484 10.484  
surf 4 pad -21.01 0 18.606 18.657 -10.484 10.484  
surf 5 pad -20.70 0 18.606 18.657 -10.484 10.484  
surf 6 pad -20.39 0 18.606 18.657 -10.484 10.484  
surf 7 pad -20.07 0 18.606 18.657 -10.484 10.484  
surf 8 pad -19.76 0 18.606 18.657 -10.484 10.484  
surf 9 pad -19.45 0 18.606 18.657 -10.484 10.484  
surf 10 pad -19.14 0 18.606 18.657 -10.484 10.484  
surf 11 pad -18.82 0 18.606 18.657 -10.484 10.484  
surf 12 pad -18.51 0 18.606 18.657 -10.484 10.484  
surf 13 pad -18.20 0 18.606 18.657 -10.484 10.484  
surf 14 pad -17.88 0 18.606 18.657 -10.484 10.484  
surf 15 pad -17.57 0 18.606 18.657 -10.484 10.484  
surf 16 pad -17.26 0 18.606 18.657 -10.484 10.484  
surf 17 pad -16.95 0 18.606 18.657 -10.484 10.484  
surf 18 pad -16.63 0 18.606 18.657 -10.484 10.484  
surf 19 pad -16.32 0 18.606 18.657 -10.484 10.484  
surf 20 pad -16.01 0 18.606 18.657 -10.484 10.484  
surf 21 pad -15.70 0 18.606 18.657 -10.484 10.484  
surf 22 pad -15.38 0 18.606 18.657 -10.484 10.484  
surf 23 pad -15.07 0 18.606 18.657 -10.484 10.484  
surf 24 cuboid -4.028 4.028 -3.805 3.805 0 60  
surf 25 cuboid -3.787 3.787 -3.570 3.570 0 60  
surf 30 pad -21.95 0 18.568 18.695 -10.984 10.984  
surf 31 pad -21.64 0 18.568 18.695 -10.984 10.984  
surf 32 pad -21.33 0 18.568 18.695 -10.984 10.984  
surf 33 pad -21.01 0 18.568 18.695 -10.984 10.984  
surf 34 pad -20.70 0 18.568 18.695 -10.984 10.984  
surf 35 pad -20.39 0 18.568 18.695 -10.984 10.984  
surf 36 pad -20.07 0 18.568 18.695 -10.984 10.984  
surf 37 pad -19.76 0 18.568 18.695 -10.984 10.984  
surf 38 pad -19.45 0 18.568 18.695 -10.984 10.984  
surf 39 pad -19.14 0 18.568 18.695 -10.984 10.984  
surf 40 pad -18.82 0 18.568 18.695 -10.984 10.984
```

```
surf 41 pad -18.51 0 18.568 18.695 -10.984 10.984
surf 42 pad -18.20 0 18.568 18.695 -10.984 10.984
surf 43 pad -17.88 0 18.568 18.695 -10.984 10.984
surf 44 pad -17.57 0 18.568 18.695 -10.984 10.984
surf 45 pad -17.26 0 18.568 18.695 -10.984 10.984
surf 46 pad -16.95 0 18.568 18.695 -10.984 10.984
surf 47 pad -16.63 0 18.568 18.695 -10.984 10.984
surf 48 pad -16.32 0 18.568 18.695 -10.984 10.984
surf 49 pad -16.01 0 18.568 18.695 -10.984 10.984
surf 50 pad -15.70 0 18.568 18.695 -10.984 10.984
surf 51 pad -15.38 0 18.568 18.695 -10.984 10.984
surf 52 pad -15.07 0 18.568 18.695 -10.984 10.984
surf 29 cuboid -4.128 4.128 -3.905 3.905 0 60
surf 80 cuboid -4.378 4.378 -4.155 4.155 0 60
surf 26 cyl 0 0 42.3 0 60
surf 27 cyl 0 0 41.8 0 60
surf 90 cuboid -52.3 52.3 -52.3 52.3 -10 72.5
surf 28 cyl 0 0 25
surf 100 pz 60
surf 200 pz 0
surf 210 cuboid -100 100 -100 100 -60 120
——define cells——
cell 1 1 uranium -1
cell 2 1 uranium -2
cell 3 1 uranium -3
cell 4 1 uranium -4
cell 5 1 uranium -5
cell 6 1 uranium -6
cell 7 1 uranium -7
cell 8 1 uranium -8
cell 9 1 uranium -9
cell 10 1 uranium -10
cell 11 1 uranium -11
cell 12 1 uranium -12
cell 13 1 uranium -13
cell 14 1 uranium -14
cell 15 1 uranium -15
cell 16 1 uranium -16
cell 17 1 uranium -17
cell 18 1 uranium -18
cell 19 1 uranium -19
cell 20 1 uranium -20
cell 21 1 uranium -21
cell 22 1 uranium -22
cell 23 1 uranium -23
cell 40 1 aluminum -30 1
cell 41 1 aluminum -31 2
cell 42 1 aluminum -32 3
cell 43 1 aluminum -33 4
cell 44 1 aluminum -34 5
cell 45 1 aluminum -35 6
cell 46 1 aluminum -36 7
cell 47 1 aluminum -37 8
cell 48 1 aluminum -38 9
cell 49 1 aluminum -39 10
cell 50 1 aluminum -40 11
```

cell 51 1 aluminum -41 12
cell 52 1 aluminum -42 13
cell 53 1 aluminum -43 14
cell 54 1 aluminum -44 15
cell 55 1 aluminum -45 16
cell 56 1 aluminum -46 17
cell 57 1 aluminum -47 18
cell 58 1 aluminum -48 19
cell 59 1 aluminum -49 20
cell 60 1 aluminum -50 21
cell 61 1 aluminum -51 22
cell 62 1 aluminum -52 23
cell 24 1 aluminum 25 -24
cell 25 1 bsteel 29 -80
cell 26 1 swater 30 31 32 33 34 35 36 37 38 39 40 41 42 43 44 45 46 47 48 49 50 51 52 -25
cell 27 1 outside 28 100 200
cell 28 1 swater -28 80
cell 29 1 swater -29 24
cell 30 3 swater -28
cell 31 3 void 28
lat 2 1 0 0 11 11 11
3 3 3 3 3 3 3 3 3 3
3 3 3 3 3 3 3 3 3 3
3 3 3 3 1 1 1 3 3 3 3
3 3 3 1 1 1 1 1 3 3 3
3 3 1 1 1 1 1 1 1 3 3
3 3 1 1 1 1 1 1 1 3 3
3 3 1 1 1 1 1 1 1 3 3
3 3 3 1 1 1 1 1 3 3 3
3 3 3 3 1 1 1 3 3 3 3
3 3 3 3 3 3 3 3 3 3 3
3 3 3 3 3 3 3 3 3 3 3
cell 32 0 fill 2 -27
cell 33 0 bsteel 27 -26
cell 35 0 salt 26 -210
cell 34 0 outside 210
——material definition——
mat uranium -0.4
92235.86c -0.93
13027.86c -0.0
92238.86c -0.07
mat water -1 moder lwtr1 1001
1001.86c 0.667
8016.86c 0.333
therm lwtr1 lwtr.10t
mat aluminum -2.7
13027.86c -1
mat steel -7.84
26054.86c -0.97
12026.86c -0.01
6000.86c -0.02
mat boron -2.3
5010.86c 0.19900
5011.86c 0.80100
mix bsteel steel -0.99
boron -0.01

```
mat kaol -2.2
13027.86c 0.118
14028.86c 0.118
8016.86c 0.529
1001.86c 0.235
mat salt -2.163
11023.86c 0.5
17035.86c 0.5
mat mkpc -1.86
19039.70c 0.05
12024.70c 0.05
15031.86c 0.05
8016.86c 0.53
1001.86c 0.32
mix swater water -0.75
salt -0.25
mix wmkpc
mkpc -0.7
water -0.3
mat mica -2 19039.70c 0.05
12024.70c 0.14
13027.86c 0.05
14028.86c 0.14
8016.86c 0.55
1001.86c 0.09
——criticality calculation settings——
set pop 1000 100 10
Plot of the geometry
plot 3 2000 2000 25
```